From A to B, Statistical Modelling of the Ecology of Ants and Badgers

Pierre Nouvellet

Doctor of Philosophy

The University of Sussex

October 2010

The University of Sussex
Pierre Nouvellet
DPhil.

From A to B: Statistical Modelling of the Ecology of Ants and Badgers

Summary

Biological systems involve features/behaviours of individuals and populations that are influenced by a multitude of factors. To explore the dynamics of such systems, a statistical description offers the possibility of testing hypotheses, drawing predictions and more generally, assessing our understanding.

In the work presented, I analyse the properties of various biological systems of two very different organisms: Pharaoh's ants (*Monomorium pharaonis*) and badgers (*Meles meles*). The basis of the work, in the two projects on these biological systems, relies heavily on data collection and explaining observations using quantitative methods such as statistical analysis and simulations.

In the first part of this thesis, I describe animal movement in space and time using data collected on the foraging behaviour of ants. A new model is presented which appears to reflect, with a high degree of accuracy, the behaviour of real organisms. This model constitutes the basis of the second chapter in which the qualities of searching strategies are explored in the context of optimal foraging. The final chapter of first part of this thesis concludes with a detailed analysis of the rate of exploration of individuals. As an essential part of foraging, the rate of individuals leaving their nest is analysed using collected data, and contrasted with results derived from a mathematical model.

The second part of this thesis focuses on badgers. A first chapter explores the significance of palate maculation that is observed in badgers and relates their symmetry to parasitic infection. I then explore the population dynamics of a population of badgers subject to natural variation in climatic conditions. A first analysis is based on local climatic conditions, while a second analysis focuses on a more general property of climate (i.e. its unpredictability) to infer population dynamics.

Declaration

I hereby declare that this thesis has not been and will not be, submitted in whole or in part to another University for the award of any other degree.

.....

Pierre Nouvellet, October 2010.

Acknowledgements

The work presented here would not have been possible without the efforts and support of many whom I would like to thank.

Firstly, my supervisors, Jonathan Bacon, David Macdonald and David Waxman, offered me valuable guidance during each step of the journey. They always encouraged me with a positive attitude, which greatly heightened my motivation.

My work in Oxford would not have been possible without the great help of Christina Buesching and Chris Newman, who both acted as unofficial supervisors. Thanks to them, I will keep 'warm' memories of badger trapping.

My time at Sussex University was certainly fruitful thanks to my many office-mates and many members of staff and I should thus express my gratitude. A special thank to: Mark Broom, Paul Craze, Tomer Czaczkes, Adam Eyre-Walker, Jeremy Field, Tony Grossman, Christophe Grueter, Alan Hodgkinson, Joel Peck, Vini Pereira, Francis Ratnieks, Martyn Stenning, Nina Stoletzki and Sacha Vignieri.

While in Oxford, the many discussions over tea with members of the badger project were certainly helpful. I'd like to thank specially: Geetha Annavi, Karen DeVries, Stephen Elwood, Alex Rey, Simon Sin. I am extremely thankful for all members of the Leys community and Steve who not only helped us a great deal during trapping but also were great company. Also for the nice time in Oxford, not always in the office, to name a few, thanks to: Ruairidh Campbell, Adam Dutton, Paul Johnson, Thomas Merckx, Inigo Montes, Tom Moorhouse, Jed Murdoch, Greg Rasmussen, Diana Roberts, Marion Valeix and Nobby Yamaguchi.

I also thank both my examiners, Tim Roper and James Marshall, for helpful discussion and comments that significantly improved this work.

A special thanks to my family and friends, in France as well as in UK, who bear with me rambling on about ants or badgers. Finally, last but not least, to have shared my daily worries, happy moments and many moods, thank you Mei.

Contents

Preface

This thesis is the result of 3 years of research as a DPhil student and, as stated in acknowledgements, would not have been possible without numerous collaborations in particular with my supervisors. In this preface, I intend to attribute, in some detail, the involvement of each party.

The first research chapter (chapter 2) was based on an idea of my own, on random walks of ants. It developed into the final form, in collaboration with Jonathan Bacon and David Waxman and appendices A2.1-3 are largely a contribution of David Waxman.

Chapter 3 wouldn't have been achieved without Jonathan Bacon's initial input. I designed and performed all simulations and the detailed statistical analyses presented. Appendices A3 were largely a contribution of David Waxman.

Chapter 4 was initiated by common discussion between Jonathan Bacon, David Waxman and me. Appendices A4.1-3 represent a common contribution from David Waxman and myself.

Chapter 5 comes from an original idea of David Macdonald to investigate asymmetry of palate maculation. Data were collected, mainly by Christina Buesching and Chris Newman, before my arrival (between 1994 and 1997), and my involvement started with the digitisation of palate drawing. *Animal models* were constructed and analysed together with Hannah Dugdale, while other analyses are work of my own. Data on parasitic infections came from Chris Newman's own DPhil research.

Chapter 6 was motivated after the completion of Macdonald *et al*. (2009). The long-standing interests of David Macdonald and Chris Newman for climatic interplay with population dynamics were the initial driving forces for this work. The methods of data analysis and the analyses themselves are my own work.

Chapter 7 was an idea of my own, and I completed all analyses presented.

Glossary of symbols

AICc: Akaike Information Criterion corrected for small sample size.

α: turning angle between successive step.

β_0: intercept in a general(ised) linear model.

$\beta's$: coefficients in a general(ised) linear model.

ΔT_j and ΔR_j: temperature and rainfall unpredictability index for year j in chapter 7.

D: diffusion coefficient.

Δt: time interval between two individual leaving the nest.

ζ: parameter defining the distribution of turning angle for a given time interval.

G: number of individuals in a group.

h^2: narrow-sense heritability.

$M(t)$: distance travelled up to time t.

n: the number of ants initially present in the nesting area.

N: a sample size.

P: payoff of a walking pattern, as the benefit of the foraging bout relative to its energetic cost.

QAICc: quasi-AICc, corresponding to the AICc corrected for a variance inflation factor.

r: the probability of any individual ant leaving the nesting area per unit time.

$\boldsymbol{R}$: vector representing both components of the displacement.

R_m, R_o and: R_o^{-1} May and October rainfall and rainfall from the previous year.

s: sensory range, i.e. distance from which an individual is able to recover a food item.

SE: standard error

$\sigma^2(t)$: mean square displacement.

T: time scale of correlation.

T_f, T_m and T_s: February, May and September temperature.

$\boldsymbol{\tau}$: time-intervals, between recorded positions in chapter 2 and 3, between count of ants that left the nesting area in chapter 4

V_A: genetic additive variance.

V_P: phenotypic variance.

X and Y: displacement along X and Y axis, the displacement is defined as the distance moved relative to the initial position (at time zero).

Chapter 1

General Introduction

This thesis includes work intended for journal publications. As such each chapter contains its own detailed introduction. For this reason, this first chapter, as a general introduction, merely intends to set the general background.

Biological systems, in a broad sense from single cells to communities of organisms, are characterised by a high level of complexity. A striking feature of those systems is their dynamical properties. Characterising their variation in space and time is of fundamental interest to understand their structures as well as their possible functions. A classical example in biology would be the study of the beak sizes of Darwin's finches (for a review see Grant 1999). By characterising the spatial and temporal distributions of beak sizes and seed sizes in the Galapagos Islands, the structure of beak size could be correlated with the distribution of seed sizes. The function of various beak sizes emerged as an adaptive feature of the system and selective pressures on the birds could be hypothesised, tested and verified.

Characterising variation in space and time, thus dealing, as seen above, with spatial or temporal distributions, would not be possible without the use of statistics. Statistical analyses are indeed increasingly used in a biological context. Together with mathematical modelling, they provide valuable tools to explore the degree of our understanding, by setting rational limits to the expectation of observations under a certain set of assumptions. This is crucially important as our intuition is often misleading. A good example is given by the *birthday paradox*: what is the probability that 2 or more people in a group of 30 students share the same birthday? We might be surprised at the result of approximately 70%, and see patterns in actual results when there is none. Statistics rely heavily on the concept of *falsification*: a theory, characterised by a set of assumptions, is considered valid unless sufficient support, based on observations, is found to reject it. Together with the principle of *parsimony*, this approach allows the choice of the simplest theory to adequately explain observations.

As already hinted in the previous section, the most rigorous mathematical and statistical treatment of data would be useless without a careful gathering and knowledge of the data themselves. An example given by Whitlock and Schulter (2008) (in Chapter 1) illustrates extremely well the danger of potentially flawed data. A study of cats (Whitney and Mehlhaff 1987) reveals that cats falling from the 7th floor of a building sustained more injuries than those falling from below. However, surprisingly, cats falling from more than seven floors seemed to exhibit fewer injuries, and this was attributed to cats relaxing *'and this change to the muscle cushions the impact'*. Whitlock and Schulter (2008) subsequently remarked:

> *'Our strong suspicion is that not all falling cats were taken to the vet, and that the chance of a cat making it to the vet was affected by the number of stories it has fallen. Perhaps most cats that tumble out of a first or second floor window suffer only indignity, which is untreatable. [...] At the other extreme, a cat plunging 20 stories might also avoid a trip to the vet, heading to the nearest pet cemetery instead.'*

It is clear from this example that a proper data collection, and in-depth knowledge of the data, is paramount to any statistical analysis.

Assuming cautious data collection, statistical modelling may rely on pre-existing models or the model itself may need to be constructed. In relatively simple cases, e.g. when rules of behaviour are simple, construction of a model might offer the best alternative as it allows an accurate description of the processes. In more complex cases, where a more holistic approach is needed, e.g. if relating complex population dynamics to climate, well established models (such as a General(-lised) Linear (mixed) Model) might be more suitable.

In this thesis, I explore two different biological systems, in two different species, Pharaoh's ants (*Monomorium pharaonis*) and badgers (*Meles meles*). The seeming disparity in systems studied should not hide the common scientific approach between the two projects. To study two very different organisms also offers the advantage of learning a different set of methods (e.g., experimental set-up/field work) and a different set of issues and literature, while using similar scientific methodologies. It also has the (dubious) advantage of increasing the number of DPhil supervisors. Through the two projects, the basis of the work relies heavily on both data collection and explaining observations using quantitative methods (statistical analysis, simulations *etc*.).

Throughout the thesis, my general aim is to gain a deeper understanding of the ecology of these two species. To achieve this, I will rely on creating, developing and using a variety of modelling tools appropriate to the situation and species under investigation. While trying to understand the foraging behaviour of ants, I could control for very specific environmental conditions, allowing me to answer fundamental question about their behaviour. On the other hand, understanding the ecology of wild living badgers allowed me to explore complex interactions between their individual characteristics, their population characteristics, both in relation to their environment. The two systems offer the advantage of conducting experimental studies for ants and longitudinal studies for badgers allowing me to explore their ecology at different time scale. In turn the different time scale opened question linked to individual behaviour on one hand and population behaviour on the other.

Ants, as well as many other social insects, are known to display self organisation characteristics, where complex behaviour emerges from simple rules (Bonabeau *et al.* 1997). The relatively simple nature of individual behaviour I was interested in allows an accurate statistical description of the processes and their simulations in *silico* as well as in *vivo* (Halloy *et al.* 2007). During these 3 years, I have explored the foraging abilities

of Pharaoh's ants. By using carefully designed laboratory experiments, I was able to control for many factors, allowing observations to be very specific. In the first research chapter (chapter 2), I establish and explore a new model describing their movement, which can then be applied to evaluate optimal foraging efficiency in a range of situations (given in chapter 3). Finally another essential characteristic of animal foraging is the rate at which individuals engage in exploration, and I propose a detailed model for this process and contrast it with actual observations (chapter 4). Because of the relative simplicity of the behaviours, and our control over experiments, it is possible to model in-depth and de-*novo* the behaviours and I test the validity of the constructed model using observations.

In contrast, when studying animals in the wild, a more holistic approach is needed to account for uncontrolled factors affecting biological systems. To gain knowledge in the relevant approaches of statistical modelling, I present work undertaken on badgers. In England, badgers (*Meles meles*) are socially-living medium-sized carnivores. They have been studied for over 30 years in Wytham Woods, 5km North-West of Oxford, UK (Kruuk 1978c). This thesis relies specifically on intensive trapping records collected since 1987. My involvement in data collection, for the last 3 years, allowed me to gain knowledge of field procedures (e.g. trapping and handling procedures) as well as data analyses. In the 3 chapters focusing on badger ecology, I make extensive use of well established statistical procedures. The first chapter of this section (chapter 5) explores the determinants of skin maculation in the upper palate of badgers. Use of a generalised mixed model (Crawley 2007) would allow the investigation of a potential link between the symmetry of maculation and early developmental stress from parasitoses. We also explore heritability components using a specifically designed analysis of variance components known as the *animal model* (Kruuk 2004). In the two final 'data' chapters (chapter 6 and 7), I explore population dynamics using the Capture-Mark-Recapture framework (White and Burnham 1999) associated with multi-model selection tools (Burnham and Anderson 2002). Specifically the interactions between climate and population dynamics are investigated.

Part I:

From A to B, Statistical Modelling of the Ecology of Ants and Badgers

Cases arising from Studying Ants

Chapter 2

Fundamental Insights into the Random Movement of Animals from a Single Distance-related Statistic

A slightly modified version of this chapter was published in *American Naturalist,* 174, (2009). Authors of the paper are listed below:

Pierre Nouvellet, Jonathan Bacon, David Waxman

Abstract

Statistical theories of animal movement have often been based on models of random walks where movements take place in discrete steps and occur at discrete times**.** The multiplicity of distributions required in these approaches to describe animal movement (i.e., the distributions of angles, discrete steps, and times), have effects that cannot be simply disentangled, and hence cannot be unambiguously determined. In this first research chapter, we present a mathematical formulation of *continuous* animal movements. In this new framework, it is shown that a single time-dependent distance statistic, the mean square displacement, which may be directly measured or mathematically modelled, is a central determinant of such random walks and encapsulates key information about the statistical properties of animal movements. The model and methodology presented here not only allow the determination of what were previously viewed as independent aspects of animal movements, such as the distribution of angular changes in direction, but also, because of the new emphasis on the mean square displacement, may open up a new set of questions concerning animal movement and related phenomena. The results established in this chapter are directly applied to the foraging behaviour of Pharaoh's ants and very close agreement is found between observation and theory.

2.1 Introduction

Establishing the rules underlying the movement of animals (Kareiva and Shigesada 1983; McCulloch and Cain 1989**)** and cells (Nossal and Weiss 1974; Zygourakis 1996) is of fundamental interest in biology and related disciplines. A concept that has proved indispensable in this area is that of a *correlated random walk*, where the direction of a single step of the walk is statistically related to the direction of previous steps (Kareiva and Shigesada 1983; McCulloch and Cain 1989; Nossal and Weiss 1974; Zygourakis 1996; Bovet and Benhamou 1988; Codling *et al.* 2008).

Generally, a correlated random walk of animals is understood to describe movements that take place in two dimensions and occur at discrete times. Such walks typically rely on three distinct distributions: (i) the distribution of times between the discrete steps, (ii) the distribution of step lengths, and (iii) the distribution of turning angles at each step (Kareiva and Shigesada 1983; McCulloch and Cain 1989; Nossal and Weiss 1974; Zygourakis 1996; Codling *et al.* 2008; Patalak 1953; Turchin 1991; Byers 2001). Other models of movement have been constructed where time is initially taken as continuous, but subsequently is approximated as being discrete, in order to facilitate analysis (Bovet and Benhamou 1988, Codling and Hill 2005). These previous studies have focused on estimating parameters, such as the mean distance moved in a single step and the mean cosine of turning angles between subsequent steps (Kareiva and Shigesada 1983). This is in order to predict the mean square displacement and compare predictions of the models with the behaviour of real organisms.

In the present chapter, we introduce and analyse what we believe is a new model for the movement of animals in an unstructured territory. Crucially, our model describes the *continuous* movement of animals. Our model follows from a minimal modification of Brownian motion, and incorporates correlations between the direction of movements at different times. The resulting random walks are short-tailed in character, in the sense that the distances moved, in a finite time, have a *finite* variance. Random walks with infinite variances (long-tailed Levy walks) have been considered elsewhere in a related context (Viswanathan *et al.* 1996; Edwards *et al.* 2007).

The mean square distance associated with animal movement (also known as the mean square displacement), has long been recognised as an important aspect of animal

behaviour (Kareiva and Shigesada 1983; McCulloch and Cain 1989). This quantity also plays a particularly prominent role in the present work. We present, here, what we believe is the simplest model of *continuous* animal movement where correlations are included. We show that essentially all results for the model can be derived, once we have determined the relationship between mean square displacement and the time taken for the displacement to occur. The central role of mean square displacement, as a function of time, is an exact feature of the model; it arises from the intimate way the mean square displacement is determined from correlations between directional changes. More generally, it is plausible that a substantial amount of information, of direct relevance to animal movement, is contained in the dependence of the mean square displacement on the time for the displacement to occur.

We have applied the model presented here to a significant biological problem: the foraging behaviour of Pharaoh's ants. The quality and quantity of data from observations of the ants provide a stringent test of the model.

The following list summarises key findings of the model and the results presented here.

(1) The displacements, which are achieved over a given time interval, have a distribution which is determined solely by the *mean square displacement* over this time interval. The resulting distribution of displacements has an isotropic Gaussian form. These properties hold for any random walk model with a distribution which obeys a simple diffusion equation, however the model of the present work generally encompasses non-diffusive behaviour.

(2) The model is applicable to animal positions that have been recorded at a set of equally spaced times (data of this form follow from filming as well as other methods of recording positions). From the data, a piecewise linear approximation of each animal's path is constructed by joining the positions that were recorded, at adjacent times, by straight lines. The set of directional changes of all lines of the paths of many animals yields a distribution of angular changes. With τ denoting the time-interval between recordings of position**,** the model predicts that the distribution of angular changes is determined *solely* from the *ratio* of *mean square displacements* that are established over time intervals of τ and 2τ. In particular, there are no parameters that require fitting in order to determine this distribution.

(3) Mean square displacements, which are established over the times τ and 2τ, generally change when either the time-interval of data sampling, τ, is changed, or the data set is resampled, so the effective time-interval of sampling is changed. The model predicts that the changed mean square displacements will change the angular distribution in a predictable manner**.** Generally, the angular distribution is *not* a robust quantity, but one that varies according to the precise value adopted for the sampling time-interval; the angular distribution can thus be viewed as an object that is entirely *created* by the precise method of data recording. The impact of resampling on angular distribution was the subject of previous detailed studies (see Bovet and Benhamou, 1988; Codling *et al.* 2005).

(4) Application of the model to the foraging behaviour of Pharaoh's ants, by a detailed analysis of digital video recordings of their movements, indicates that the mean square displacement, of the ants' paths, deviates considerably from being directly proportional to time. This is the characteristic of an anomalous form of diffusion (Codling *et al.* 2008), which is a phenomenon that has been seen in a number of theoretical models **(**Bartumeus *et al.* 2008). In the context of the present work, this anomalous diffusive behaviour is theoretically predicted and empirically found to be directly manifested in the distribution of angles associated with ant paths. This anomalous diffusive behaviour allows us to very simply estimate an important timescale in the problem which concisely characterises the correlations underlying the random walk.

2.2 Model of a Persistent Random Walk

In the present work we introduce a model of animal movement, with the aim of applying it to real organisms to further our understanding of their behaviour. The model describes properties of the "displacement" of an animal. The displacement of an animal at time *t* is its position at this time, *relative* to its position at time $t = 0$. Since the animal moves in two dimensions, the displacement involves two coordinates and is written $\mathbf{R}(t) = \big(X(t), Y(t)\big)$. By definition, the displacement vanishes at time $t = 0$.

When constructing the model, we restricted ourselves to the very *simplest* piece of mathematics capable of governing continuous changes of the displacement over time (a linear differential equation). Such an equation must incorporate the observed tendencies of animals to have some level of persistence in their direction of movement. These tendencies presumably arise from a combination of neuronal activity and the biomechanics of movement. In the absence of a detailed knowledge of these factors, and recognising that there are effectively (or genuinely) random aspects of the problem, we incorporated a degree of randomness into the equation governing the displacement (full details of the model are given in Appendix A2.1). The random components in the equation governing the displacement (and which represent random tendencies to move and change direction) are allowed to be arbitrarily correlated with themselves over time. This is a very simple and natural way to incorporate the tendency of animals to move with some persistence of direction. We encapsulate *all* unknown determinants of movement of the model in a specification of the correlations.

Like any modelling in biology, assumptions do need to be made. Here we assume that the animals are foraging, but not purposefully heading in a particular direction (which, for example, occurs when they are migrating). The validity of this assumption can be tested on real data sets, by the absence of a directional preference, and this assumption makes the present work a possible starting point for further studies, where additional assumptions about the general patterns of movement may be included in the equation governing the displacement (see Appendix A2.1 and Eq. (A1)).

The mean square displacement that is established after time *t* is $E\left[X^2(t) + Y^2(t)\right]$ where $E[...]$ denotes an average or expected value. Displacement here specifies the changes in

position relative to the initial position. The term squared displacement was initially used by the seminal paper of Kareiva and Shigesada (1983). We write the mean square displacement as $\sigma^2(t)$:

$$\sigma^2(t) = E\left[X^2(t) + Y^2(t) \right]. \qquad (2.1)$$

We note the mean square displacement has the form of a variance (see theoretical results below for details).

The model allows the mean square displacement, $\sigma^2(t)$, to be explicitly expressed in terms of correlations of the "random tendencies to move", as is shown in Appendix A2.2. Thus all emphasis can be shifted from correlations to the mean square displacement, $\sigma^2(t)$. We adopt the view that $\sigma^2(t)$ is the object containing all unknown determinants of movement of the model. This model exhibits considerable flexibility, since many different possible choices can be made for the dependence of $\sigma^2(t)$ on time, *t*.

We note here three special cases of the dependence of the mean square displacement on time.

(i) $\sigma^2(t)$ is a constant, independent of time *t*. This is the extreme limit of so-called *subdiffusive* behaviour (Codling *et al*. 2008), which generally corresponds to $\sigma^2(t)$ having a *slower* than linear growth with time *t*. Subdiffusion is a feature found in some models of animal movement (Codling *et al*. 2008). It can arise when there are negative correlations in directional changes, and the animal paths have the tendency to "backtrack" on themselves.

(ii) $\sigma^2(t)$ is proportional to time *t*. This corresponds to conventional diffusion and is a feature seen in many models of animal movement at long times (Kareiva and Shigesada 1983). If $\sigma^2(t)$ is proportional to *t* for all times then we have *Brownian motion* (Brown 1828) and this arises when correlations in directional changes exist over only the very shortest of timescales.

(iii) $\sigma^2(t)$ is proportional to t^2. This occurs when an animal moves at a constant speed in a fixed direction (but different individuals generally have different speeds and

different directions). This can be described as ballistic motion and can arise when correlations in directional changes are positive and exist over very long timescales. Ballistic motion is the extreme limit of *superdiffusive* behaviour (see e.g., Codling *et al.* 2008), and generally corresponds to $\sigma^2(t)$ having a *faster* than linear growth with time *t*.

2.3 Theoretical Results

All results given in this Section are derived from a detailed mathematical analysis of the model given in Appendix A2.3. We begin the presentation of these results by noting that within the framework of the model, both the *x* and *y* coordinates of the displacement of an animal at time *t* have very simple statistical descriptions. They are each *independent* normal random variables with mean zero and variance $\sigma^2(t)/2$ and Eq. (2.1) follows from this. Despite the extreme simplicity of the distributions of *x* and *y* (normal distributions), there are highly nontrivial characteristics of the paths of individual organisms because of the presence of correlations, as will become apparent in the distribution of angles, given below.

While our model is fully continuous, it may be applied to situations where the positions of the animals are sampled/recorded at only the discrete times $0, \tau, 2\tau, 3\tau, \ldots$ Such sampling would result, for example, from a film or video recording of the animal positions or from telemetry.

Given this sampling, we construct the piecewise linear approximation of a path by joining the adjacent positions of an animal at the discrete times $0, \tau, 2\tau, 3\tau, \ldots$ via straight lines. The angular changes of the adjacent straight lines allow a definition of the turning angles, α. Figure 2.1 illustrates a piecewise linear path which was constructed from movements of a single animal (an ant) that was recorded at discrete times.

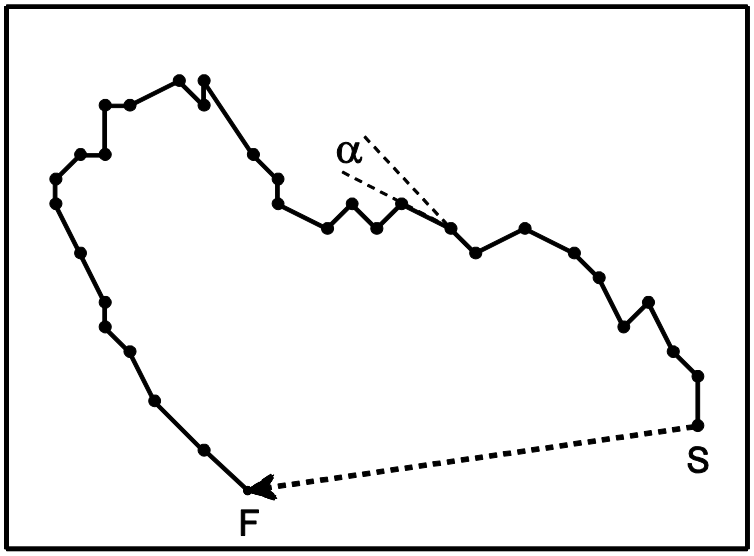

Figure 2.1

A plot of the piecewise linear approximation of the continuous path of a single animal (an ant from experiments which are described later), when its position was sampled at time intervals of $\tau = 0.125$ seconds. The filled dots represent the sampled positions, while the straight solid lines connecting the dots constitute the piecewise linear construction of the path. The particular path illustrated is of four seconds duration and hence contains 33 positions. The path starts at position S and finishes at position F. From one time step to the next, the directions of the linear segments generally change. One angle, α, is illustrated between the adjacent linear segments joining the positions of the animal at times 1.000, 1.125 and 1.250 seconds. We adopt the convention that angles are positive (negative) if made in anticlockwise (clockwise) direction. The angle illustrated corresponds to an anticlockwise change and hence is positive. The dashed arrow shows the displacement of the animal from its starting point after the four seconds of movement.

The distribution of turning angles for discretely sampled paths is, remarkably, found to depend on only a single parameter $\zeta \equiv \zeta(\tau)$ which is completely determined from the mean square displacement, $\sigma^2(t)$, via

$$\zeta \equiv \zeta(\tau) = \frac{1}{2}\frac{\sigma^2(2\tau)}{\sigma^2(\tau)} - 1. \qquad (2.2)$$

The parameter ζ can vary from $-\frac{1}{2}$ to 1. The lower limit of this range follows from the mean square displacement having behaviour associated with the extreme limit of *subdiffusion* (i.e., $\sigma^2(t) = \text{constant},$ independent of *t*). The upper limit follows from the extreme limit of *superdiffusion*, which is ballistic motion ($\sigma^2(t) \propto t^2$). Brownian motion ($\sigma^2(t) \propto t$) leads to the intermediate value $\zeta = 0$.

Up to a reasonable approximation, the parameter ζ is proportional to the mean value of the cosine of the turning angles, $E[\cos\alpha]$, namely $\zeta \approx (4/\pi) \times E[\cos\alpha]$ (the exact relation between ζ and $E[\cos\alpha]$ is given in Eq. (2.4), below).

With angles, α, lying in the range of $-\pi$ to π radians, the distribution of turning angles, for a given value of ζ, is written $\phi(\alpha;\zeta)$ and is found to take the exact form

$$\phi(\alpha;\zeta) = \frac{(1-\zeta^2)}{2\pi}\frac{\sqrt{1-\zeta^2\cos^2\alpha} + \left[\arctan\left(\frac{\zeta\cos\alpha}{\sqrt{1-\zeta^2\cos^2\alpha}}\right) + \frac{\pi}{2}\right]\zeta\cos\alpha}{(1-\zeta^2\cos^2\alpha)^{3/2}}. \qquad (2.3)$$

This distribution is illustrated in Figure 2.2.

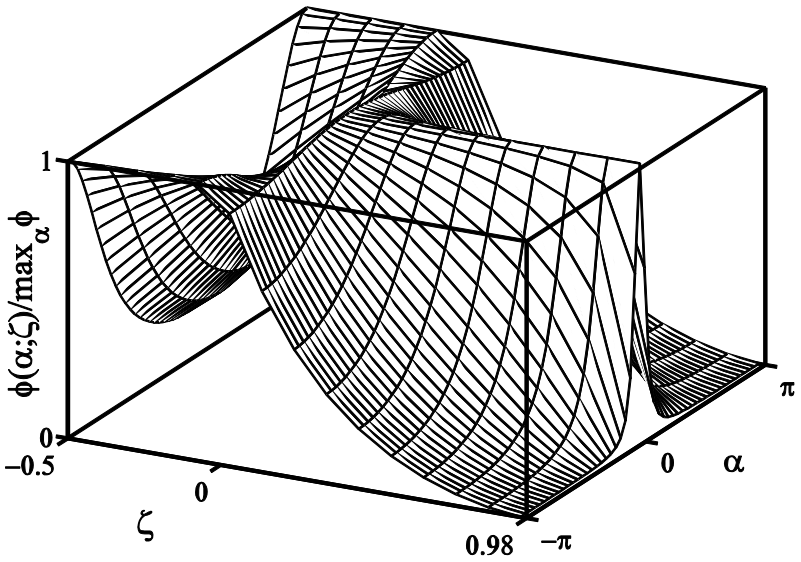

Figure 2.2

A plot of the ratio $\phi(\alpha;\zeta)/\max_\alpha \phi$ against angle, α, and parameter ζ, where $\phi(\alpha;\zeta)$ is the distribution of angles for a given value of ζ and $\max_\alpha \phi$ is the maximum value of $\phi(\alpha;\zeta)$ over all angles. In the Figure, angles are measured in radians. The distribution $\phi(\alpha;\zeta)$ takes various forms, depending on the value of ζ. When ζ is negative, the distribution is a U shaped function of α (due to the presence of *negative correlations*). When $\zeta = 0$ the distribution is uniform in α (as would occur in *Brownian motion*). When ζ is close to 1 (which corresponds to near *ballistic motion*), the distribution is a sharply peaked function of α. The maximum value of $\phi(\alpha;\zeta)$ varies strongly with the value of ζ. For example, when $\zeta = 0$, the maximum value is $(2\pi)^{-1}$, while when ζ tends to 1, the maximum value tends to infinity. Plotting the ratio $\phi(\alpha;\zeta)/\max_\alpha \phi$ allows a direct comparison of the shape of the distribution for different values of ζ, without being confounded by the very different maximum heights. If the angular distribution is required for a given value of ζ, the complete result for the distribution is given in Eq. (2.3).

As shown above, the distribution of angles depends on just a single parameter, $\zeta \equiv \zeta(\tau)$, which therefore has an exceptional status in the theory. The value of ζ is a defining characteristic of paths that have been sampled at discrete time-intervals of τ. All statistics of paths that provide a direct measure of correlations in directional changes, depend only on ζ. For example, the mean (i.e., expected) value of $\cos\alpha$, namely $E[\cos\alpha]$, is explicitly given by

$$E[\cos\alpha] = \frac{E(\zeta) - (1-\zeta^2)K(\zeta)}{\zeta} = \frac{\pi}{4}\zeta + \frac{\pi}{32}\zeta^3 + O(\zeta^5) \qquad (2.4)$$

where $K(\zeta)$ and $E(\zeta)$ denote complete elliptic integrals of the first and second kind, respectively (Abramowitz and Stegun 1965). The smallness of the coefficient of ζ^3 in Eq. (2.4) allows the mean value of $\cos\alpha$ to be quite reasonably approximated by just the leading term in ζ, namely $E[\cos\alpha] \approx (\pi/4)\zeta$, with all higher order terms omitted (as pointed out above).

Within the model, the time-interval of sampling, τ, can be arbitrarily chosen. We can exploit this feature to provide an estimate of an important timescale in the problem that concisely characterises the decay of correlations of the random tendencies that give rise to the random walk, and which we have assumed arise from neuronal activity and the biomechanics of movement. The existence of such a timescale, say *T*, is also equivalent to the assumption that the mean square displacement, $\sigma^2(t)$, depends on time *t* only in the combination *t/T*. We have considered correlations that decay as $\exp(-|t|/T)$ or $\exp(-t^2/(2T^2))$. The resulting forms of $\zeta(\tau)$ that follow from these have common features. In particular, they both decrease as the sampling time, τ, is increased, and have a largest value, $\zeta(0)$, of unity. When the value of the sampling time is close to the timescale T, i.e., when $\tau \approx T$, we find the value of $\zeta(\tau)$ is close to $1/2$. This suggests a simple but practical *estimate* of the correlation time associated with movement, namely it is the choice of sampling time, τ, that leads to $\zeta(\tau) = 1/2$.

As an alternative method of characterising correlated random walks, some authors have introduced a statistic termed 'sinuosity' (Bovet and Benhamou 1988; Bovet and Benhamou 1991; Benhamou 2004). This statistic has been primarily defined for random walks with discrete step lengths, and as such is not obviously directly relevant

for the fully continuous random walks considered in the present work. We note, however, that a formulation has been provided that relates sinuosity to mean square displacement *at long times* (Benhamou 2004). We plan, elsewhere, to investigate the relation between the different approaches.

2.4 Data Analysis Procedure

To complement the theoretical results, it is necessary to have a practical means of extracting information from the data. We work on the assumption that we have a number of distinct animal paths, where animal positions are known at the times 0, τ, 2τ, 3τ, **…** The results we require are estimates of quantities such as the mean square displacement at the times τ and 2τ, namely $\sigma^2(\tau)$ and $\sigma^2(2\tau)$, and the distribution of angular changes of direction along paths. Our procedure is to extract and use the maximum number of independent positions/displacements, and hence the maximum information, from the positional data in our possession. We adopted the following procedure to achieve this. Focussing on a single animal path, we extracted all *x* and *y* coordinates of the animals at the times $2j\times\tau$ and $(2j+1)\times\tau$ with $j=0,1,2,...$ This information allows us to directly determine a set of squared displacements of data sampled at time intervals of τ along a single path. Pooling the data over all paths allows a good estimate of $\sigma^2(\tau)$. Next, extracting all *x* and *y* coordinates of the animals on a path at the times $2j\times\tau$ and $(2j+2)\times\tau$ allows us, in a similar way to estimate $\sigma^2(2\tau)$. In an analogous way, all angular changes in direction can be determined from the *x* and *y* coordinates that were extracted from the positional data, and an empirical distribution can be determined.

2.5 Application of the Theory to Pharaoh's Ants

We applied the theoretical results to the foraging paths taken by individual ants of the highly invasive, pheromone laying, multi-queen species *Monomorium pharaonis* (Pharaoh's ants). These ants were allowed access, via a bridge from their nest, to a previously inaccessible area (henceforth termed the *arena*) and filmed at the rate of 8 frames per second. Each frame was stored in a digital format, and analysed to determine the mean position (i.e., the mean value of the x and y coordinates) of every ant that had left the nest and was exploring the arena (see Appendix A2.4 for details of experimental setup). This gave the positions of each ant in the arena, every 0.125 seconds, but did not identify which of the positions, in different frames, correspond to a given ant. To make such an identification, we adopted the procedure where, given the position of a particular ant in one frame, the position of the ant closest to it, in the next frame, is taken as the actual position of the ant in that frame. We estimate that over a path lasting up to 120 seconds (i.e., approximately 10^3 frames), and for the density of ants observed in our experiments (approximately 10^3 ants/m^2), this simple procedure correctly identifies 98% of the positions visited by a single ant (see Appendix A2.5 for details of the accuracy of path identification). Having determined the positions of one ant at different times, we performed a piecewise linear reconstruction of its path.

In order to have a balanced dataset, and to avoid any edge effects associated with ants entering or leaving the arena, we restricted analysis to paths of 30 seconds duration that were located near the centre of the arena. In this time interval, Pharaoh's ants can move a significant distance - of the order of 200 body-lengths.

We carried out an analysis of the pixels (picture elements) of the digital video recordings of the ants in the arena. This allowed us to determine the time that ants spent in each pixel. Putative ant trails may be defined as regions of the arena where an appreciable time was spent by the ants. We estimate that appreciable *changes* in occupancy of such putative trails occurred on the timescale of tens of minutes. Thus during any 30 seconds time interval, at any time throughout a 70 minutes experiment, there was negligible excess usage of a trail compared with any other region (see Figure 2.3). Thus during the 30 seconds time intervals where ant movements were analysed for this work, the ants acted as *effectively independent agents* that were *not* following trails.

This motivates modelling the movements of individual ants as continuous random walks that are independent of the random walks of other ants.

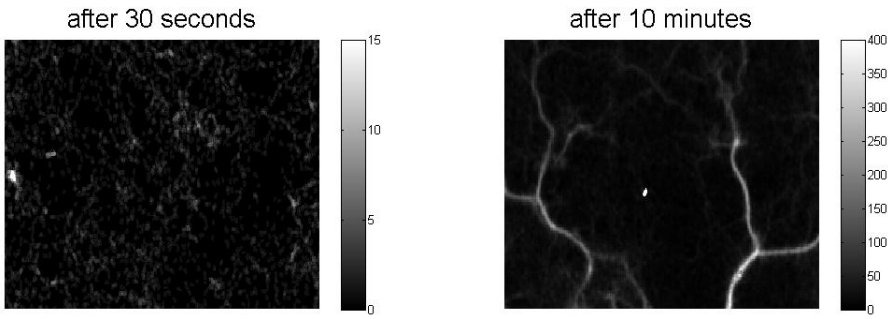

Figure 2.3

Superimposition of 60 (left) and 1200 (right) frames (2 frames per second). Clearer pixels indicate positions repeatedly visited by ants. It is clear that at a timescale of tens of minutes (right), ants used preferred area establishing a network of trails; while at timescale of 30 seconds (left) no trails could be visualised.

The digital video recordings yielded the positions of the ants every 0.125 seconds. Figure 2.1 contains the actual piecewise linear path constructed for one particular ant, over a 4 seconds time interval. From the digital video recordings, we determined the distributions of displacements, over a number of 30 seconds time intervals, during the course of the experiment.

We verified (using the Kolmogorov Smirnov test) that in excess of 95% of these distributions were not significantly different from a normal distribution. We note that if the distribution of displacements over a given time interval *t* is normally distributed, and has a variance, $\sigma^2(t)$, then a direct consequence of normality is that the ratio of "mean displacement" to "root mean square displacement" is independent of the variance,

$\sigma^2(t)$ (Bovet and Benhamou 1988) and hence the choice of time interval, *t*. With the magnitude of displacement written $\|\mathbf{R}(t)\| = \sqrt{X^2(t) + Y^2(t)}$, this ratio has the value

$$E\left[\|\mathbf{R}(t)\|\right] \Big/ \sqrt{E\left[\|\mathbf{R}(t)\|^2\right]} = \sqrt{\pi/4} \approx 0.8862 \qquad (2.5)$$

(Bovet and Benhamou 1988; see also the discussions about this in Codling *et al.* 2008). The intuitive explanation of Eq. (2.5) is that in an isotropic normal distribution (e.g. $\mathbf{R}(t)$ is uniformly distributed in all directions and normally distributed), there is only a single length present, namely $\sigma(t)$. As a consequence, both $E\left[\|\mathbf{R}(t)\|\right]$ and $\sqrt{E\left[\|\mathbf{R}(t)\|^2\right]}$ are directly proportional to $\sigma(t)$), such that their ratio is a constant, independent of $\sigma(t)$. Direct calculation verifies this explanation (see Appendix A2.3 for an explicit derivation of Eq. (2.5)).

The result of Eq. (2.5) may be used to check normality of the distribution of displacements, without requiring any knowledge about the time dependence of $\sigma^2(t)$. Results for the actual numerical value of the ratio, $E\left[\|\mathbf{R}(t)\|\right] \Big/ \sqrt{E\left[\|\mathbf{R}(t)\|^2\right]}$, calculated from our ant data, are given in Table 2.1.

time interval, t (seconds)	1	2	4	6	10	15	20	30
$E\left[\left\|\mathbf{R}(t)\right\|\right]\Big/\sqrt{E\left[\left\|\mathbf{R}(t)\right\|^2\right]}$	0.88	0.887	0.892	0.89	0.888	0.882	0.883	0.883
$\sigma^2(t)/\sigma^2(1)$	1	3.3	9.7	17.3	34.4	56.9	78.5	121.3

Table 2.1

A table exhibiting ratios of the *mean displacement* to *root mean square displacement* of foraging ants, as a function of time interval. When the displacement that occurs over a time interval of t, namely $\mathbf{R}(t)$, follows a normal distribution with variance $\sigma^2(t)$, the ratio $E\left[\left\|\mathbf{R}(t)\right\|\right]\Big/\sqrt{E\left[\left\|\mathbf{R}(t)\right\|^2\right]}$ is independent of $\sigma^2(t)$ (and hence time), and takes the constant value $\sqrt{\pi/4} \approx 0.8862$ (see (Bovet and Benhamou 1988) and Appendix A2.3). This relationship was tested for paths of 30 seconds duration that were observed at various points throughout a 70 minutes experiment. We present here the ratio that was calculated from data for the 30 seconds paths that were observed between 40 and 42 minutes of the experiment. The table illustrates the close agreement of the experimental results for this ratio, to the prediction of a normal distribution. A similar close agreement was found for 30 seconds paths at different times throughout the duration of the experiment (results not shown). The final row of the table gives the ratio of mean square displacement of the ants that was established over a time interval of t, to the mean square displacement for a time interval of t = 1. The final row indicates the substantial degree of broadening of the distribution that occurs, up to 30 seconds.

In the theory presented here, the ratio $E\left[\|\mathbf{R}(t)\|\right]\Big/\sqrt{E\left[\|\mathbf{R}(t)\|^2\right]}$ is predicted to take a fixed value of $\sqrt{\pi/4}$ (see Eq. (2.5)), which is completely independent of the way the mean square displacement, $\sigma^2(t)$, varies with time, *t*. By contrast, the distribution of angular changes is predicted to explicitly depend on the way $\sigma^2(t)$ varies with time, *t* (since the angular distribution depends on $\sigma(2\tau)$ and $\sigma(\tau)$ - see Eqs. (2) and (3)). To investigate the angular distributions associated with the Pharaoh's ants, we first investigated the mean square displacement, $\sigma^2(t)$. A typical form for the observed time dependence of $\sigma^2(t)$ is given in Figure 2.4.

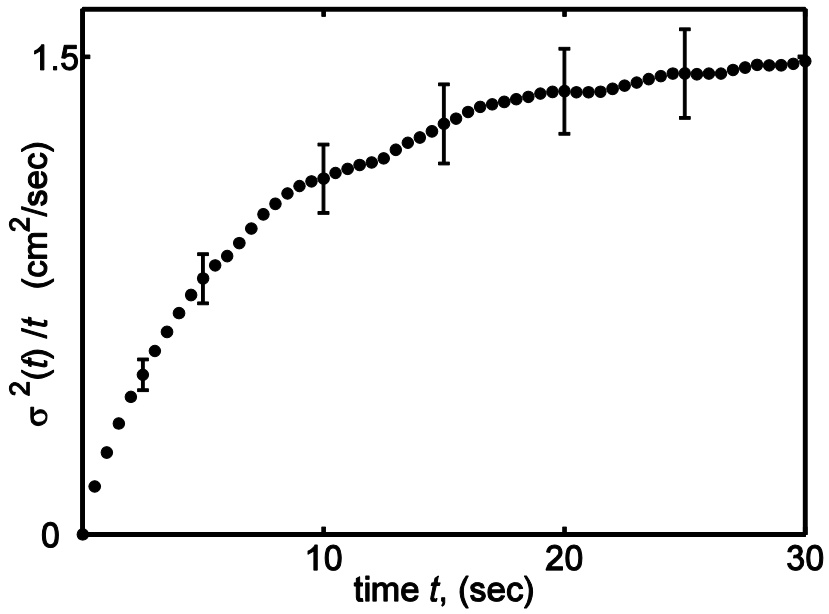

Figure 2.4

The observed mean square displacement of the ants observed in the experiments, that is established after a time interval of *t*, is written $\sigma^2(t)$. In the Figure, the ratio $\sigma^2(t)/t$ is plotted against *t* from data collected for Pharaoh's ants. The error bars represent the standard deviation of $\sigma^2(t)/t$. For *n* normally distributed displacements with a sample mean square displacement of $\sigma_s^{\,2}$, the standard deviation is estimated as $\sqrt{2/(n-1)}\sigma_s^{\,2}/t$. With σ_p^2 the population variance, this estimate follows from $(n-1)\sigma_s^{\,2}/\sigma_p^2$ having a χ_{n-1}^2 distribution. The plot suggests that at relatively long times, the ratio $\sigma^2(t)/t$ approaches a constant value. An approach of the ratio to a constant value indicates an approach to conventional diffusion behaviour, with $\sigma^2(t) \propto t$. It is evident that $\sigma^2(t)/t$ does not have a constant value for short times. This indicates a substantial deviation of $\sigma^2(t)$ from being proportional to *t*. Such behaviour is termed *anomalous diffusion* **(**see e.g., Codling *et al.* 2008**).**

Previously, we introduced the sampling time-interval τ. This quantity can, in theory, be freely chosen. However with our data there is a restriction; because of the mode of data recording adopted, τ must be an integer multiple of 0.125 seconds (there will be a similar restriction with any positional data that is recorded at discrete times). With our data it is possible, for example, to make a choice for τ such as $\tau = 1$ second. After this choice has been made, the mean square displacements for the times τ and 2τ can be found and using these, the value of the parameter $\zeta(\tau)$ (Eq. (2.2)) may be established. The resulting value of $\zeta(\tau)$ allows us, via Eq. (2.3), to determine the angular distribution that is predicted by the theory. No additional information or parameters are required to determine the angular distribution.

We extracted the maximum possible information from our data to calculate $\zeta(\tau)$, using *all* non-overlapping displacements that make up a path, as described above in the Data Analysis Procedure. We note that a path of just a *single* ant that is observed for *t* seconds may contain a considerable amount of relevant information since it consists of $t/(2\tau)$ non-overlapping displacements that may be used in the calculation of $\zeta(\tau)$.

The above process can be repeated for different *choices* of the sampling time-interval τ. The theory makes explicit predictions for the qualitative and quantitative shape of the angular distribution, for different values of τ, given knowledge of the mean square displacement, $\sigma^2(t)$. The angular distributions, so predicted, can be directly compared with the angular distributions that are arrived at by directly measuring angular changes of direction. Some illustrative findings are given in Figure 2.5.

Under a model of a correlated random walk, increasing the sampling time interval is, intuitively, expected to cause the distribution of turning angles to become more Brownian-like, since correlations in the direction of movement are expected to decay over time. Equivalently, the distribution of turning angles, derived from just the mean square displacement, $\sigma^2(t)$, is expected to broaden, given the observed behaviour of $\sigma^2(t)$, when the sampling time interval is increased (Figure 2.4). This is indeed what is seen in Figure 2.4 (see also specific studies on this effect: Bovet and Benhamou 1988 and Codling and Hill 2005).

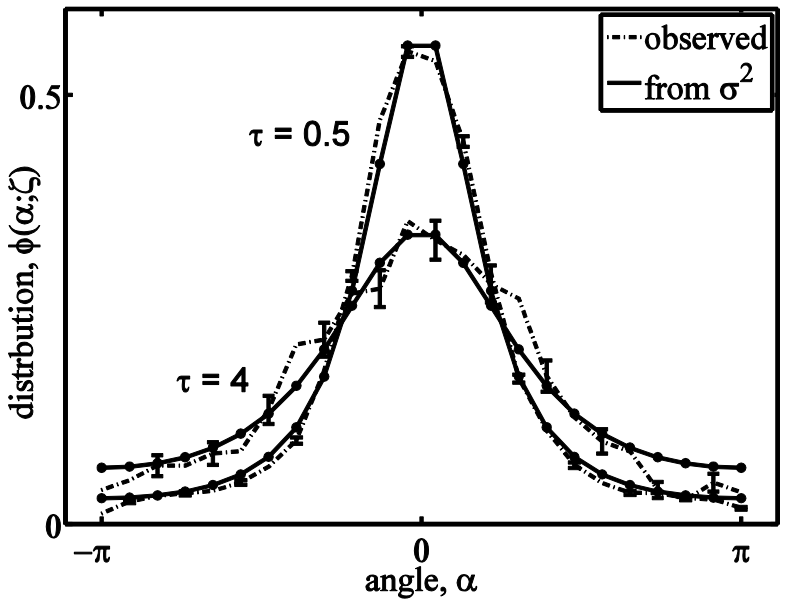

Figure 2.5

Analysis of the piecewise linear construction of recorded ant paths. The paths, sampled at time-intervals of τ, allow determination of the distribution of turning angles by directly measuring angles, as for example would be possible from Figure 2.1. Two separate choices for τ, were adopted in the Figure. The resulting angular distributions are marked with broken lines and the error bars give the standard deviation in the distributions. From the same paths, determining the mean square displacements at times τ and 2τ, and then using Eqs. (2) and (3), allows the theoretical angular distribution to be calculated without knowledge of the observed angles (see the Data Analysis Procedure for the method of determining $\zeta(\tau)$). The theoretical formulation applies for an arbitrary value of the sampling time τ. The theoretical curves are marked with dots connected with solid lines. There is very good quantitative and qualitative agreement between the angular distributions predicted by the theory (from measured mean square displacements) and the actual distributions obtained from measuring all angles. This lends strong support to the key role played by the mean square displacement, $\sigma^2(t)$. A goodness of fit procedure (as a function of sample size) is presented below (see Table 2.2).

A quantity that is widely used to describe the angular distribution, namely the mean cosine of angles, $E[\cos\alpha]$ (Kareiva and Shigesada 1983), can be determined by directly measuring angles, or alternatively by using the observed mean square displacement and Eqs. (2) and (4). To assess the effect the size of the sample has on the predictions of the present work, we have resampled the data by randomly choosing a smaller sample (i.e., a subset of all the ants we observed). For 100 samples of *N* ant paths (*N* = 10, 20,…, 150), we determined the standard deviation of $\cos\alpha$ from direct calculation of angles that we measured directly, with those using the value of $\zeta(\tau)$ for each sample and the distribution of angles, Eq. (2.3). It has been suggested (Bovet and Benhamou, 1988) that the angular distribution contains less noise than the mean displacement and thus the former should be prefrentially used in calculations. Comparing the standard deviation of $\cos\alpha$ from the two approaches, however, yields broadly comparable results (see Table 2.2).

We showed above that when the sampling time, τ, takes a value such that $\zeta(\tau)=1/2$, then it is close to an assumed unique correlation time *T*, associated with the random movement of the animals. By interpolating the values of $\zeta(\tau)$, as a function of τ, over the entire 70 minutes duration of the experiment, we estimate that $\zeta(\tau)=1/2$ for $\tau\approx 2.3\,\text{sec}$. This is thus our estimate of the *correlation time, T*, associated with the correlated random movements of the population of ants under investigation. This value of *T* is a robust feature of correlations of directional changes and hence of the underlying mechanisms that drive the ant movements.

	$T = 0.5$					$T = 4$				
N	10	20	50	100	150	10	20	50	100	150
$SD_1 \times 10^2$	4.1	2.4	1.5	0.9	0.6	7.4	4.7	3.0	1.7	1.1
$SD_2 \times 10^2$	7.1	4.1	2.4	1.6	1.0	12.5	7.8	4.8	3.3	2.0

Table 2.2

An estimate of the standard deviation of $\cos\alpha$ from samples of data of size N. The standard deviation of $\cos\alpha$, when calculated from the directly measured angles, is denoted SD_1. The standard deviation, when calculated from Eq. (2.3), (i.e., just using knowledge of the mean square displacement) is denoted SD_2. The standard deviation of $\cos\alpha$ was estimated by randomly choosing, without replacement, a subset of 100 ant paths of size N. The original data set contained 216 paths. The values of SD_2 are slightly higher than the corresponding values of SD_1, reflecting the fact that when 'n' angles can be extracted from a path, then $\zeta(\tau)$ is determined from 'n/2' values (see the Data Analysis Procedure, above).

2.6 Discussion

In previous work, it has been asserted that when it is required "to describe in detail the spatial structure of animals' actual paths, it is indispensable to specify the distribution of changes of direction" (Bovet and Benhamou 1988). Most theoretical studies (Othmer, Dunbar and Alt 1988; Bartumeus *et al.* 2008; Bartumeus *et al.* 2005; Benhamou 2004; Bovet and Benhamou 1991) and empirical studies (Crist *et al.* 1992; Crist and MacMahon 1991; Garcia *et al.* 2007; Challet *et al.* 2005) have consequently used a description of animal movement based on a characterisation of the distributions of 'turning angles' and 'step lengths'. Early work on kinesis (Gunn, Kennedy and Pielou 1937), where motion was described in term of speed (O-kinesis) and path sinuosity (K-kinesis), has, most likely, influenced the present formulation of correlated random walks.

Here, we present a mathematical model, along with associated theoretical results, which relate directly to observations of the continuous movements of animals. Constructs, such as step length, do not appear in our theoretical description. However, any recording technique that captures images at discrete times, *by its fundamental nature*, produces a discrete time description of the data, and our analysis and modelling have accommodated data with this basic feature.

The mean square displacement of the moving animals plays a central role in our theory, since it contains information necessary for an essentially complete description of a continuous correlated random walk. In particular, from the piecewise linear approximation of animal paths derived from a discrete time description, an angular distribution can be produced, and it is apparent that this distribution is *created* by the mode of recording and does not have a fundamental significance or existence in its own right. This is emphasized, in Figure 2.5, by the change in the angular distribution which results when the discrete time of sampling of the data is changed. The change of shape of the distribution, derived from direct experimental observation of real organisms (Pharaoh's ants), is well explained in terms of the mean square displacement - as predicted by the theory. We hold the view that the robust quantity underlying animal movement are particular *functions* that characterise the statistics of the problem, namely a correlation function, or equivalently, the mean square displacement, $\sigma^2(t)$. Any

model that can be cast in the form of Eq. (A1), and has a correlation function that only depends on the time interval $t_1 - t_2$ (see Appendix A2.1) will be fully characterised by $\sigma^2(t)$.

The issue of re-sampling and its implication for the angular distribution has been previously explored (Bovet and Benhamou 1988; Hill and Hader 1997; Codling and Hill 2005), while Bartumeus *et al.* (2008) did consider angular distributions and the effect on resulting simulated movement paths. Here we have presented an alternative approach, where the time dependence of $\sigma^2(t)$ contains key information needed to characterize the angular distribution, and we have shown that knowledge of this quantity predicts angular statistics with broadly comparable accuracy to those derived directly from measuring angles of directional change within paths. Hence properties that have been previously discussed, such as smoothing of angular distributions, due to resampling, also hold in the present work.

An additional feature of our model is that it uses information from the mean square displacement, $\sigma^2(t)$, and so covers different regimes of time, including behaviour at long time intervals, where the motion is close to that of Brownian motion, as well as in the short time regime, where the effects of correlations play a significant role. This leads to a full formulation for the probability distribution of the displacements of animals, and their mean distance travelled at any time after starting (for a discussion on the short time regime, see Wu *et al.* 2000). This is of special interest when making the comparison with discrete step, discrete time models. In many of such models, many quantities of interest are really only defined for the long time regime, where the number of discrete steps is used as an approximation of time (Bovet and Benhamou 1988). By contrast, the continuous time description presented here allows us to characterise the behaviour and implications of correlations over relatively short timescales and to derive the "correlation time" that is directly related to the actual level of correlation in the observed paths.

We note that the model presented here relaxes some assumptions commonly made for the sake of mathematical simplicity rather than direct biological relevance. These include (i) the assumption of constant velocity (see Codling *et al.* 2008) and (ii) the assumption of independence of step length and angular changes in direction (Kareiva and Shigesada 1983). Furthermore, because the angular distribution of a piecewise

linear discrete path appears as a by-product of changes in the mean square displacement, as shown in the present work, the need for characterising and using complicated angular distributions (Codling *et al.* 2008; Byers 2001; Bartumeus *et al.* 2008) may be avoided.

The results presented here are designed to accommodate the most common methods of data collection, namely filming/digital video recording and telemetry (radio tracking, GPS, radio frequency identification - RFID). On a practical side, and probably of particular interest for ecological studies, knowing the mean value of the displacement in the asymptotic long time regime, where $\sigma^2(t)/t$ is independent of time *t*, can yield an estimate of the diffusion coefficient, and hence allow a quantitative description of the dispersal of organisms. This can be done without knowledge of particular paths of individuals, but from an average over all displacements at a given time, providing this time is suitably large. An estimate of the correlation time, *T*, gives an indication of the minimum time at which to sample the population's mean square displacement, since when $t >> T$, the quantity $\sigma^2(t)/t$ is expected to approach a constant value (see Figure 2.4).

The work presented here provides a new perspective on the description, and hence study, of animal movement, via a statistical model that is centered on the mean square displacement, $\sigma^2(t)$. This quantity encapsulates key features of animal movement, with a number of other characteristics subordinate to it. We suggest that future progress, along the lines of the present work, may lie in two directions. The first direction is measuring how the mean square displacement, $\sigma^2(t)$, varies with time *t*. It would be natural to consider a variety of different organisms, in different contexts, and then proceed to produce plausible models and explanations of the observed forms of $\sigma^2(t)$. The second direction would lie in investigating the optimisation of resource discovery, in an evolutionary ecological context. The present work suggests that modifying the nature of the search paths is equivalent to modifying a single function, namely $\sigma^2(t)$. A mathematical formulation of search strategy, in terms of $\sigma^2(t)$, may thus be possible.

2.7 Acknowledgements

We thank Edward Codling, Don DeAngelis, Andrew Edwards and Andrew Solow for constructive suggestions and Larissa Conradt, Jeremy Field and Marie Harder for helpful discussions.

Chapter 3

Exploring Exploration: Finding which Foraging Strategies are Optimal, when Resources are Randomly Distributed

Abstract

Accurate description and simulation of animal movement is of crucial importance when investigating the strategies that optimally search and exploit food resources. In the previous chapter, we presented a model of a correlated random walk which accurately describes the movement of real ants. Here, we use this model to simulate the movement of virtual ants. In contrast to previous approaches, which artificially describe these movements as occurring in a sequence of discrete jumps, at random times and at random angles, our previous work models movement realistically as *continuously* occurring, as indeed it is for a wide range of organisms.

In the present study, the simulations are used to examine optimal foraging, focusing on central-place vs. nomadic lifestyles, group vs. solitary foraging, the influence of the sensory range of the individuals, and the distribution of food in the environment.

Nomadic foragers are predicted to walk in a ballistic fashion to achieve optimal foraging efficiency except where the food is normally distributed in term of quality and space with respect to the nest. In contrast, central-place foragers are predicted to display characteristics of both Brownian and ballistic motion to achieve optimal foraging in different circumstances. In particular, straighter motion is more efficient when the animal's sensory range is large, multiple individuals simultaneously forage, they are able to gather lot of food and when the quality of food is widely distributed. If walking patterns are selected to reduce the variance (or risk) in foraging efficiency, as well as the average efficiency, more Brownian like movements may be expected in some circumstances.

3.1 Introduction

Foraging is an essential component of animal behaviour, and is fundamental in the study of animal ecology (Begon *et al*. 2006a; Stephens *et al*. 2007; Stephens and Krebs 1987). Foraging strategies determine the amount of food gathered by individuals, and therefore affect their survival and, more generally, their fitness (Morrison 1978). Thus foraging is under selective pressure, and many studies have examined the foraging strategies that many animals employ and the extent to which these strategies appear optimal (Cezilly and Benhamou 1996; Krebs *et al.* 1978; Macarthur and Pianka 1966; Pyke 1984).

An essential characteristic of foraging strategy, in our view significantly understated in the framework of optimal foraging theory (Bovet and Benhamou 1991; Stephens and Krebs 1987), is the nature of the paths that animals actually adopt while foraging. Animal movement is the primary factor determining the rate of encounter between predator and prey, or the rate that grazers encounter food sources (Pyke 1978; Pyke 1981; Zimmerman 1979). Thus the precise walking pattern (e.g. the general rules of movement, not the precise trajectory) of an individual is likely to have been significantly shaped by selective forces.

Some very early studies of this topic introduced the concept of animal movement being a random walk (Pearson 1905a; Pearson 1905b; Rayleigh 1905). More recent work refined this concept to that of the correlated random walk, in which the movement of an individual at a particular time is related to its previous movements. Such walks account for the persistence in movement that is typically observed in animal paths (Bovet and Benhamou 1988; Codling *et al.* 2008; Kareiva and Shigesada 1983; McCulloch and Cain 1989). In modelling animal movements these authors have treated the walks as a sequence of discrete steps that occur at discrete times. Such models are characterised by distributions of time steps, step lengths, and angular changes in the direction of movement (Bovet and Benhamou 1988; Codling *et al.* 2008). The same framework has been used to characterise observed animal paths (Fortin 2003; Fortin *et al.* 2005; Kareiva and Shigesada 1983).

The foraging efficiency of animals with different walking patterns in different situations has been examined in some extent by modelling (Benhamou 1992; Bovet and

Benhamou 1991; Pyke 1978; Pyke 1981) and simulation (Pyke 1978; Williamson 1981; Zimmerman 1979). In the present chapter we present extensive simulations of animal movement, derived from a recently published model of correlated random walks in *continuous* time (Nouvellet *et al*. 2009, see Chapter 2). This model is characterised by just two parameters: a diffusion coefficient and a time scale of correlation. The framework adopted allows extensive simulation of animal paths with different walking patterns in different environments.

In particular, we examine the impacts of the spatial distribution of food and the distribution of food quality on animals having a nomadic (or harvester) lifestyle (Pyke 1978) or a central-place forger lifestyle (Bovet and Benhamou 1991; Hamilton and Watt 1970). We also explore the effects of different sensory ranges, and whether the animals forage alone or with conspecifics. This study is restricted to continuous random walks that are characterised by 'short-tailed' distributions; we do not explore the foraging efficiency of Levy walks/flights, which have been examined in other studies (Bartumeus *et al.* 2005).

3.2 Modelling and Simulating Animal Movement

In this study we carry out extensive numerical simulations of animal movements. We explore the range of behaviours that result from (i) changing a single time-parameter associated with correlations of movement (defined below) and (ii) the impacts of different lifestyles. These explorations are used to compare the efficiency of different strategies for finding food. To successfully model movements in two dimensions, we adopted a model of a correlated random walk in continuous time (Nouvellet *et al.* 2009). The model is the simplest form of a continuous random walk that incorporates persistence in the direction of movement. This model has been shown to capture, remarkably well, the observed behaviour of the foraging behaviour of ants (Nouvellet *et al.* 2009). Here we use it to generate simulated animal paths that are characterised by two parameters: (*i*) a time-scale of correlations in movements, T, and (*ii*) a diffusion coefficient, D ,associated with long time (i.e. long term) diffusive behaviour of a set of organisms.

3.2.1 Important features of the model

An overview of the model used can be found in Chapter 2 (section 2.2), and a more detailed description is found in Appendix A2.1 and A2.3. Of special theoretical interest, Appendix A2.3 shows how a Wiener process can be view as particular case of our model.

Essentially we model the tendency of displacements to change randomly, but with some persistence of direction, with displacement defined as the position of the individual relative to its starting position: $\boldsymbol{R}(t) = (X_t, Y_t)$ with each individual starts from position $\boldsymbol{R}(0) = (X_0, Y_0) = (0,0)$.

We further define a *correlation function* (see Chapter 2) that determines the persistence of movement. This correlation can take a wide range of form and for the purpose of this chapter we define it as:

$$\Delta(t) = \frac{1}{2T} e^{-\frac{|t|}{T}}. \qquad (3.1)$$

This form of the correlation function satisfies the natural assumption that correlations in movement decrease when their time interval of separation is increased. We note the correlation function is symmetric around *t=0*, such that the tendency to move is equally correlated with future and previous moves. Finally it should be noted that the correlation function defined is an autocorrelation, as

Previous analysis (see Chapter 2) showed that such a form for the correlation time leads to very good fit between the mean square displacement and time.

3.2.2 Comparing like with like

Modifying the two parameters characterising the animal paths in our model (namely the diffusion coefficient, *D*, and the time-scale of correlations, T) yields paths with very different qualitative properties. In particular:

- increasing the diffusion coefficient increases the rate of dispersal of the organism.
- increasing the time-scale of correlations increases the straightness of the paths.

Henceforth, a particular *walking pattern* refers to the general features associated with paths resulting from a particular diffusion coefficient and a particular time-scale of correlations.

As well as having different qualitative properties, changes in parameters have also nontrivial implications regarding the *speed* of the organism. For the model presented, the total distance walked up to time t, denoted $M(t)$, varies from animal to animal and hence is a random variable. It is important to distinguish between the total distance walked, $M(t)$, and the displacement, $\boldsymbol{R}(t)$. The total distance walked represents the length of the 'curved path' and thus is proportional to the 'number of steps' walked by an animal, while the displacement is a vector measure of the position reached from the starting point. Thus an animal could have walked a large total distance, but its displacement could be quite small, for example if its path intersected with itself many times.

The total distance walked up to time t, $M(t)$, has an average over many individuals (an expected value) of $E[M(t)]$, which is proportional to time (see Appendix A3.1). Therefore the expected speed, v, of a given walking strategy, is:

$$v = \frac{E[M(t)]}{t} = \sqrt{\frac{\pi\Delta(0)D}{2T}} \tag{3.2}$$

In this work we simulate the paths of individuals with different walking patterns, in order to compare their relative foraging efficiencies. To facilitate the analysis, we only compare bouts of foraging with the same duration and which are constrained to have the same mean speed. Given that the overall duration of a foraging bout is fixed, this means the two sets of simulated paths (i.e., paths with different values of the correlation time, T) will have the same mean length, so we can meaningfully compare them.

By constraining speeds to the same mean value, simulated paths with a specific value of the correlation time have a diffusion coefficient whose value is completely determined. This feature restricts the possible combinations of parameters that need to be considered. In particular, one value of T leads, in our simulations, to a specific value of the diffusion coefficient, D, namely:

$$D = \frac{4T}{\pi} v^2 \qquad (3.3)$$

3.2.3 Simulated walks

We simulated (see Appendix A3.2 for details) n = 1000 paths for each walking pattern. We tested 107 different walking patterns, characterised by 107 different values of T, ranging from T = 0.1 to T = 20. These resulted in 107 values of D, ranging from D = 51 to D = 10,185, that kept the mean speed constant (Equation 3.3). Figure 3.1 illustrates 2 typical examples of these paths and highlights how changing just one parameter affects the qualitative properties of a walk. A small value of T is associated with a thorough search in a small area, while a large value of T is associated with a more extensive search. If time units are considered minutes, then in our simulations, individuals are allowed to forage for 50 minutes and their positions are recorded every 1.5 seconds. The set of (1000 x 107) simulated paths constitute the basis of all our subsequent analyses.

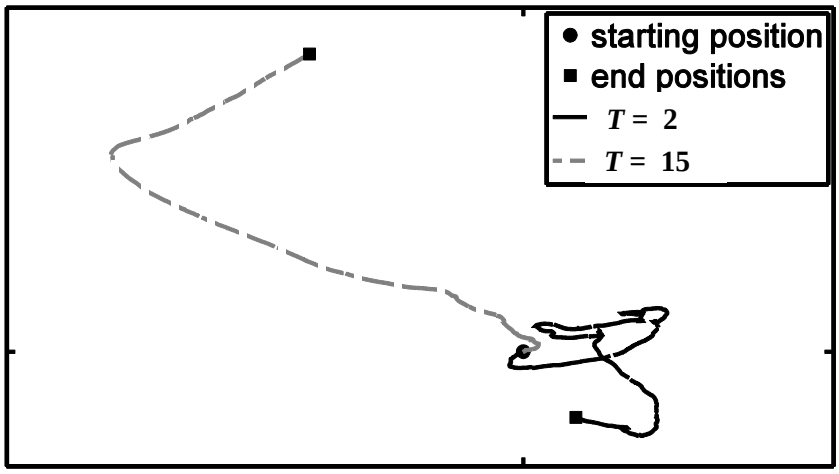

Figure 3.1:

Typical paths of 2 different walking patterns, associated with 2 values of the correlation time, T. As T increases, the 'straightness' of the search paths decreases. When T is very small, the movement is close to Brownian motion. To keep the mean speed constant, an increase of T is associated with an increase in D, resulting in faster rates of diffusion. In the two cases illustrated, T takes the values [2, 15] and the corresponding values of D (that lead to the same mean speed) are $[1018.6\ ; 7639.4]$.

3.3 Assessing the Efficiency of Foraging Strategies

To assess the relative efficiencies at finding food, we compare different walking patterns in various situations. For each walking pattern (i.e. for each value of T), two life-history strategies are considered: (*i*) the animal stays in its final position (the defining property of a *nomadic* strategy) or (*ii*) it returns to its initial home position via a straight path (the defining property of a *central-place* strategy).

Table 3.1 summarises the characteristics of a variety of different cases affecting foraging. In the first row, all characteristics are defined as being the default characteristics, and in subsequent rows, we explore how the efficiency of various walking patterns is affected by the change of one parameter.

Model	Value of T	Regular/random position of food	Sensory range	Number of individual G	Duration of foraging bouts	Distribution of food quality
Default conditions	T takes 107 values between $[0.1; 20]$	Regular	$s = 0.5$	$G = 1$	$t = 50$, with 40 positions per unit-time	Uniform
Case 1	Default	Default	Default	Default	Default	Default
Case 2	Default	Random	Default	Default	Default	Default
Case 3	Default	Default	s takes 10 values between $[0.5; 5]$	Default	Default	Default
Case 4	Default	Default	Default	G takes 9 values between $[5; 100]$	Default	Default
Case 5	Default	Default	Default	Default	Until F_{max} is reached. F_{max} takes 5 values between $[50; 800]$	Default
Case 6	Default	Default	Default	Default	Default	$\mathcal{N}(0; \sigma^2)$, σ^2 takes 7 values between $[10; 1000]$

Table 3.1

A summary of the environmental characteristics and parameters values used in different cases.

3.3.1 Defining foraging efficiency

For the simulations, we assume that each individual forages in an environment containing discrete food items. We define s as the 'sensory range' of the species. It is the maximum distance at which an individual can detect a food item. Each food item that lies within the sensory range, *s*, of the simulated position of an animal will be considered to have been consumed/collected. Each food item can be consumed/collected only once (there is no replacement of food during the foraging bout of one individual), and replacement occurs at the end of a foraging bout.

For the i'th individual with a walking pattern characterised by a correlation time of T, we define the benefit of the walk as '$B_{i,T}$' and this equals the total number of food items consumed/collected during the foraging bout. We further define $M_{i,T}$ as the total distance walked during the foraging period, and $R_{i,T}$ as the absolute displacement (direct distance to the starting position) after the foraging period. The total distance walked and (for central-place foragers) the final displacement are viewed as costs associated with foraging.

Finally we define $P_{i,T}$, the payoff of a particular walking pattern, as the benefit of the foraging bout relative to its energetic cost. The payoff is the rate at which food items are retrieved per unit distance walked. For a nomadic strategy, the payoff is defined as the total amount of food retrieved divided by the distance walked, $M_{i,T}$, during the foraging bout. As each walking pattern is tested using $n = 1000$ individual paths, the expected payoff, $E[P_T]$, given a walking pattern is approximated by the average of the simulated walks:

$$E[P_T] \sim \frac{1}{n} \sum_{i=1}^{n} \frac{B_{i,T}}{M_{i,T}} . \quad (6)$$

For a central-place forager, the benefit of the foraging remains the amount of food retrieved, $B_{i,T}$, but the energetic cost of the bout includes not only the distance walked, $M_{i,T}$, but also the direct distance to return to the initial position, $R_{i,T}$. Again the expected payoff, $E[P_T]$, for a given walking pattern is approximated by an average of the thousand walks simulated for a particular walking pattern:

$$E[P_T] \sim \frac{1}{n} \sum_{i=1}^{n} \frac{B_{i,T}}{M_{i,\tau} + R_{i,T}} . \quad (7)$$

The efficiency of different walking patterns and different life-history strategies (nomadic or central place foraging) can therefore be directly compared.

3.3.2 Influence of the walking pattern on food retrieval in a static environment

In this first case, food items are regularly distributed (see appendix A3.3) and are consumed/retrieved by the walker if they lie within a sensory distance of $s = 0.5$ of all positions visited (see Table 3.1). A single individual is allowed to forage during a bout that lasts a fixed time period, $t = 50$ units of time. For each walking pattern, the expected payoff and the variance of the payoff are estimated from simulations.

Different walking patterns yield different efficiencies of finding food (Figure 3.2). The efficiency of nomadic foragers increases with the value of T (and hence also D). Movement in a straight line ('ballistic movement') would thus appear to be the optimal walking strategy for this kind of life history. Given the same walking pattern, central-place foragers always have a lower efficiency because they have the additional cost of returning to their starting position. Central-place foragers appear to have an optimal walking pattern for an intermediate value of the correlation time. We estimate that for the particular parameters used, the optimal payoff was reached for a correlation time of $T = 1.1$.

The standard deviation in payoff for nomadic foragers appears to reach a minimum when $T = 2.6$, while for central-place foragers a minimal standard deviation in payoff was reached for $T = 0.3$. If a forager weights the outcome of its foraging bouts in term of both its expected payoff but also its variance (a proxy for the risk of encountering no food), it seems likely that a lower value of T might be optimal for both foraging lifestyles.

We note that optimality of the walking pattern could be further investigated by including starvation into our simulations.

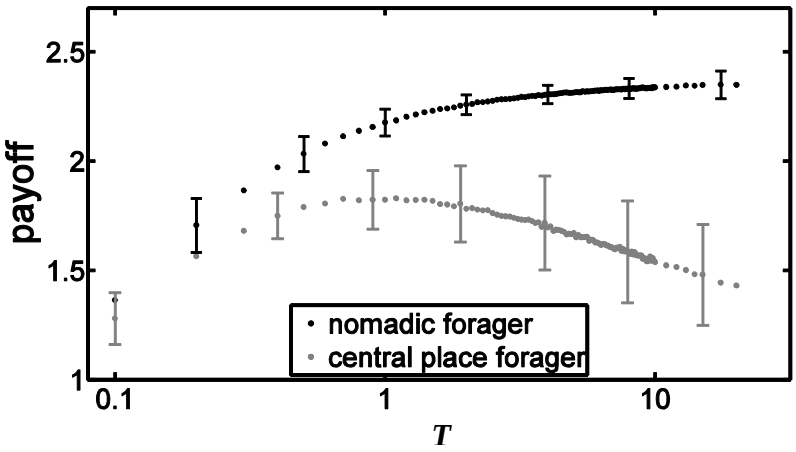

Figure 3.2:

Efficiency of the search strategy, P_T (ratio of number of items found per unit distance walked), as a function of different walking patterns. The payoff values used in the figure are the average payoff of foraging walks of 1000 individuals. Grey dots denote averagedpayoffs for nomadic foragers. Black dots denote payoffs for central-place foragers – this cost includes both the distance walked foraging and the distance to return to the initial position. The latter displays an optimal value of T that maximizes payoff. Error bars indicate the standard deviation in payoff which are calculated from the 1000 simulated walks.

3.3.2 Influence of the walking pattern on food retrieval in a variable environment

An alternative scenario posits an animal making the same walk (literally the same path) each day but the positions of food items change daily, although the mean density of food remains constant. This provides the opportunity to examine optimal foraging in a highly variable environment.

In this second case (Table 3.1), the position for each food item is randomly located in the area covered by the paths previously calculated (see Appendix 3.3). For a given walk, changing the position of food items results in a different payoff; we can thus establish the influence of a variable environment.

While the benefit of a particular walk varies between environments, the distance walked during the foraging bout and the displacement from the initial position remain constant.

Given the same food density as in the previous simulation (Figure 3.2), we observe no differences in the mean payoff from the previous case (Figure 3.3). This set of simulations, however, allows the evaluation of the impact of environmental variation on food retrieval. We observe that more straight line (‘ballistic’) movements, of both nomadic and central-place foragers, lead to decreased variation in payoff due to environmental variability.

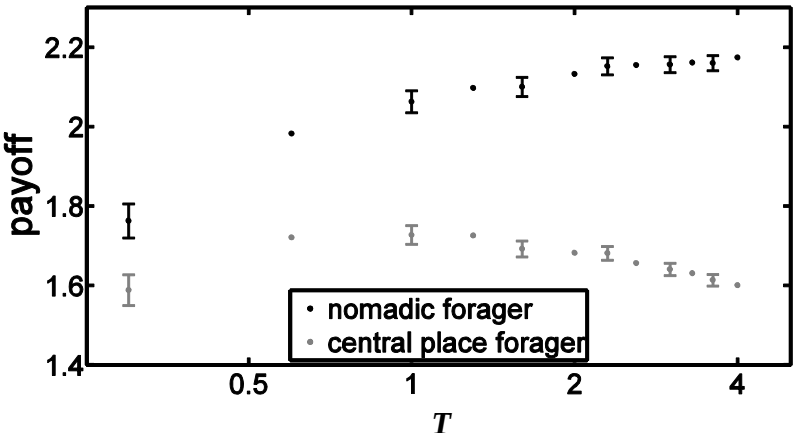

Figure 3.3:

Efficiency of the search strategy, P_T (ratio of number of items found per unit distance walked), with different values of the correlation time, T. The payoff represents an average of 1000 individuals foraging in 500 distinct environments. For a given walking pattern, the mean payoff does not differ from that shown in Figure 3.2, however the variation due to environment (shown by the error bars) decreases as the correlation time increases. For a given walking pattern, mean payoff for each environment was calculated and standard deviation in the average payoff over the 500 environments was calculated to estimate the standard error.

3.3.3 Influence of the sensory range, s, on optimal foraging strategy

To determine how sensory range influences optimal foraging strategy, we modelled a situation in which animals could detect, and thus collect, food from different distances (namely the values of the sensory range, s, which are shown in Table 3.1).

The first value of sensory range, $s = 0.5$, yields exactly the same result as presented in Figure 3.2. As the sensory range increases, the payoff for both nomadic and central-place foraging increases as expected (Figure 3.4). For nomadic foragers, the optimal strategy given any values of the sensory range is straight line ('ballistic') movement (Figure 3.4a). However for central-place foragers, as the sensory range increases, the optimal walking strategy shifts towards higher values for the timescale of correlations, τ (Figure 3.4b). For central-place foragers, the optimal strategy seems to be - the further you sense, the straighter you should walk.

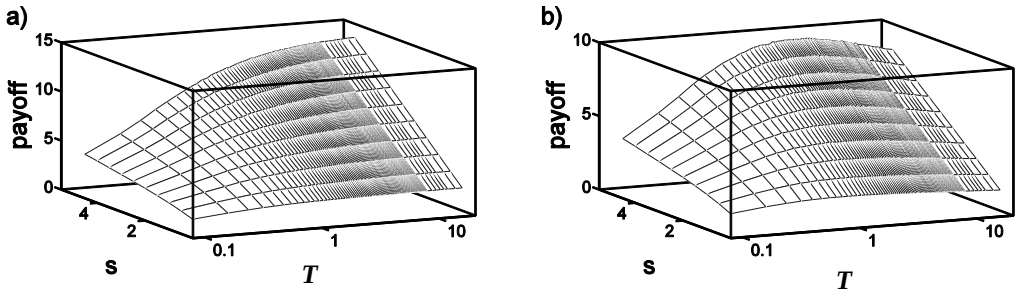

Figure 3.4:

Payoff or efficiency of the search strategy, $E[P_T]$ (ratio of number of items found per unit distance walked), with different values of the correlation time, T, and different values for the sensory range s. Payoff is an average of 1000 individual foraging bouts. Figure a represents payoff for nomadic foraging, while Figure b represents payoff for central-place foraging. For a given sensory range, central-place foraging displays an optimal value of T that maximizes the payoff; the value of T at the optimal payoff increases as the sensory range increases.

3.3.4 Influence of the number of individuals simultaneously foraging on optimal strategy

The natural environment is likely to contain a number of individuals foraging simultaneously. To determine the effects of forager density on optimal foraging, we simulated foraging bouts in which *G* individuals (with *G* ranging from 5 to 100) foraged simultaneously, but without interaction, in an environment in which the food was uniformly distributed. The simulations finished when the G individuals had completed their foraging walks. In this situation, each foraging bout (characterised by a value of T and a value of G) was repeated 1000 times by randomly choosing a different set of G individual walks from the initial simulated walks.

Because the number of items an individual gathers depends on the total number of foraging individuals, we define a *group benefit* rather an *individual benefit*. Specifically, for a group of G individuals that retrieve a total of F food items, the benefit is considered as the shared benefit, e.g. the total amount of food from the group divided by its size: $B = F/G$.

As seen in Figure 3.5, the expected payoff always decreases as the group size increases, reflecting the sharing of benefits. Nomadic foragers, regardless of the group size, should walk in a ballistic way to achieve optimal foraging (Figure 3.5a). In contrast, central-place foragers display the optimal time scale of correlations which increases as the group size increases (Figure 3.5b). In other words, to achieve optimal foraging, each central-place forager should straighten it own walk as the group size increases.

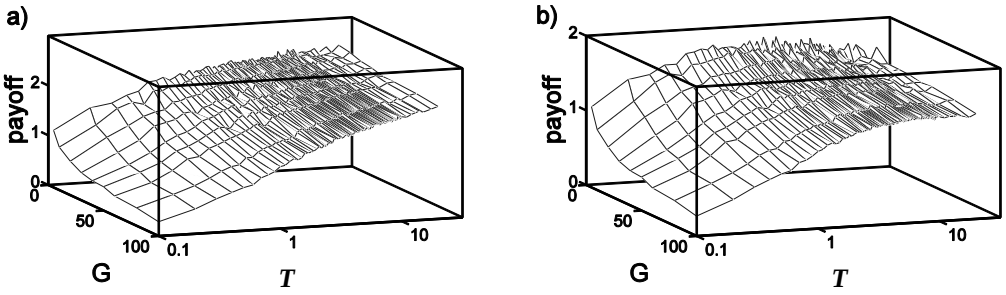

Figure 3.5:

Efficiency of the search strategy, $E[P_{G,T}]$ (number of items found per unit distance walked), with different values of the correlation time, T, and different values of the group size, *G*. The data are an average of 1000 groups of *G* foragers. Figure a shows payoffs for nomadic foraging, while Figure b shows payoffs for central-place foraging. For a given group size, the latter displays an optimal value of the correlation time, T, which maximizes the payoff. Note that the value of T at the optimal payoff increases as the size of the group increases.

3.3.5 Influence of the quantity of food that individuals are allowed to retrieve on an optimal foraging strategy

To examine the effects of restricting the total number of food items that could be gathered on any animal walk (i.e., reflecting limits to the number of food items an animal can carry or ingest), we estimated the payoff for each value of the correlation time, T that was achieved while foraging from 50 to 800 evenly distributed food items. In this case, a foraging bout is considered finished when the individual had gathered a critical number of food items, F_{max} (see Table 3.1). We chose a range of F_{max} which ensures that the walk with the smallest benefit could achieve the values of F_{max}.

No qualitative changes are observed for nomadic foragers (Figure 3.6a); thus their optimal walk remains a ballistic one. For central-place foragers, the greater the number of food items allowed to be gathered, the larger is the optimal time scale of correlations (Figure 3.6b).

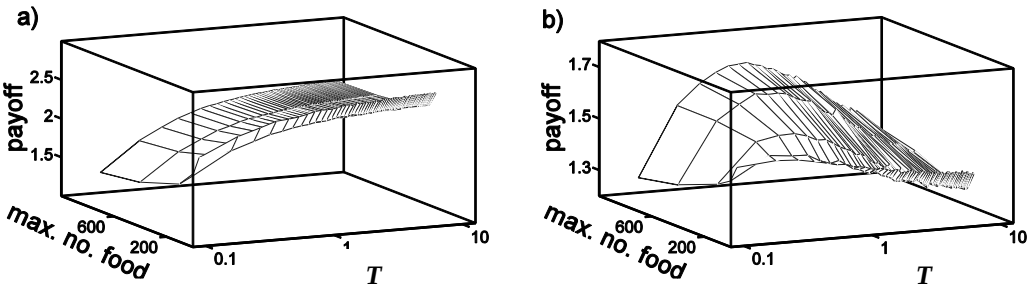

Figure 3.6:

Payoff or efficiency of the search strategy, $E[P_{N,T}]$ (ratio of number of items found per unit distance walked), with different values of the correlation time, T, when a foraging bout stops after the gathering of *N* food items. The payoff represents an average of 1000 simulated walks. Figure a shows the payoff for a nomadic forager, while Figure b represents payoff for a central-place forager. For a given *N*, the latter displays an optimal combination of $[T, D]$ that maximizes the payoff, and the value of T at the optimal payoff increases as the food load *N* increases.

3.3.6 Influence of distribution of food quality on an optimal foraging strategy

Finally, we examined cases where the quality of food item is not uniform; each food item has a value dependent on its distance from the walking start point. The value of each food item follows a normal distribution which, centred at the walk starting point, has a standard deviation of σ (see Appendix 3.3). This is plausible as animals may have previous knowledge/experience about the food distribution they are living in, and elect to live in the centre of the 'patch'. Alternatively, individuals living serendipitously at the centre of the patch will be more successful than those living elsewhere which may die because of lack of resource.

We estimated the payoff for different values of the correlation time, T, with 7 values of σ ranging from 10 to 1000. For small values of σ, an optimal walking pattern that was characterised by small values of T was apparent for both nomadic and central-place foragers (Figure 3.7). As the variance increases the optimal value for the time scale of correlation also increased for both types of foraging. However the increase in T was larger for nomadic foragers (Figure 3.7a) than for central-place foragers (Figure 3.7b).

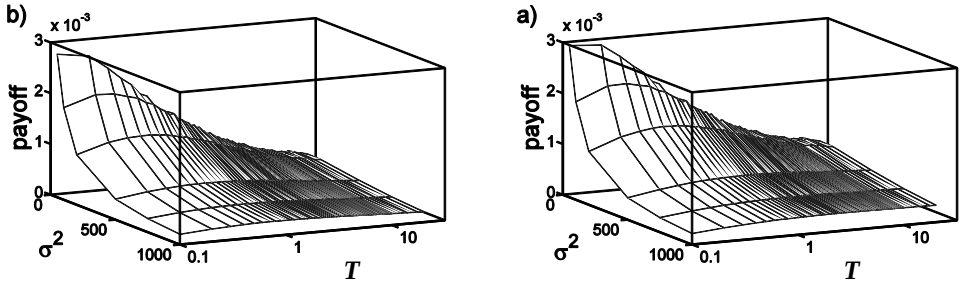

Figure 3.7:

Payoff or efficiency of the search strategy, $E[P_T]$ (ratio of number of food items found per unit distance walked), with different values of the correlation time, T, when food is normally distributed with variance σ^2. The payoff represented is an average of 1000 simulated walks. Figure a shows payoffs for nomadic foragers, while Figure b represents payoffs for central-place foragers. If the food quality is very narrowly distributed around the centre, then both nomadic and central-place foragers have an optimal (small) value of T that maximises the payoff. As food quality becomes more widely distributed, the optimal value of T increase for each forager lifestyle, although it increases more markedly for nomadic foragers.

3.4 Discussion

While describing and comparing foraging strategies, an essential concept is the rate at which an individual finds the resource it searches (Stephens and Krebs 1987). It is clear that this encounter rate depends on the characteristic movements of the individual or species (Benhamou 1992; Bond 1980; Morrison 1978). The fundamental challenge that emerges is the realistic characterisation of animal movements (Kareiva and Shigesada 1983). Previous approaches have been largely influenced by early work on kinesis (Gunn *et al.* 1937), and tend to view movement as a succession of discrete steps of different lengths, and in different directions (Bovet and Benhamou 1988; Kareiva and Shigesada 1983; McCulloch and Cain 1989). These descriptions of movement have been used to characterise observations in real animals as well as to simulate virtual agent movement.

The present chapter develops this theme by simulating trajectories of animal movement using a recently published continuous time based model (Nouvellet *et al.* 2009, see Chapter 2). While this model shows an excellent match between simulated and real ant movements, it also reveals the artificial nature of describing movement via a distribution of angular changes of direction. It was shown that the distribution of changes in direction is highly dependent on the observation time scale, and is completely determined by the relation between a distance statistic (the mean square displacement) and time (Nouvellet *et al.* 2009, see Chapter 2). Of critical importance for the study presented here, the model allows an exact stochastic description of trajectories, and thus provides a more realistic framework for the simulation of animal movement than was hitherto possible. These simulations have allowed us to predict the foraging efficiency of organisms in different situations, the first being the distinction between nomadic and central-place foraging (Hamilton and Watt 1970; Mirenda and Topoff 1980). We found significant differences between the optimal walking patterns for these two lifestyles. Except in the special case when food quality is strongly centred to the animal's initial position, nomadic foragers achieve better efficiency when walking in a ballistic manner, while central-place foragers always achieve optimal foraging for intermediate values of correlation time, which leads to their thorough search patterns. Interestingly the variance associated with the payoff of a walking pattern is minimised for lower than the optimal correlation time. In addition to the mean expected payoff, if

the *predictability* of encountering food of a particular walking pattern is also under selection pressure, then more thorough, convoluted searches might be expected for both nomadic and central-place foragers. In contrast, we note that the variance associated with the stochasticity of the environment would tend to push for larger values of the correlation time. Again, if the predictability of food gathering is under selection, we expect more ballistic searches to be optimal in highly variable environments.

Nomadic foragers are expected to walk ballistically if selected on mean efficiency, regardless of their sensory range, the number of individual simultaneously foraging, or the amount of food they can to gather. Only when food quality is centrally distributed is an intermediate walking pattern (Brownian with some persistence in movement) optimal.

Central place foragers are predicted walk in a more random fashion when their sensory range is low, the number of individual simultaneously foraging is low, when they are limited by the amount of food they can gather, or when the quality of the food is centrally distributed. To our knowledge, using our model of a correlated random walk in *continuous* time, this study is the first to explore such an extensive range of situations under the same framework model and in such deep parameter space.

By using our more realistic model of animal movement and relying on extensive computer simulations, we were able to confirm some earlier predictions of optimal walking patterns (Bovet and Benhamou 1991; Cezilly and Benhamou 1996; Harkness and Maroudas 1985; Mirenda and Topoff 1980; Morrison 1978; Pyke 1978; Pyke 1981; Roese *et al.* 1991; Zimmerman 1979; Zollner and Lima 1999).

In his study food depleted is not replaced between foraging, and to study the influence of food replenishment on foraging strategies was outside the scope of this work (but see Bartumeus *et al.* 2005). We can however predict that if food is replaced during a foraging bout, a smaller distance travelled from the starting position might lead to equivalent food efficiency compared to a no-replacement situation. Thus we can predict that in those situations a central place foraging strategy might become beneficial over a nomadic strategy.

Many studies of optimal foraging have examined the effect of patchy distribution of (food) resource (Dejean and Benhamou 1993; Krebs *et al.* 1974; Macarthur and Pianka 1966; Perry and Pianka 1997; Possingham 1989; Stillman and Sutherland 1990). It is

argued, and experimentally observed, that animals change their walking pattern to achieve optimal foraging in heterogeneous environments (Benhamou 1992; Dejean and Benhamou 1993). Organisms are expected to walk in a convoluted fashion within a high-density food patch and straighter between patches. These conclusions are intuitively related to the study presented here, i.e. considering the patches as single food items the optimal strategy is the same within or between patches but viewed from a higher spatial scale (thus leading to more ballistic motion between patches).

In conclusion, this chapter provides some new insights in the selective pressure associated with different walking patterns. It seems important that, as well as maximising the mean efficiency, reducing the risk associated with a particular strategy (the variance in efficiency of finding food) might be of considerable importance for animals. Also, this study could be further developed but including methods used to risk sensitive studies (McNamara and Houston 1992), where the payoff obtained from foraging is linked by some qualitatively defined function to the fitness of individuals. Finally, given the relatively shallow slopes around the optimal walking pattern found, it is likely that the sensitivity of the efficiency to change in walking pattern is relatively low, leading to multiple walking strategies with very similar foraging efficiencies.

Chapter 4

Testing the Level of Ant Activity Associated with Quorum Sensing; an Empirical Approach Leading to the Establishment and Test of a Null-Model

A slightly modified version of this chapter was accepted for publication in *Journal of Theoretical Biology*. Authors of the submitted paper are listed below:

Pierre Nouvellet, Jonathan Bacon, David Waxman

Abstract

On the basis of experimental observations, this chpater develops two well-defined mathematical models for the level of activity of Pharaoh's ants within their nesting area, with the aim of providing a more general understanding of animal activity. Under specific conditions, we observe that the activity of ants within their nesting area appears to show no dependence on their density. Making the assumption that all ants move independently of one another, this behaviour can be mathematically modelled as a random process based on the binomial distribution. Developing the model on this basis allows an exponential distribution to be exposed that underlies the time-intervals between ants leaving the nesting area. Such a distribution is present, irrespective of whether the ant population in the nesting area remains constant or steadily depletes, and suggests that ant-ant interactions do not play any significant role in determining ant activity under these experimental conditions.

The mathematical framework presented plays the role of a null model that will have a wide range of applications for detecting other determinants of activity-level (not addressed in this study) including environmental and social factors such as food availability, temperature, humidity, presence of pheromone trails, along with intraspecific and interspecific interactions outside the nest, and more generally. The null model should have applications to a range of organisms.

Lastly, we discuss our data in relation to a recent study of ants leaving their nest (Richardson *et al*. 2010) in which the null model was rejected in favour of record dynamics, where ant-ant interactions were conjectured to play a role.

4.1. Introduction

Organisms frequently monitor the density of conspecifics in their immediate vicinity and modify their behaviour appropriately. For example, some bacteria secrete diffusible signals, for which they also express specific receptors, in order to signal and monitor their density. This mechanism was first discovered in the bacterium *Vibrio fischeri*; this species uses this technique to ensure that free-living bacteria, which are at low density in the sea, do not indulge in metabolically expensive luminescence, except when living symbiotically, at high density, in the light organs of some marine fish and squid. This mechanism was first called 'quorum sensing' by Fuqua *et al*. (1994). It has subsequently emerged that bacteria ubiquitously use both intra and inter-species communication to regulate a range of behaviours, notably co-ordinated control of pathogenicity towards their unfortunate host (Miller and Bassler, 2001).

Social insects also exhibit a number of clear examples of behavioural responses to the density of conspecifics. The Argentine ant, *Linepithema humile*, tends to make convoluted exploratory pathways at high ant density, but these become straighter as ant density decreases (Gordon, 1995). This is in broad accordance with the predictions of models of behaviour, based on optimal searching (Adler and Gordon. 1992). The ant *Leptothorax albipennis*, after damage to its nest, sends out ants to find new nesting sites. When the number of ants at a potential new nest site first reaches a threshold value (or density), this triggers a local consensus decision to switch from recruitment by tandem running, to the speedier mechanism of carrying ants (and brood) from the old nest to the newly chosen site (Pratt et. al., 2002). Scout bees from a swarm of *Apis mellifera* investigate potential new nest sites and, on returning to the swarm, communicate the quality of the new nest site by the vigour and duration of their waggle dances. The better sites therefore recruit more bees. Once a quorum of about 15 bees is established at a potential new site, those bees returning to the swarm perform a piping behaviour to prime the entire swarm for flight to the new site (Seeley *et al*., 2006; Visscher and Seeley, 2007).

Given these well documented cases, not least in ants, where the behaviour of organisms depends on their density, we have investigated whether there is any evidence that the

density of Pharaoh's ants, *Monomarium pharaonis*, within a nest, has any significant influence on their level of activity.

Our investigations, based on two different types of experiment, test whether there is an analogue of quorum sensing in Pharaoh's ants. In one experiment, we measured the times at which ants left their nesting area, when taking a specific foraging route, and were allowed to return to their nesting area. As a consequence, the mean ant density within the nesting area remained constant throughout the experiment. This rate of leaving was compared directly to a situation in which the ants were strictly prevented from returning to their nesting area after taking the foraging route, in which case the mean density of ants progressively decreased over time. As we shall argue, the measured rate at which ants leave their nesting area is a measure of their level of activity. Given this, our measurements probe the degree to which the level of activity of the ants is affected by their density.

To explore these issues in detail, we also formulated mathematical models. Rather than using models with deterministic rules for the behaviour of each ant, we constructed and tested two null statistical models, in which individual ants move randomly and *independently* of one another. These models yield results that show remarkable similarity to our direct behavioural observations. We conclude that under the experimental conditions we established, Pharaoh's ants move with a level of activity that is, to very high accuracy, independent of the number of other ants encountered in the nesting area. That is, they make decisions to move as independent agents without any hint of behavioural change associated with the density of ants.

The simple experimental methodology and null-model mathematical framework we present here provide a solid foundation for further investigations that can precisely determine the influence of controllable environmental and social perturbations on the activity of ants and other organisms. Examples of such perturbations include changes of food supply, temperature, humidity, along with intraspecific and interspecific interactions outside the nest. We finally note and discuss a recent study of ants leaving their nest (Richardson *et al*., 2010) in which data appear best fitted by more complex mathematics – a model of ants exiting that involves *record-dynamics*, implying some kind of ant-ant interactions.

4.2. Ant Activity: an Experimental Approach

4.2.1 Experimental set-up

We used the Pharaoh's ant, *Monomorium pharaonis*, in our experiments. Pharaoh's ants are a well-studied, highly invasive, unicolonial species (Sudd, 1960; Fourcassie *et al*., 1994) in which a number of seminal aspects of self-organising foraging behaviour has been elucidated (e.g. Jackson *et al*., 2004). The ants were kept at a constant temperature of 25°C and constant level of humidity of 40%, and deprived of sugar for a period of two days prior to an experiment. During an experiment, the ants were able to leave their nesting area (i.e., the brood chamber and its immediate vicinity), via a bridge. Application of a coating of fluon (*fluon* PTFE, *Blades biological*) to the far end of the bridge, which was vertical, caused all ants walking on the coated region of the bridge to fall from the bridge.

In one experiment, the far end of the bridge was located within the nesting area, so that all ants falling off the bridge re-entered the nesting area (see Figure 4.1). We call this 'leaving with replacement'. We observed that after falling, the ants carried out a range of different behaviours, and there was no evidence of the ants learning to repeatedly use the bridge.

In the second experiment, the far end of the bridge was located above a container that was physically inaccessible from the nesting area. Ants falling into this container were unable to return to the nesting area during the course of an experiment (see Figure 4.1). We refer to this as 'leaving without replacement'.

The times at which ants fell were recorded for experiments 'with replacement' and 'without replacement'; both types of experiments were repeated for 4 different colonies of Pharaoh's ants. Below we illustrate our findings with results and figures from (i) a single experiment 'with replacement' and (ii) a single experiment 'without replacement.' In Appendix A4.1 we present summary statistics for the experiments carried out on the different colonies. The quantitative results differ between colonies, due to differences in uncontrollable aspects, such as the precise colony size. However, for a given experimental setup, the general conclusions, that we report, hold for all experiments of that type that were carried out.

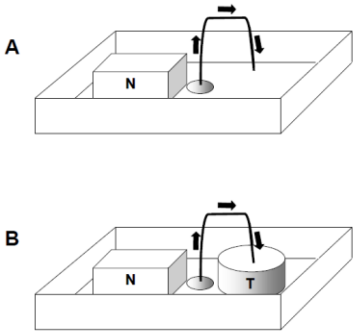

Figure 4.1

Apparatus used to determine the rate that ants leave the nesting area. A). Ants were able to climb the wire bridge (thick line) in the direction of arrows. On encountering the fluon covered vertical far end of the bridge, ants fell to the ground and hence directly returned to the nesting area in which the nest (N) was situated. B) Ants walking along the bridge in the direction marked by the arrows fell into the trap (T) which had fluon coated walls; the ants were therefore unable to return to the nesting area during the period of the experiment. Rates of falling from the far end of the bridge were used as the proxy for ants leaving the nesting area in both experiments.

All of the statistical analysis presented in this work was performed using the software package MATLAB (The Mathworks).

4.3 Results

4.3.1 Ants falling with replacement

When the number of ants that have left the nesting area 'with replacement' is plotted against time, it is found to closely correspond to a linear change (Figure 4.2).

The distribution of *time-intervals* between adjacent ants leaving the nesting area (Figure 4.3) has the appearance of an exponential distribution.

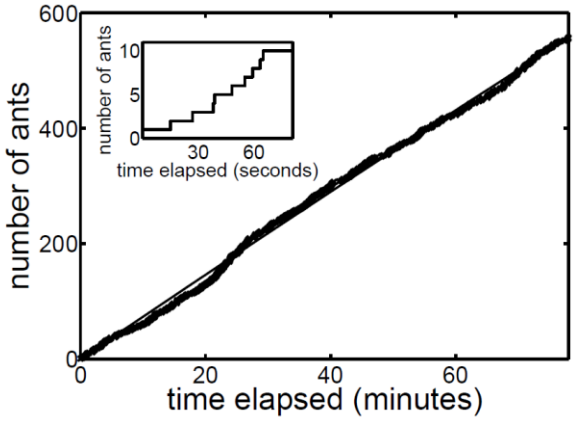

Figure 4.2

A plot illustrating the cumulative number of ants (shown as a thick black line comprising individual data points) that have left the nesting area 'with replacement', as a function of time. The thin straight line was derived from linear regression. In this particular experiment, on average, 0.12 ants were leaving/second. The rate of activity, as characterised by the rate of leaving, did not appreciably change with either the time that had elapsed since the start of the experiment or the number of ants that had left the nesting area. A visual estimate indicated that approximately 300 ants were in the nesting area. Thus some ants must have left the nesting area at least twice during the experiment. The inset is a 'zoom' of the first 80 seconds of the main figure, to show the actual discrete unit changes in number. The horizontal lines in the inset figure represent the time-intervals between adjacent ants leaving.

We cannot directly use a Kolmogorov-Smirnov test (Hogg and Tanis, 2006) to determine whether this distribution is genuinely exponential since the distribution contains a parameter (the inverse of the mean time-interval) which would need to be estimated from the data (Lilliefors, 1969; Broom *et al*., 2007). Instead, we used an Anderson-Darling test (Anderson and Darling, 1952; see also Kvam and Vidakovic, 2007) to determine whether the distribution of time-intervals follows an exponential distribution. The test revealed that there was no significant difference ($p = 0.113$) between the observations ($N = 585$) and an exponential distribution, and led to a value of a mean time-interval between ants leaving the nesting area of 8.283 seconds (see Table 4.1).

A plot of the time-intervals produced during the entire course of an experiment (Figure 4.4) strongly suggests that the distribution of time-intervals is independent of the time elapsed since the start of the experiment; linear regression of time-interval against time elapsed from the start of the experiment confirmed the absence of significant trend ($N = 585$, $p = 0.56$).

The simplest interpretation of these data is that the ants move independently within the nesting area, without any aggregation (Parrish and Edelstein-Keshet, 1999, Ame *et al*., 2004, Jeanson *et al*., 2005, Lauzon-Guay *et al*., 2008) or recruitment behaviour (Wilson, 1962), and some ants randomly encounter the bridge and use it to leave the nesting area. The mean rate with which ants fall from the bridge has, we assume, contributions from both the geometry of the problem (the larger the diameter of the wire, constituting the bridge, the larger the probability of encountering it) and the level of activity of the ants (the more active or fast-moving the ants, the greater the chance they have of encountering the bridge). Under a fixed experimental geometry, the mean rate with which ants leave the nesting area is used in the present work as a measure of ‘ant activity’.

The results obtained for ants leaving their nesting area ‘with replacement’ indicate that their activity remained essentially constant during the entire duration of the experiment. Furthermore, a linear increase over time of the mean number of ants leaving the nesting area and an exponential distribution of time-intervals between adjacent ants indicates that the ants leave the nesting area as a Poisson process (see e.g., Haigh, 2002).

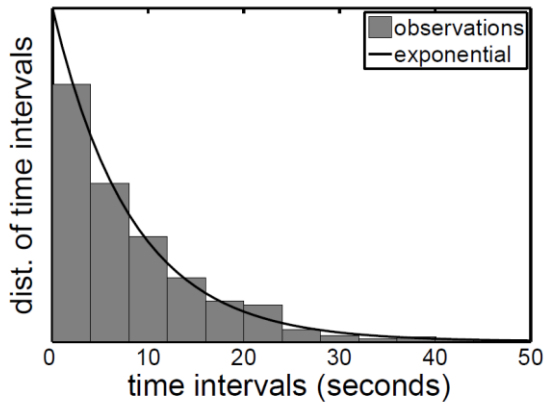

Figure 4.3

A plot, for a single experiment, which illustrates the distribution of time-intervals between consecutive ants leaving the nesting area, under the scenario "leaving with replacement". This distribution is found not to be significantly different from an exponential distribution (solid curve), using an Anderson-Darling test (see Table 4.1). The graph is consistent with ants moving independently of each other and undergoing a stochastic process (a Poisson process) that is "memory-less" (Hogg an Tanis, 2006).

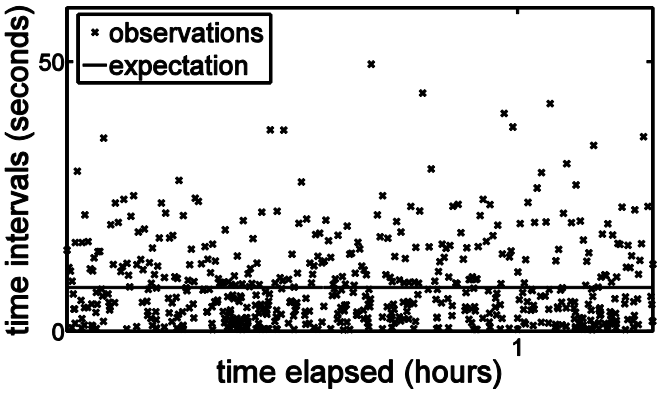

Figure 4.4

A plot, for a single experiment, which illustrates the distribution of time-intervals between consecutive ants leaving the nesting area, under the scenario "leaving with replacement". This distribution is found not to be significantly different from an exponential distribution (solid curve), using an Anderson-Darling test (see Table 4.1). The graph is consistent with ants moving independently of each other and undergoing a stochastic process (a Poisson process) that is "memory-less" (Hogg an Tanis, 2006).

	Test	outcome	AD-statistic	KS-statistic	P-value
replacement	Exponential	Accepted	1.02	-	0.113
No replacement	Exponential	Rejected	9.8	-	<0.001
	Underlying exponential shape	Accepted	-	0.058	0.35
	Exponential with shifting parameter according to Equation 4.8	Accepted	-	0.025	0.92

Table 4.1

In Table 4.1, we test the exponential nature of the distribution of time-intervals between ants leaving their nesting area. In the top row, the exponential nature of the distribution, when replacement is allowed, is confirmed. The following rows show the distribution of time-intervals when replacement is not allowed. First, the "raw" distribution of time-intervals is shown not to be exponentially distributed. Then using a different method (Broom et. al., 2007), we find evidence for the underlying exponential shape of the distribution, but with a parameter that slowly changes with time. Our model for this predicts a changing parameter, and furthermore, predicts the nature of the change. We transform the time-intervals, by rescaling them by their expected value, and the resulting distribution was predicted to be exponential with a parameter of unity. We tested this using a Kolmogorov-Smirnov test (final row).

4.3.2 Ants falling without replacement

When ants left their nesting area 'without replacement,' the number falling from the bridge per unit time decreased as the number of ants in the nesting area decreased. This is apparent in Figure 4.5, in which the cumulative number of ants that had left the nesting area is plotted against the time elapsed since the start of the experiment.

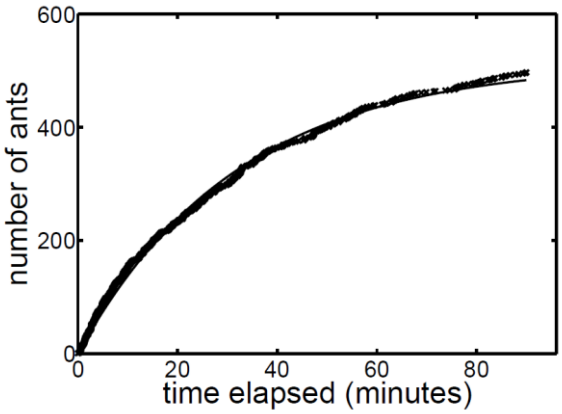

Figure 4.5

A plot of the cumulative number of ants that fell as a function of time. Ants fell into a new area and were not allowed to return to their nesting area, hence this is a "without replacement" experiment. Initially, there were an average of 0.21 ants leaving/second, but this rate of exploration decreased over the course of the experiment, as the number of ants within the nesting area decreased. The solid curve, derived from the mathematical model (see Eq. 4.6), represents the expected cumulative number of fallen ants.

A decrease in the rate of ants leaving the nesting area over time is expected if their level of activity remains independent of the density of ants in the nesting area, since as time proceeds there are fewer ants within the nesting area, and hence fewer likely to encounter the bridge. The question is whether the observed decrease in the rate of leaving is *fully explained* by simply a reduction in the number of ants, or whether the level of the ants' activity is modulated beyond this - due to the decreasing *density* of the

ants. We address this question later on, when we mathematically formulate a null model of the problem.

In experiments where ants leave their nesting area without replacement, we have verified that the distribution of time-intervals between consecutive ants leaving (Figure 4.6) deviates significantly from an exponential distribution. Results of an Anderson-Darling test for one particular experiment, given in Table 4.1, illustrate this ($N = 496$, $p < 0.001$).

However, we hypothesised that the distribution is fundamentally exponential in character, but the parameter characterising the distribution (the inverse of the mean time-interval) is a function of the time elapsed since the start of the experiment, and hence changes during the course of an experiment. The lengthening time distribution, as a function of elapsed time, is clearly shown in Figure 4.7.

To investigate this hypothesis, we employed a statistical approach that tests only the underlying shape of the distribution, and is insensitive to time-dependence of the parameter in the distribution (Broom et. al., 2007). This test uses the ratio of adjacent time-intervals, and this transformation of the data yields a new probability distribution which is independent of the parameter of the original distribution. We found no evidence to reject an underlying exponential *shape* of the distribution (Table 4.1, $N = 496$, $p = 0.35$). As a consequence, the overall distribution of time-intervals can be well-characterised as an exponential distribution, but with a parameter whose value depends on the time elapsed since the start of the experiment, and which changes during the course of an experiment.

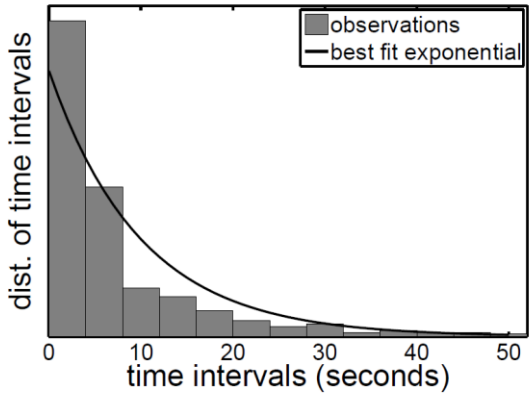

Figure 4.6

Distribution of time-intervals between ants leaving 'without replacement'. The solid curve is the best-fit exponential distribution (by fitting the distribution from the data). It is apparent that the data (histogram) deviates from the exponential distribution and an Anderson-Darling test (Table 4.1) confirms that this difference is statistically significant.

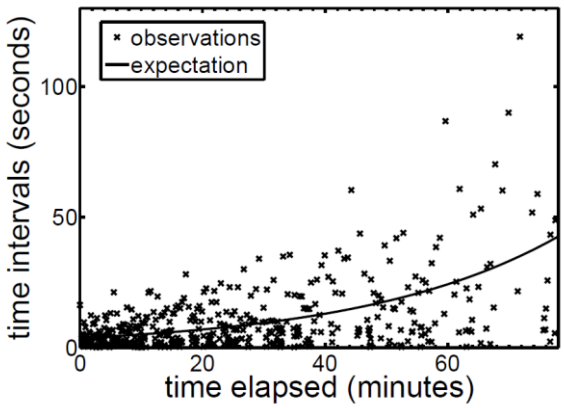

Figure 4.7

A plot, in a single "without replacement" experiment, of the time-intervals of consecutive ants leaving as a function of the time elapsed since the start of the experiment. The time-intervals clearly increase during the course of the experiment - as the number of ants remaining in the nesting area decreases. The values for the expected mean time-intervals (curved line) were derived from the mathematical model (see Eq. 4.8)

4.4 Conclusions from the Experimental Approach

In the first experiment, where replacement is allowed, the ants appear to display behaviour that is consistent with them moving independently of one another with a behaviour characterised by (i) a mean rate of leaving that does not change during the course of an experiment and (ii) with an exponential distribution of time-intervals between adjacent ants leaving the nesting area. While (ii) implies (i), we note that *any* stationary distribution of time-intervals would, by definition, lead to a constant value of the mean time-interval. The exponential distribution obtained shows that, under these experimental conditions, the way the ants leave the nesting area is a memoryless stochastic process (i.e., a random process where past events have no impact on the present; see e.g., Hogg and Tanis, 2006).

In the second experiment where ants leave their nesting area without being replaced, the ants' rate of leaving decreased with time, as the number of ants in the nesting area also decreased. While this might be consistent with some level of communication or collective behaviour, e.g., ants being less active as they 'sense' that the ant density within the nesting area decreases, the exponential nature of the distribution of time-intervals that arises (albeit with a time-dependent parameter) suggests that a random, memoryless stochastic process also underlies the observations in this second experiment.

In the next section, we construct formal models for the problem, and derive expressions for (i) the rate of ant departure from the nesting area and (ii) the distribution of time-intervals, and proceed to fit these model predictions to the data and compare the level of agreement.

4.5 Stochastic Process Underlying Ant Exploration

We present idealised models of the above experiments which allow a complete mathematical description of the outcomes (details are given in Appendix A4.2). In the models, individual ants are assumed to move independently of one another within the nesting area (as they appear to do so outside a nest; see Nouvellet et. al., 2009).

In the experiments, ants left the nesting area if they encountered the bridge, climbed it and then fell off. To express all of this in a succinct way, we shall describe the ants as 'leaving' the nesting area via an 'exit.' We shall explore two models associated with two different exiting scenarios:

(i) Ants randomly leave the nesting area by the exit, but are then immediately returned to the nesting area. This is 'leaving with replacement'.

(ii) Ants randomly leave the nesting area by the exit, but are prevented from returning. This is 'leaving without replacement'.

We shall establish a statistical description of the two different scenarios to predict how the number of ants leaving their nesting area changes with time, under the null assumption that ant activity does not change, irrespective of whether the ants are replaced or prevented from returning to the nesting area.

To describe the problem, it helps to think of time as occurring in a discrete set of steps; the discrete step-size could have a genuine reality, such as the smallest time-interval that can be resolved in an experiment. We initially formulate the problem in this way (Appendix A4.2) but do not pursue the implications of discrete time-steps in this work (although this may have applications elsewhere). Thus all results presented below hold when the time-step size is vanishingly small (i.e., when time is continuous).

Two parameters characterise the problem:

n = the number of ants initially present in the nesting area (4.1)

r = the probability of any individual ant leaving the nesting area per unit time (4.2)

(r is assumed the same for every ant).

The probability of an individual ant leaving per unit time, r, encapsulates both the geometry of the problem, and also the level of ant activity. In principle, r need not be a constant, but could depend on quantities such as the corpulence of the ants (Robinson *et al*., 2009) or their density. For the mathematical analysis we present, we shall assume r is a constant, corresponding to a constant level of activity, and shall investigate the degree to which the data is compatible with this assumption.

The number of ants leaving during a time-step is the outcome of random sampling, where every ant in the nesting area has an equal probability, *r*, of finding and using the exit.

When leaving occurs with replacement, the number of ants that have exited by a time *t* from the start of the experiment, $N(t)$, is found to be a random variable with a Poisson distribution with parameter *nrt* (see Appendix A4.2 for details). Thus with $P(k,t)$ the probability that *k* ants have exited by time *t* since the start of the experiment, we have

$$P(k,t|\text{with replacement}) = (nrt)^k e^{-nrt}/k! \qquad (4.3)$$

where *k* = 0, 1, 2, ..., and *k* can be arbitrarily large.

When replacement is prevented, the number of ants that are present in the nesting area decreases with time. Thus if, by time *t*, a total of $N(t)$ ants have exited then $n - N(t)$ ants remain in the nesting area and the random sampling, which determines which ants leave the nesting area, leads to $n - N(t)$ having a binomial distribution with parameters n and e^{-rt} (see Appendix A4.2 for details). The form of the probability parameter e^{-rt}, that occurs in the Binomial distribution, yields the intuitively plausible result that the probability of an ant remaining in the nesting area decreases exponentially with time.

Given the distribution of the number of ants remaining in the nesting area, it directly follows that the number of ants that have left by time *t*, namely $N(t)$, which is *the* observable quantity in these experiments, has a binomial distribution with parameters n and $1 - e^{-rt}$.

The probability that *k* ants have left without replacement by a time *t* since the start of the experiment is shown in Appendix A4.2 to be given by

$$P(k,t|\text{without replacement}) = \binom{n}{k}(1 - e^{-rt})^k e^{-(n-k)rt}\,. \qquad (4.4)$$

Here $\binom{n}{k}$ is a binomial coefficient, and *k* = 0, 1, 2, ..., *n*, hence *k* has a largest value equal to the total number of ants in the colony.

The models presented here rely heavily on the assumption of independence of movement of different ants *within* the nesting area (hence the validity of binomial sampling and the constancy of *r*). In particular, it is assumed that the departure of one ant does not statistically influence other ants to leave. Thus the models presented are equivalent to a particular null hypothesis, namely independence of movement within the nesting area and random exiting. If there are significant differences between the predictions of the models and the observations then it will be an indication of non-independence of the movements of the real ants.

Having characterised the process of ants leaving their nesting area, it is possible to derive how the expected number of ants that have left the nesting area depends on the time, *t*, that has passed since the start of the experiment. When replacement is allowed, it is a standard property of the Poisson distribution of Eq. (3) that the expected number of ants that have left is

$$E[N(t)|\text{with replacement}] = nrt \tag{4.5}$$

(see e.g., Haigh 2002).

In a similar way, it follows from Eq. (4.4) that when replacement is not allowed, the expected number of ants that have left is given by

$$E[N(t)|\text{without replacement}] = n(1 - e^{-rt}). \tag{4.6}$$

When rt is small ($rt \ll 1$) Eqs. (4.5) and (4.6) yield similar results but when rt becomes large compared with unity the two results become quite different. In particular, the result of Eq. (4.5) can reach any size, whereas that of Eq. (4.6) can only reach a maximum of *n* because there are only a total of *n* ants in the nesting area.

Finally given the processes of departure from the nesting area - described above - the distribution of time-intervals between two individual ants leaving, written $\varphi(\Delta t)$, can also be inferred (see Appendix A4.2).

With replacement, the distribution of time-intervals follows an exponential distribution:

$$\varphi(\Delta t|\text{with replacement}) = nre^{-nr\Delta t}. \tag{4.7}$$

Without replacement, the distribution of time-intervals follows an exponential distribution, with a time-dependent parameter:

$$\varphi(\Delta t, t|\text{without replacement}) = \lambda(t)e^{-\lambda(t)\Delta \text{t}} \qquad (4.8)$$

where

$$\lambda(t) = nre^{-rt}. \qquad (4.9)$$

Thus without replacement, the observed time-intervals are drawn from an exponential distribution that *depends on the actual time of observation*. For example, the probability of observing a time-interval larger than 1 second, at the start of an experiment, will be different to the probability of observing a time-interval larger than 1 second at 60 minutes into the experiment. However, this dependence of the distribution on the time of observation can, by a simple time-dependent rescaling of observed time-intervals, be removed. The procedure is to divide a time-interval that is observed at time *t*, written $\Delta\text{t}(t)$, by its expected value (written $E[\Delta\text{t(t)}]$ and equal to $1/\lambda(t)$) at this particular time. We thus define the rescaled time-interval, $R = \Delta\text{t}(t)/E[\Delta\text{t(t)}]$ and this can be verified to have an exponential distribution, similar to that of Eq. (4.8), but with a parameter that is not of the form of $\lambda(t)$ of Eq. (4.9), but rather with a parameter that has the time-independent value of unity.

4.6 Contrasting Data with the Predictions of the Models

Given the data and the null-models proposed above, we now re-analyse the data to estimate the parameter-values of the models and compare the level of agreement between models and data.

4.6.1 With replacement

When ants fell with replacement, the model for this case predicts that they leave the nesting area at a constant mean rate that follows from Eq. (4.5): $E[N(t)] = nrt$. Linear

regression yielded the thin straight line in Figure 4.2 with $nr = 0.12$ (N = 585, p<0.001, R^2 = 0.997). In this situation it is not possible to obtain separate estimates of n and r; only the product of the two can be estimated, representing the number of individuals falling per second (and thus depending on both the size of the colony and the level of activity of the ants). The observed time-intervals between individual ants leaving thus appear to be drawn from a distribution that is indistinguishable from an exponential distribution (solid line in Figure 4.3, Table 4.1). The mean time-interval between individual ants leaving appears uncorrelated with time (Figure 4.4, straight line). We observe a very close agreement in the estimation of nr using either (i) the number of ants that have left as a function of time: $nr = 0.12$ (via linear regression) or (ii) from the distribution of time-intervals: $nr = 0.12$.

4.4.2 Without replacement

When ants left without replacement, the expected number of ants that had left and the observed number (as a function of elapsed time), showed a high level of agreement (Figure 4.5), and allowed us to estimate that there were initially n = 515 (95% CI [511, 518]) ants present in the nesting area, and the probability of any ant leaving, per second, was found to be $r = 5.2 \times 10^{-4}$ second^{-1} (95% CI [5.1×10^{-4}, 5.3×10^{-4}]). Additionally, the underlying distribution of time-intervals was predicted to be an exponential distribution with a time-dependent parameter. From the data, the exponential nature of the underlying distribution was demonstrated (Table 4.1). The time-dependence in the parameter of the distribution is illustrated by the curved line in Figure 4.7.

Finally, given a distribution with an underlying form that is exponential, but with a time-dependent parameter, the scaling of each observed time-interval by its expected value leads to a new random variable, R, that has a distribution that is predicted to be exponential, with a parameter of unity. Figure 4.8 shows the distribution of time-intervals, when scaled by their expected values.

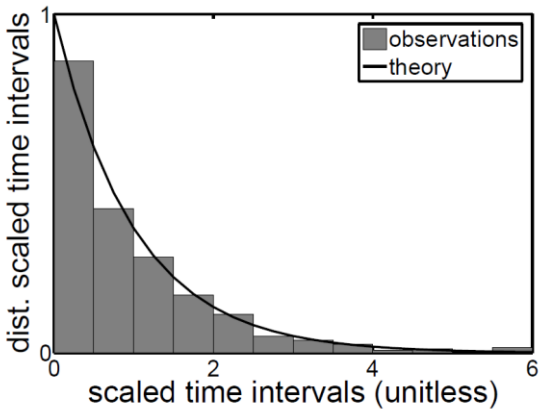

Figure 4.8

Distribution of time-intervals between ants leaving without replacement. Each time-interval has been scaled by its expected value (given by $1/\lambda(t)$ of Eq. (4.8)). The model for this predicts that such scaled time-intervals are drawn from an exponential distribution with an expected value of the scaled time-interval of unity. The distribution of the scaled values is not statistically and significantly different from an exponential distribution, as confirmed by a Kolmogorov-Smirnov test (Table 4.1).

The scaled time-interval values, i.e., R cannot be distinguished from exponentially distributed values (solid line Figure 4.8, Table 4.1) using a Kolmogorov-Smirnov test. We note that ants continue to behave in this statistically predictable fashion, despite their density decreasing to approximately 10% of its starting value during the course of an experiment.

4.7 Event Based Analysis

So far the analysis presented has been in terms of the relation between ants leaving a nesting area and the time elapsed since the start of an experiment. In Appendix A4.2 we show that direct predictions of the models, resulting from focussing on ‘events’, i.e., the dropping of individual ants without regard to the time they occurred, are the following:

(i) In the case of 'leaving with replacement,' where Δt_j is the random time-interval to the next ant dropping after the j'th event (the j'th ant dropping), the quantity $U_j = \exp(-nr\Delta T_j)$ is predicted to be a random number that is drawn from a uniform distribution on the interval 0 to 1. This property follows from the ΔT_j being predicted to be exponentially distributed.

(ii) In the case of leaving without replacement, the quantity $V_j = \exp(-(n-j)r\Delta t_j)$ associated with the j'th event is also a random number that is drawn from a uniform distribution on the interval 0 to 1.

The set of 'event'-based quantities U_j and V_j from experiments with and without replacement is shown in Figure 4.9.

The quality of the uniform distributions obtained provides further evidence of a Poisson process-like stochasticity underlying ants leaving their nesting area. Statistically, a Kolmogorov-Smirnov test (test statistic K) indicates that there is no significant deviation of the distribution of the U_j and V_j from a uniform distribution (for the U's: $K \approx 0.04$ giving $p \approx 0.37$; for the V's: $K \approx 0.02$ giving $p \approx 0.95$).

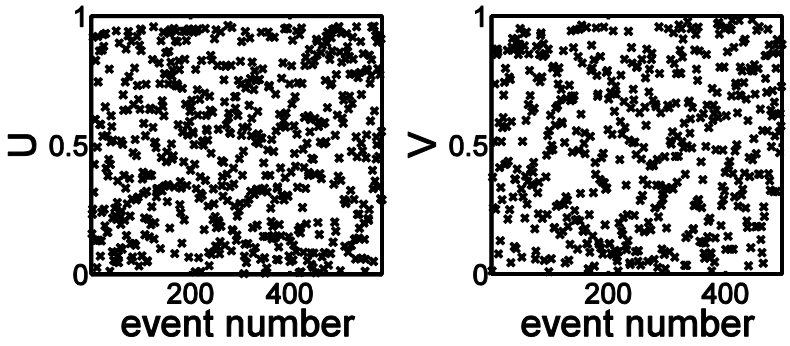

Figure 4.9

Transformed time-intervals for the ant escape with replacement, *U*, and for no-replacement, *V*, are plotted against event number. If the predictions of the models were exact, *U* and *V* would be drawn from uniform distributions over the range 0 to 1. The distributions of *U* and *V* are found to not be significantly different from uniform distributions using a Kolmogorov-Smirnov.

4.8 Comparing our Model with a log Poisson Process

Our findings are quite different from a recent study by Richardson at al. (2010) on the ant *Temnothorax albipennis.* By RFID tagging ants in each colony, these authors were able to examine the timing of ants leaving the nest when not allowed to return (so directly comparable to our non-replacement experiment) and the case in which ants were allowed to return but only those ants leaving the nests for the first time were recorded. They claim their data were better modelled by *record dynamics* (a Poisson process in logarithmic time, suggesting strong interactions between the components of the system – i.e., the ants) rather than a null model of exponential decay (Poisson statistics in linear time, where components of the system act independently).

A detailed comparison of the log Poisson process and our model is presented in Appendix A4.3. In this section we merely discuss the main findings of this Appendix and propose an objective way by which future studies could distinguish between the two processes.

The defining property of a log Poisson process is that the difference of the logarithm of the time of adjacent events is exponentially distributed. This leads us, under a reasonable approximation, to conclude that in a log Poisson process, the time intervals are exponentially distributed and the mean time interval, between adjacent events, increases linearly with time (see Appendix A4.3). This can be contrasted with our study in which time intervals are also time dependent and exponentially distributed, but the mean time intervals increase exponentially with time. Thus while there is similar qualitative behaviour of the mean time interval of both models, there is a genuinely quantitative difference.

For future research on similar system, we propose the following steps:

1. Observe the fit in a plot of the number of individuals that leave, against time, with the expectations from each model. To obtain the expectation from our model, one would need to use a non-linear fit of the data to Equation 4.6 of our model (thus obtaining estimates of r and n). For a log Poisson process (see Appendix A4.3), one would need to fit the data to $E[t_k] = (1-c)^{-k} \approx \exp(ck)$ (i.e., estimate the value of c when k is the number of individuals that had left).
2.
    a. Observe and test nature of the distribution of the time intervals divided by their expected value, $R = \Delta t(t)/E[\Delta t(t)] = \Delta t(t)\, nre^{-rt}$, using a Kolmogorov-Smirnov test. Under our model, the distribution is expected to be exponential with a parameter that has the time-independent value of unity.
    b. Observe and test nature of the distribution of the time intervals in log time, $\ln(t_{k+1}) - \ln(t_k)$, using an Anderson-Darling test. Under a log Poisson process, this distribution is expected to be exponential.

If after performing these tests, neither process better fits the data, Occam's razor would dictate that our model should be adopted because it is more parsimonious. Indeed using an analogy to a physical system, Richardson *et al*. (2010) argue that a log Poisson process reflects underlying interactions between individuals while our model does not make such an assumption. Furthermore, we add that our model is derived from a concrete mathematical description of the process (leading to biologically interpretable parameters) rather than an analogy to a physical phenomenon.

4.9 Discussion

In this work, we have made observations of animal activity, and modelled this phenomenon from basic principles. Specifically, we have focussed on the rate at which individual Pharaoh's ants (*Monomorium pharaonis*) leave their nesting area. We have found a high level of agreement between observations and two null models presented here, which assume both independence of ant movement and random departure of ants from the nesting area. Our observations, within the context of the models, have allowed us to produce an estimate of the size of a colony and consistent estimates of the value of the parameter linked with the activity-level of the study organisms.

The models presented here treats the dynamics of ants leaving their nesting area as being the outcome of a set of independent 'decisions', where the 'choice' of one ant to leave does not affect other ants' decisions. While we do not deny the presence of interactions between individual ants within the nesting area, the high level of agreement between observations and theory (such as an exponential distribution of time-intervals) indicates that such interactions do not have any significant impact on the level of ant activity – at least under the experimental conditions investigated here.

In our first experiments, in which ants were allowed to return to the nesting area, the constant density of ants cannot trigger any density/quorum sensing mechanisms, and hence cannot activate any behavioural changes. However in the second set of experiments, where individuals were not allowed to re-enter the nesting area, the density of ants declined substantially; by the end of the experiment the density had a value of about 10% of the value at the start of an experiment. It would, *a priori*, have been reasonable to expect some behavioural effect because ants have been shown to be sensitive to the density of conspecifics in their vicinity (Wilson, 1984), and a change in their density, alone, could have acted as a form of feedback impinging on their level of activity and hence on their stochastic leaving-behaviour. This would manifest itself in the probability of any single ant leaving per unit time, r, depending on the number of ants in the nesting area. In the data analyses presented, we assumed a constant value of r and obtained an extremely high level of agreement between models and data. Furthermore, under 'leaving without replacement', Figure 4.9 illustrates the values taken by the random variable V that was introduced in an event based analysis, and was

predicted to have a uniform distribution under the assumption of constant *r*. The distribution of *V* does not significantly change with the number of events; a Kolmogorov-Smirnov test indicates that the distribution of the 50 first elements of *V* is not significantly different from that of the last 50 elements ($p \approx 0.50$). This implies that for the experiment without replacement, no density dependence was observed, suggesting that these Pharaoh's ants were leaving their nesting area as independent agents, seemingly oblivious to the dramatic decrease in ant density that was occurring within the nesting area during the course of an experiment.

An independent paper (Richardson *et al*., 2010), suggested a log Poisson process might underlie the dynamics of ants leaving their nest. Using an analogy to a physical system, they concluded that this was evidence for interactions between individuals. Based on our comparison of the two models (see Appendix A4.3), we remain largely unconvinced by their conclusions. However, possible differences between the two studies might be due to intrinsic interspecies differences or ecology but could also be related to the feeding status of the animals. In our experiments, hungry ants may well default to behaving autonomously with a high tendency to forage. But when fed *ad libitum* (Richardson *et al*. 2010), interactions between returning fed ants and nest mates, signalling levels of food availability outside the nest, will be important in determining the rate of subsequent exploration (Hölldobler and Wilson 1990). Similarly honeybees (Seeley, 1995) and bumblebees (Dornhaus and Chittka, 2004) increase their exit rate from the hive/nest in response to returning bees signalling bountiful nectar availability in the environment.

We conclude that the level of activity observed, under the experimental conditions of the present work, in which ants were deprived of sugar for the 48 hours prior to the observations, can be well explained by individual ants acting independently of each other, i.e., with a fixed probability of leaving the nesting area/unit time. Interestingly, for experiments without replacement, this leads to the distribution of time-intervals between individual ants leaving the nesting area being exponential, but with a mean value that changes with time, as the number of ants remaining in the nesting area varies with time. If, for example, we had used the distribution of time-intervals over the entire course of an experiment, then we would not have discovered the underlying exponential distribution. This character of the distribution could thus be termed cryptic, since it is not readily apparent from the overall results of an experiment. Using our model for this,

this cryptic exponential distribution can be exposed, via a time-dependent rescaling of time-intervals. The fundamental nature of the stochasticity in this situation was therefore revealed.

Despite the somewhat counterintuitive predictions of our models for real organisms, their predictive power underlines their utility. Our experimental set-up and models may offer interesting opportunities for further exploration into other determinants of activity level, which could likely include both environmental and social factors, e.g., food availability, temperature, humidity, presence of pheromone trails, intraspecific and interspecific interactions outside the nest.

Part II:

From A to B, Statistical Modelling of the Ecology of Ants and Badgers

Cases arising from Studying Badgers

Chapter 5

Mouthing Off about Fitness: Palate Asymmetry Reveals Impact of Juvenile Parasitoses in the European Badger (*Meles meles*)

A slightly modified version of this chapter was accepted for publication in *Journal of Zoology* and is currently in press. Authors of the submitted paper are listed below:

Pierre Nouvellet, Christina D. Buesching, Hannah L. Dugdale, Chris Newman, David W. Macdonald

Abstract

Fluctuating asymmetry has been observed to relate to measures of fitness in a variety of species. In this chapter we investigate the relationship between palatine marking (maculation) symmetry and the developmental impacts of coccidial endo-parasites in the European badger (*Meles meles*).

We found young individuals with the most severe intensity of infection to be less symmetrical. The relationship persists in adulthood indicative of a lasting developmental relationship between physiological challenge and the symmetry of melanin deposition.

Maculation also shows a quadratic trend with age, with increasing size and decreasing symmetry in young individuals (i.e. less than 4 years old), contrasted by decreasing size and increasing symmetry in older individuals (i.e. more than 4 years old).

Selection had no obvious impact on maculation pattern. We acknowledge that sexual selection based on these markings is unlikely, i.e. the palate is difficult for conspecifics to observe, however as this trait demonstrated a link to individuals' capacity to cope with parasitic infection we speculate that this trait may have heritable corollaries, under selection pressure. Heritability was estimated using the statistical framework commonly referred to as the animal model (Kruuk 2004). Heritability in the size of maculation was found (h^2 = 0.51) but not in its symmetry. There was a positive relationship between relatedness and spatial organisation of the marking. The following suggestion is made: relating pairwise coefficient of co-ancestry to pairwise spatial correlation for 2-Dimensional traits might be more sensitive to evaluate genetic dependence than commonly used methodology (i.e. animal model).

Finally, despite external factors influencing the pattern of maculation with time, sufficient stability of the marks were found to allow suitable individual's recognition in a small badger population (less than 50 individuals).

5.1 Introduction

Phenotypic variations (here, variation in marking patterns) are by definition influenced by life history as well as genetic variation. Some markings (and other comparable external features), are heritable (Frankel 1991; Guenther *et al.* 1993; Nurnberger *et al.* 1995; Woolf 1989), and have been proposed as signals of individual genetic quality, particularly based on their symmetry (Gangestad and Thornhill 1999; Malyon and Healy 1994; Moller *et al.* 1996; Scheib *et al.* 1999). On the other hand, ontogeny, physiological stress, and environmental conditions are all known to influence bilateral symmetry (Edler 2001; Malyon and Healy 1994; Mateos *et al.* 2008). Mark symmetry can therefore provide an honest signal (visible or not) of condition; that is, asymmetry may indicate the "poor" quality of an individual relative to symmetric individuals, with possible consequences of reduced viability or attractiveness as mates (Mateos *et al.* 2008). In this context, 'Fluctuating Asymmetry' (VanValen 1962) (random deviation from perfect symmetry) has become a common measure of developmental stability, i.e. ability of an individual to buffer its development against random perturbations (Roff and Reale 2004; VanDongen *et al.* 1999). Early stress might thus influence the symmetry of individuals, making symmetry an indicator of the "quality" of individuals. In this context, heritability of symmetry is not a required characteristic *per se*.

A wealth of studies has shown the potential for using external markings as a recognition tool in research studies across a wide range of taxa (Childerhouse *et al.* 1996; Dufault and Whitehead 1995; Van Tienhoven *et al.* 2007). In mammals, skin colouration and markings vary between individuals, and have been used in demographic studies (Arzoumanian *et al.* 2005; Forcada and Aguilar 2000; Karlsson *et al.* 2005). Fur colouration and pattern are commonly used in photographic capture-mark-recapture methods (Karanth and Nichols 1998; Kelly 2001). This non-invasive method of identification has proven useful as it is inexpensive and reliable, with a low impact on animal welfare.

European badgers, *Meles meles*, in common with other mammals (including humans; (Brown 1964), display melanin deposition (maculation) on their hard (maxillary) palate. Badgers are known to undergo considerable juvenile morbidity and mortality due to endo-parasitic infections. At the age of *ca*. 12–14 weeks, cubs are heavily infected with

coccidial parasites (*Eimeria melis* prevalence > 65%), with deleterious consequences for survival (Anwar *et al*. 2000; Newman *et al*. 2001c). Here we investigate the relationship between parasitism and maculation patterns, hypothesising that severe parasitism may induce increased developmental asymmetry.

Sleeman *et al*. (2001) also proposed that drawing the maculation on the upper palate of badgers might provide a cost effective and reliable back-up method for distinguishing between known individuals, assuming the (so far untested) stability of the maculation over time. This would be useful where other forms of identification, such as inguinal tattoos (Cheeseman and Harris, 1982) may no longer be interpretable, for example, to identify road traffic accident victims. We test this proposition in a dense population of individually-known badgers.

The following summarises key hypothesis tested in this study:

1) Badgers undergo considerable stress at an early age from a coccidial parasitic infection. This early stress may reflect on the characteristics (i.e. size and symmetry) of maculation of badger's upper. The parasite would thus influence maculation pattern in young individuals as well as in adults.
2) As observed in human population (Brown 1964), palate maculation of badger may be age dependent.
3) As the maculation seems individually characterised, a heritability component of the marking pattern might be present and selection might act on this trait.
4) Finally individual badgers might be indentified by their maculation patterns thus offering a non-intrusive method to distinguish individuals.

5.2 Materials and Methods

5.2.1 Upper palate marking sample collection

Data were collected at Wytham Woods, 6 km north west of Oxford, in central England, UK (GPS ref: 51:46:26N; 1:19:19W) (Macdonald and Newman 2002; Macdonald *et al.* 2004a). Badgers have been studied continuously at this site since the 1970s (Kruuk 1978a; Kruuk 1978c) and the population has been trapped at least three times per annum since 1987 (for detailed description of methods see Macdonald and Newman 2002). All trapping and handling procedures were in accord with the UK Animals (Scientific Procedures) Act, 1992. On first capture, each badger was given a unique and persistent identifying tattoo in the inguinal region (Cheeseman and Harris, 1982).

Between 1994 and 1997 inclusive, the pattern of melanin deposition (maculation) on the hard palate (defined as the semilunar maxillary area delimited by the alveolar ridge and the posterior uvula: see Figure 5.1) was also recorded (drawn), in terms of absolute coverage, coverage symmetry, and pattern stability over time.

Following sedation, with 0.2 ml/kg of ketamine hydrochloride, badgers were laid dorsally and their mandible opened gently and tongue depressed to facilitate exposure of the palate. Using a standard palate template, with regard to teeth (and tooth alveoli, where teeth were absent), palate ridges and septum, 971 drawings (from N = 323 individual badgers) were made (and confirmed for consistency between observers). Given the limited gape and size of the badger's mouth, time restrictions of having animals under sedation and combined with the detailed reference points afforded by palate morphometry (e.g. marking position and extent can be assessed relative to other buccal landmarks), drawing proved to be an effective, readily comparable and reliable method of collecting these data. Comparing 25 drawings of the same palate at a single time from two different drawers (who drew the majority of the 971 drawings) revealed the mean similarity of the 25 drawing was 90% (standard error in the mean similarity: 0.7%). Mean similarity between two drawings was defined as the proportion of pixels, from a digitised image of the drawing (see below), which share a common status (mark or unmarked).

Template-derived drawings were subsequently scanned to create digital images as photography of the palate was constrained by jaw gape. A Matlab, MathWork® procedure was programmed to recognise key template features, which resulted in a set of images at the same resolution with overlapping template features (see Figure 5.1 for template), but differing marking characteristics.

Henceforth, marking size refers to the number of pixels representing melanin deposition (excluding the template image), and marking symmetry refers to the number of pixels (not already marked in the template) that share a common bilateral status (as marked or unmarked, i.e. maculated or un-maculated / total number of pixels compared). Although marking size would commonly be modelled as a Poisson variable (as a counts of the number of marked pixels), and symmetry as a Binomial variable (numerator: number of pixels that share a common bilateral status, denominator: number of pixels compared), given that each picture included around 40 thousand pixels both variables could be approximated effectively by a normal distribution and thus we subjected them to Gaussian statistical treatment. Direct observations of the distributions of marking size and symmetry among badgers confirmed the approximate Gaussian nature of these distributions.

5.2.2 Parasite load

Coccidiosis load i.e. prevalence and intensity of *Eimeria melis* infection, was measured between 1994 and 1997. Administration of a warm, soapy water enema induced a faecal sample, which was then collected and examined by microscopy. Following Anwar *et al.* (2000), excreted oocyst counts were used as a measure of parasitic infection. *Eimeria melis* typically parasitises juvenile individuals (i.e. cubs) (see Newman *et al.*, 2001), thus we use the parasite load for this population class in our analyses. Using these data from juveniles (N = 130), we constructed a general linear mixed model (GLMM) in order to assess whether cub parasite load influenced contemporary marking size and symmetry (i.e. cub's marking size and symmetry); where variation in marking size, or symmetry, were predicted by parasite load, as covariate, and tattoo number, as a random factor. By running another model without parasite load, as covariate, and using a likelihood ratio test, we examined the significance of including parasite load in the model.

As immunity to coccidial parasitoses develops with maturity, infection is rare in the adult population, and apparent only mostly in cubs. We were thus able to test further whether the evidence for an interaction between maculation and parasitic infection persisted into adulthood. Cub infection, adult age and tattoo number were used as predictors of adult marking size and symmetry using a GLMM. In the model, age (with quadratic effect – see results for justification) and parasite load (as a cub) were included as covariates, along with their interactions, and tattoo number (to account for repeated measures of the same badger; 225 out of 323 badgers had repeated measures) was included as a random factor. Using a restricted likelihood method (REML), we constructed two models, with- and without- parasite load, followed by an analysis of deviance (likelihood ratio test), which informed us of the significance of including parasite load as a predictor of palate marking size or symmetry (Crawley 2005; Crawley 2007). Statistical analyses were performed with *R 2.8.0* software and the package *lme4* (Bates and Maechler, 2009).

5.2.3 Marks and age

Cursory observation of the image database (i.e. the collected set of palate maculations) indicated variability unrelated to individuality. We considered that this might be a function of ontogeny (as observed in human mouth markings, Brown 1964); that is, a relationship between the extent and/or symmetry of the mark and the age of the badger, as well as observer error (i.e. ability for two observers to render identical drawings). The significance of the ontogenic relationship was assessed using a GLMM with tattoo number as a random effect. An analysis of deviance (likelihood ratio test) using models including and excluding age (Crawley 2005; Crawley 2007) was then performed. All 323 badgers were of known age, i.e. were first caught as cubs. A quadratic influence of age was also tested, along with interaction amongst fixed effect.

5.2.4 Selection and heritability

Using reproductive output as a proxy for fitness (see Dugdale *et al*. 2010 for discussion), we determined whether mark size or symmetry were under selective pressure. We tested for selection specified as directional selection differential (Lande

and Arnold 1983). Reproductive output was calculated as the total number of offspring that survived to independence, and that were trapped and assigned with parentage (both parents were assigned to 595 out of 735 cubs trapped between 1988 and 2005, inclusive; see (Dugdale *et al*. 2007b). The total count of offspring was performed for individuals that were born after 1987 and were known, or deduced, to be dead by the end of the study period as they had not been trapped in the last two years of the study (N = 201). If selection was in evidence we anticipated a relationship would be apparent between our estimation of fitness (the response variable) and mark size or symmetry. We looked for such a relationship using a generalised linear model, with a Poisson error structure (accounting for counts of offspring per individual) implemented in R. The response variables were standardised (Hereford *et al*. 2004b).

Heritability of the size of marking and pixel symmetry was then assessed using the 'animal model' (Kruuk 2004) and ASReml-W version 2.1 (Gilmour *et al.* 2006). The 'animal model' is a modification of a linear mixed effect model, where the variance-covariance matrix of the mixed effect is taken to be proportional to the genetic relationship matrix (where each individual's relationship is inferred from a pedigree and the coefficient of co-ancestry). When running the 'animal model', an analysis of variance component is performed indicating which factors (e.g. environmental or genetics factors) influence the variance observed in the trait of interest.

Age and age-squared were included as random effects as they showed a clear influence on both the size and symmetry of the markings, which were scaled by a factor of 1,000, as required by the 'animal model'. A permanent environmental effect was included as a random effect to account for repeated measures. We assessed the significance of the additive genetic variance (V_A) using a likelihood ratio test of the model with- and without- badger identity as a random effect. We estimated narrow-sense heritability (h^2), i.e. the degree of resemblance between relatives, as the ratio of V_A to phenotypic variance (V_P): $h^2 = V_A / V_P$ (Falconer and Mackay 1996).

This method for assessing marking heritability, however, was considered to be unsatisfactory in isolation. Examining the heritability of a spatial pattern requires testing whether differences in both the position and extent of the marking correspond with the relatedness between the two individuals in question. By quantifying the trait with a numerical value (as necessary for the use of the 'animal model'), we will inevitably loose information related to the spatial position (shape) of the marking. We therefore

used two comparative measurements: pair-wise co-ancestry values (Henderson 1976) (calculated using a pedigree based on 22 microsatellite loci), and similarity in marking pattern (measured as the number of pixels common to the two palate images). When relating the coefficient of co-ancestry with the similarity in marking pattern, multiple comparisons of the same two individuals were made; to avoid pseudo-replication each distinct dyadic comparison was included as a random effect.

5.2.5 Palate marking as an individual-specific diagnostic

Some individuals (225 out of 323) were caught and their palate drawn on multiple occasions (up to 10 times) facilitating the assessment of variation in melanin deposition over time. Using standard statistical concepts, if inter-individual variation exceeds intra-individual variation, then marking may predict individuality. We first tested inter- and intra- individual differences using a GLMM; as this included multiple comparisons of the same two individuals, each distinct dyadic comparison was included as a random effect.

To assess the individuality potential of palate markings further, we defined more stringent criteria. For instance in fingerprinting, given a database of fingerprints, one individual's print sampled subsequently should match previous records for that individual most closely. To test this assumption for each drawing we assessed the number of differing pixels compared to images derived from a different drawing. We anticipated that the closest match would be to an image from the same individual. We then calculated the percentage of correct assignments, which in a perfect superimposition would be 100%, i.e. positive and unambiguous identification.

The size of the database (number of distinct individuals) will, however, also influence success rate. With a large database the opportunity for finding a different individual with a similar palate mark (a 'false-positive') increases, thus the sensitivity of the technique diminishes. This effect was quantified by randomly selecting a comparative subset of n images (n ranges from 5 to 200) from the database and running an identification procedure as described above, allowing us to estimate a success rate (percentage of correct identifications), at different badger population densities. For each value of n, the procedure of re-sampling was repeated 100 times.

5.3 Results

971 palate markings were digitised from the standard field template (Figure 5.1a and b), representing 323 individual badgers, of which 225 were represented by more than 1 drawing, and 3 individuals had 10 drawings. These digital images were manipulated to extract information on the extent and symmetry of the marking. Figure 5.1c shows a superposition of all images indicating a propensity for marking to occur adjacent to dental alveoli.

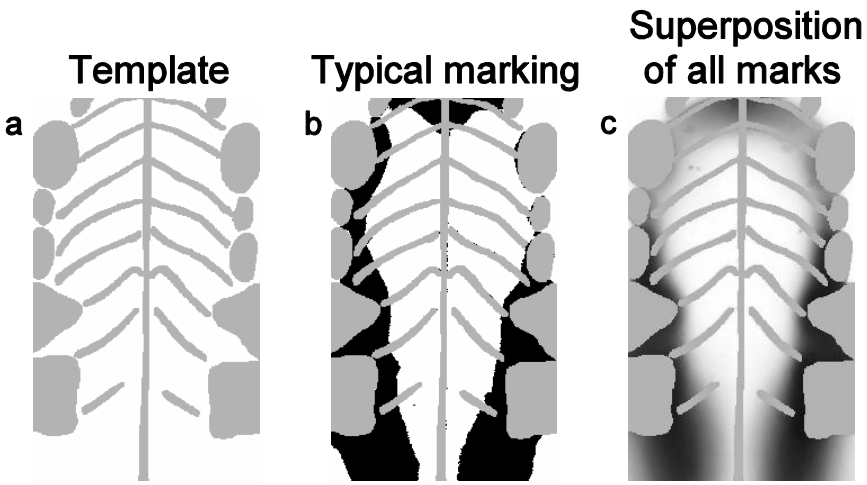

Figure 5.1

Digitised badger palate image: (a) template used for drawings, grey areas show the teeth/alveoli and maxillary-palatine ridges; (b) palate with representative markings, black areas show melanin deposits; and, (c) superposition of all 971 palate images, darker pixelation indicates the most frequently marked (maculated) area. From (c) some regions are maculated in up to 94% of the 971 badger palates observed, notably maculation is disposed towards medial-alveolar deposition (especially around the incisors and molars). Maculation variability is highly variable (range = 0 – 76%).

5.3.1 Parasite load

An increased parasite load (defined as intensity of infection of *Eimeria melis* in cubs) was linked to a less symmetrical and a smaller palate marking in cubs (Table 5.1). .

We found a significant negative correlation between cub parasite load and subsequent symmetry of the marking once that individual was an adult (Table 5.1). We also found a significant but positive correlation between cub parasite load and the size of subsequent adult palate marking (Table 5.1). While age and age square, as well as tattoo number were retained in the model presented, the interactions terms were removed as non-significant (using a likelihood ratio test, $p > 0.05$).

Therefore, cub coccidial (*Eimeria melis*) load had a negative impact on the symmetry of the marks for both cubs and adults. Conversely, high parasitic load as a cub was correlated with smaller marking extent while cub but larger marked areas when adult.

Model (tattoo number always included as random factor)	$\beta_{parasite}$ (SE)	AIC	X^2 (*df=1*)	*p*
Sym_{Cub}~ Parasite	-0.014 (0.042)	1653	554	< 0.001
Sym_{Cub}~ intercept		2204		
$Size_{Cub}$~ Parasite	-0.180 (0.145)	1872	645	< 0.001
$Size_{Cub}$~ intercept		2524		
Sym_{Adult}~ Parasite+age+age^2	-0.075 (0.044)	5663	4427	< 0.001
Sym_{Adult}~ age+age^2		10087		
$Size_{Adult}$~ Parasite+age+age^2	0.062 (0.199)	6305	4953	< 0.001
$Size_{Adult}$~ age+age^2		11257		

Table 5.1

Statistical outputs from a general linear mixed model with symmetry (sym) or size of maculation as the response variable. We present the coefficient linking the dependent variable (either symmetry or size of the maculation) to parasite load, $\beta_{parasite}$. The AIC (Akaike Information Crierion), a measure of the goodness of fit of the model is present and subsequently used during the likelihood ratio test resulting in the chi-squared test statistic, X^2, and its associated with a p-value (last column). In the upper set of models, cub's maculation is significantly related to parasite load. In the lower set of models, adult's maculation is significantly related to parasite load as a cub; also age and age^2 are included as covariates. The inclusion of parasite load is significant in all models (analysis of deviance, $p<0.001$).

5.3.2 Maculation and age

Age had a significant quadratic impact on both the symmetry and size of the palate markings. Using a likelihood ratio test in a model exploring variance in marking symmetry, inclusion of age ($\chi 2_{(df=1)} = 4262$, $p < 0.001$) and age squared ($\chi 2_{(df=1)} = 8$, $p = 0.005$) significantly increased the fit. Similarly, using a likelihood ratio test in a model exploring variance in marking size, inclusion of age ($\chi 2_{(df=1)} = 4752$, $p < 0.001$) and age squared ($\chi 2_{(df=1)} = 72$, $p < 0.001$) significantly increased the fit. Linear age had a negative impact (coefficient for age: -251, SE = 72) and quadratic age had a positive impact (coefficient for age: 27, SE = 9) on marking symmetry. Linear age had a positive impact (coefficient for age: 1994, SE = 195) and quadratic age had a negative impact (coefficient for squared age: -229, SE = 26) on marking size. Thus, in young individuals (< 4 years old), the extent of maculation increases with age, while in mature animals (> 4 years old) the maculation decreases with age according to a negative quadratic component (Figure 5.2). This relationship remained significant when controlling for badger identity. The relationship for mark symmetry follows in opposite trend (see above).

Sex and social group (linked to the geographical position) were also examined as potentially influential variables, but showed no significant effects (repectively in a likelihood ratio test we add: $\chi 2_{(df=1)} = 2.5$, $p > 0.05$ for sex and $\chi 2_{(df=1)} = 1.8$, $p > 0.05$ for social group).

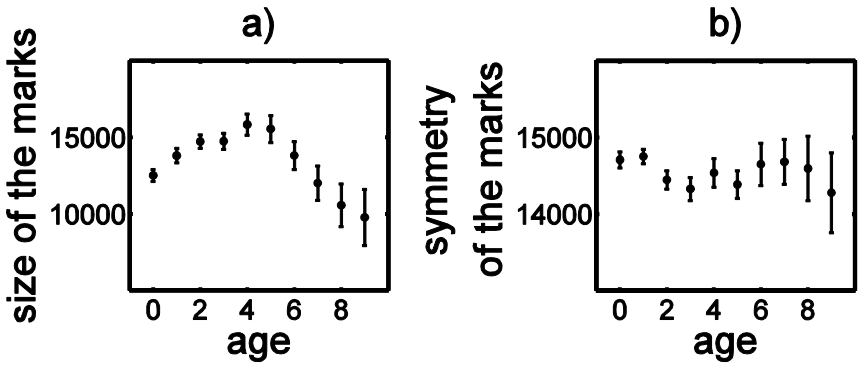

Figure 5.2

Relationship between the size (a) (in number of pixels) and symmetry (b) (in number of matching pixels between the left and right of the palate) of palate maculation with badger age (years). We present the mean sizes of the marks (in number of pixels) for each age along with their standard errors (error bars). Mean symmetries of the maculation per age (in number of pixel matching) are also presented along with their standard errors.

5.3.3 Heritability and selection

Lifetime reproductive output was determined for 326 individuals with values ranging from 0 to 18 offspring. Neither symmetry nor size of the maculation had a significant impact on lifetime reproductive output (respectively $t_{(df=209)} = -1.5$, $p = 0.14$; and $t_{(df=209)} = -0.92$, $p = 0.35$).

The symmetry of the palate marking (n = 288) did not show any additive genetic variation ($V_A = 0.00 \pm 0.00$; $\chi 2_{(df=1)} = 0.0$, $p = 1$; $h^2 = 0.00 \pm 0.00$); however, the estimate was constrained due to negative estimation during the iterations, suggesting either no V_A or a low sample size. The size of the mark, however, did show significant V_A (14.6 ± 4.1; $\chi 2_{(df=1)} = 34.7$, $p < 0.001$; $h^2 = 0.51 \pm 0.11$).

Comparing pair-wise co-ancestry values with 'palate marking' similarity (defined as number of shared pixels between two individuals; Table 5.2) identified that marking relatedness is positively correlated with genetic relatedness ($p<0.001$). This gives weak evidence (strong correlation, but shallow slope) of a genetic basis for palate marking.

Model (individual comparison included as random effect)	β_0	β_1	AICc	$\chi 2$ $(df=1)$	p
$M_{sim} \sim G_{co\text{-}an}$	31975 (15.6)	1679 (230)	7488565	53.9	<0.001
$M_{sim} \sim 1$	31998 (15.3)		7488637		

Table 5.2

Statistical output, from a general linear mixed model with Marking similarity (M_{sim}) as the response variable and genetic co-ancestry value ($G_{co\text{-}an}$) as covariate, showing a significant positive relationship (β_1 : regression slope is positive) between kinship and marking similarity. That is, individuals with greater genetic similarity tend to have slightly more similar marking patterns in both terms of extent and also spatial position. The variable β_0 represents the intercept in the model; we also present the AIC used for the likelihood ratio test and the test statistics, $\chi 2$, and its p-values.

5.3.4 Palate marking as an individual-specific diagnostic

The variation in maculation between individuals was significantly greater than the variation observed between repeat images from the same individual ($\chi 2_{(df=1)} = 53.9$, $p<0.001$, GLMM with individual pairs as random effect). On average, for the same badger re-sampled at a different time, 85% of pixels shared a common status (marked or unmarked); while between different individuals 75% of the pixels shared a common status. While the difference between these two figures reflects the individuality potential of palate marks, the latter reflects that maculation tends to occur always in similar areas (Figure 5.1c, medial-alveolar).

A "database" of 971 individual palate markings was constructed, including repeat images from re-sampled individuals ($N = 225$). 36% of images were accurately diagnostic of badger identity. The accuracy of the identification technique was assessed on its capacity to correctly identify individual badgers based on similarity (greatest number of matching pixels) of the palate maculation. As the number of images ($N = 5$ to 200, number of individuals in the database), picked randomly from the full dataset of 971, decreased, the efficiency of the procedure increased. With a smaller population

(number of individuals in the database) this technique would be more powerful, i.e. there would be less continuous variation in the sample. Population re-sampling facilitated an estimate of the efficiency of this identification technique (Figure 5.3): 70% efficiency is achieved for a population of 50 individuals.

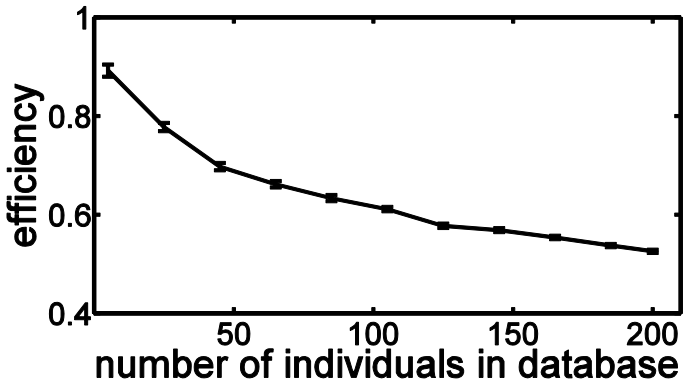

Figure 5.3

Efficiency of individual badger recognition based on palate marking as a function of number of individuals in the database. The efficiency of the recognition procedure, proportion of correct assignment, increases as the number of individuals decreases. The curve shows the mean efficiency of the procedure and its standard error (derived from 100 repetitions).

5.4 Discussion

In the field of fluctuating asymmetry, stress has been shown to impair condition during development, resulting in observable bilateral variation (Ligon *et al.* 1998; Malyon and Healy 1994; Mateos *et al.* 2008; Oakes and Barnard 1994; Polak 1997). Although there has been substantive debate in this field (Houle 1998; Lens *et al.* 2002; Palmer 2000), there remains considerable evidence to support the existence of corollaries of fluctuating asymmetry for a wide range of traits and species (Dufour and Weatherhead 1998; Edler 2001; Gangestad and Thornhill 1998; Gangestad and Thornhill 1999; Moller *et al.* 1996; Morris 1998; Strobeck 1997; Thornhill and Gangestad 1999a; Thornhill and Gangestad 1999b). Badgers undergo pronounced physiological stress levels during their first few months of life as a consequence of pandemic endo-parasitic infection, causing diarrhoea and dehydration at a sensitive stage in their development (Anwar *et al*. 2000; Newman *et al*. 2001c). In turn, the severity of this juvenile parasitic infection appears to be influential in the subsequent symmetry and extent of palate maculation. Early infection results in greater asymmetry in the marking, asymmetry that is still apparent in adults. The size of the maculation, however, reveals a more complicated pattern where parasite infection seems to first impair the development of palate marking in cubs but then to increase the melanin deposition in adult. Parasitic infection would thus appear to delay, or inhibit, the formation of palate marking during the period of peak infection. But with developing adult immuno-competence it would appear that there is a phase of 'over-compensation' in the rate of melanin deposition. It must be highlighted, however, that severely infected cubs will die (Newman *et al*. 2001), so the surviving sub-sample of adults is representative only of those individuals able to overcome the morbidity associated with infection. Maculation does however reflect early life experience and exposure to stress and provides a proxy measure from which developmental stress levels can be inferred retrospectively amongst adults.

While the life-history influence on the phenotypic presentation of the trait (Morris 1998; Thornhill and Gangestad 1999a) was clearly in evidence, genotype appeared to have a subordinate role in determining maculation characteristics. A trait has to be quantified to estimate its genetic dependence, e.g. each individual has a trait value, facilitating the estimation of the variance in the trait correlated to the relatedness between individuals (Kruuk 2004). On this basis no evidence of heritability was found for the symmetry of

maculation, although heritability was found in the size of the markings. The heritability of fluctuating asymmetry is known to be very low and most likely with dominant or epistatic effects (Leamy and Klingenberg 2005), which are non-additive and thus would not be detectable with the procedure presented here. Proximate measures of fitness, such as lifetime reproductive output, also revealed no evidence of direct selection for either size nor symmetry of the marking, which is to be expected as markings are not readily visible to other badgers. However it is possible that fluctuating asymmetry acts in a multitude of traits, some of which would be detectable by conspecifics (symmetry of face stripes), but were not measured. Under this assumption as each symmetric feature would be correlated, selection acting on one trait would be reflected on other, allowing us to detect selection on a non-visible trait.

It is clear that traits, such as maculation extent and pattern, contain more information than a single numerical value can encode, due to of their spatial nature. Other studies have used statistical descriptions of such traits using multi-factorial analysis (Woolf 1989). Here we present a somewhat simpler method involving a comparison of genetic relatedness (through the coefficient of co-ancestry) and maculation relatedness, e.g. very similar markings in terms of size, symmetry and position would be indicative of greater relatedness. From this assumption we were able to compare the similarity in the marking traits with the genetic relatedness of individuals. A weak, but significant, genetic basis for badger palate maculation was found. Comparing the spatial correlation of marks between individuals does not restrict a trait (marks) to a specific single value. Further theoretical work is needed to relate expected measures of spatial cross-correlation between the marks of two individuals and a genetic correlation (i.e. coefficient of co-ancestry), leading to estimate of true heritability of complex/spatial traits.

As demonstrated previously by a small scale study (Sleeman *et al.* 2001), our study also confirms the potential utility of palate maculation as an identity marker in small populations of badgers. The methods would not be effective in a large population (> 50 individuals); for many studies at the level of social groups, however, this technique could offer an additional non-procedural identification method (Auger-Methe and Whitehead 2007; Sleeman *et al.* 2001). Even in studies of larger populations, knowledge of the macular markings of an individual might help narrow the number of potential candidate identities, thus increasing the possibility of making the correct

assignment when other identification techniques or technologies fail, for example identifying road kills where other methods of identification may be lost or unreadable to the reporter of the casualty. The stability of markings (e.g. whale skin patterns) over time is the primary constraint when using markings for individual recognition (Dufault and Whitehead 1995; Gowans and Whitehead 2001). Although the maculations presented here showed clear age-related changes, this method could still have valid shorter-term application. The simplicity of the technique (raw comparison of pixels) contrasts with more sophisticated methods used in pattern recognition: using complex algorithms (Arzoumanian *et al.* 2005; Gope *et al.* 2005); software relying on user interaction (Van Tienhoven *et al.* 2007); or using theoretical information frameworks (Fagan and Holmes 2006; Speed *et al.* 2007). Palate maculation would be rendered more effective by developing sophisticated recognition algorithms and by using spatial information linked to trapping location / the site from which the individual's data were recovered (Road Traffic Accident). Here, we obtained reasonable success (70% success in a population of 50 individuals) even with a relatively unrefined algorithm, which compares favourably with other methods (Auger-Methe and Whitehead 2007; Kelly 2001; Van Tienhoven *et al.* 2007).

In conclusion, in this 5th chapter, we show an interesting interplay between phenotypic influences, such as juvenile parasite load (developmental stress) and age; and genetic influences (genetic relatedness, heritability) on the size and symmetry of a maculation trait. While this trait is unlikely to be subject to direct sexual selection (i.e. play a direct role in mate choice) the link between maculation and phenotypic stress is readily apparent. That such proxies for previous life-history events may exist in populations is biologically intriguing (see Morris 1998; Thornhill and Gangestad 1999a). These traits may have potential to provide powerful indicators for the developmental stresses experienced by individuals or populations, in turn informing both our understanding of animal societies and the effective application of conservation measures.

5.5 Acknowledgments

We are very grateful to Anna Santure for calculating the relationship matrix from our pedigree and to Paul Johnson for constructive comments on statistical methods. Much of this core study was generously supported by the People's Trust for Endangered Species, with additional support from the Earthwatch Institute. Work was carried out under English Nature Licences, currently 20061970 and Home Office Licence PPL 30/2318.

Chapter 6

Are Badgers '*Under the Weather*'?

Direct and Indirect Impacts of Climate Variation on European Badger (*Meles meles*) Population Dynamics

A slightly modified version of this chapter was accepted for publication in *Global Change Biology* and is currently in press. Authors of the submitted paper are listed below:

Pierre Nouvellet, Christina D. Buesching, Hannah L. Dugdale, Chris Newman, David W. Macdonald

Abstract

Weather conditions, and how they in turn define and characterise regional climatic conditions, are a primary limit on species diversity and distribution globally, and increasing variability in global and regional climates have significant implications for species and habitat conservation.

A capture mark recapture study revealed that badger (*Meles meles*) life-history parameters interact in complicated ways with annual variability in the seasonality of temperature and rainfall, both in absolute and in phenological terms. A strong predictive relationship was observed between survival and both temperature and late-summer rainfall. This link at the population dynamics level is related, at the individual level, to the weight variation between summer and autumn. In addition, fecundity was correlated with spring rainfall and temperature. We proposed and confirmed that the relationship was consistent with observed variation in the spread of a parasitic infection. Finally, fecundity during a given year correlated with autumn condition prior to parturition, relating again to weight gain.

Badger survival also correlated with late winter condition. This period is critical for badgers insofar as it coincides with their peak involvement in road traffic accidents (RTAs). RTA count during this period was strongly linked to temperature, underlining the intricate ways in which a changing climate might interact with anthropogenic agents to influence species' population processes.

Equinoctial conditions produced significant population driver effects. That is, while summers will always be relatively warm compared to winters, spring and autumn weather can be more variable and functionally delimit the 'productive' vs non-productive period of the year in terms of badger behavioural and physiological cycles.

6.1 Introduction

Climate is one of the primary limiting factors of species diversity and distribution globally, and past climatic changes have affected the composition and dynamics of natural communities (Root *et al*. 2006). Thus, anticipated changes in global and regional climates are likely to have significant implications for species and habitat conservation (Ipcc 2007a).

Ecologists are faced with assessing how highly variable climatic conditions might impact upon species and communities within destabilised ecosystems (Naeem and Li 1997; Root *et al*. 2003; Wilmers *et al*. 2002). Root *et al*. (2003) also discuss how the impacts of climate change on a population can pivot on a critical life-history event, for example through the failure in synchronicity of food supply and demand, due to phenological change. That climatic trends might sufficiently alter a species' behaviour or phenology to bring them into increased conflict with, or at risk from, human activity is an additional facet of these changing limitations on population viability (Root *et al*. 2005; Root *et al*. 2003).

The Eurasian badger *Meles meles* (Linnaeus 1758) is an exemplary species with which to consider potential climate change impacts on population dynamics. *Meles* has an extensive geographical range, stretching across Europe and Asia from the Arctic Circle to the Mediterranean, and exhibits considerable socio-spatial adaptability (Kruuk 1989; Woodroffe and Macdonald 1993).

Past analyses have suggested that badger populations are regulated principally by intrinsic factors and by the limitations of environmental conditions, such as the fluctuating availability and dispersion of resources (Carr and Macdonald 1986; da Silva *et al*. 1993; Johnson *et al*. 2002; Kruuk 1978b; Macdonald and Newman 2002). Badgers have no contemporary predators in Britain; thus, aside from disease (Newman *et al*. 2001a), there are few natural factors that could result in "top-down" population regulation (Vucetich and Peterson 2004).

Badger population densities are generally greatest in areas where mild, damp conditions make favoured earthworm prey (*Lumbricus terrestris*) readily available at the soil surface (Kruuk 1978c; Macdonald 1980; Macdonald 1983). Earthworms are sensitive to

microclimatic conditions (Fragoso and Lavelle 1992; Gerard 1967; Macdonald 1980; Macdonald 1983), consequently their distribution and abundance is highly dependent on weather patterns, and in parts of the species' range environmental conditions provide good surrogate measures for badger food supply (Johnson *et al*. 2002; Kruuk 1978b; Macdonald *et al*. 2004a). Although badgers will eat a mixed diet in the UK, for example if earthworms become scarce during droughts or frosts (Cleary *et al*. 2009; da Silva *et al*. 1993; Hofer 1988a; Kruuk 1978b; Kruuk 1978c; Kruuk 1989) they forage preferentially for earthworms when conditions permit. Variation in weather patterns can thus affect the badger's food supply considerably. Considering the nocturnal habits of both the badger and the earthworm, it is noteworthy that increasing annual mean temperature has been reported to result particularly from night-time, rather than daytime, increases, reducing the Diurnal Temperature Range (Rebetez and Beniston 1998; Tuomenvirta 2000). Previous analyses of badger population dynamics, using an earlier subset of data for the badgers of Wytham Woods (Macdonald and Newman 2002), suggested that their numbers were responding positively to changing climatic conditions, particularly winter warming (which creates a longer productive season). Here, with a much longer-term data-set, we provide evidence of a far more complex relationship between badger survival, factors known to correlate with food supply, extrinsic mortality factors and weather patterns.

Badgers have critical periods within annual cycles that are especially sensitive to climatic factors (Domingo-Roura *et al*. 2001; Kruuk 1989; Neal and Cheeseman 1996). In late summer and early autumn, badgers increase their body-fat levels (Macdonald *et al*. 2002; Neal and Cheeseman 1996), an adaptation to cope with food scarcity during harsh winter conditions (Fowler and Racey 1988). As seasonal weight gain is dependent upon resource availability, climatic conditions during this sensitive period influence contemporaneous badger survival both in terms of modifying food availability and with regard to thermal-stress on the badgers' metabolic rate when foraging above ground. Thus, climatic conditions associated with lower gain in weight during this period should also militate for lower survival rates. Additionally, lower survival and weight gain in one year might also militate for lower fecundity during the following spring; a time when neonatal cubs experience a high level of coccidial parasitic infection, which induce considerable juvenile mortality (Anwar *et al*. 2000; Newman *et al*. 2001a). Thus we also test whether fecundity is influenced directly by spring climatic conditions,

particularly whether low measures of fecundity are associated with higher cub parasite loads.

In addition to "natural" extrinsic factors limiting badger populations, the species is affected by the anthropogenic impacts of road traffic accidents (RTAs; (Clarke *et al*. 1998; Davies *et al*. 1987; Neal and Cheeseman 1996; Skinner *et al*. 1991). Annually, between 30-66% of national adult and post emergence cub mortality in the UK can be attributed to RTAs (Clarke *et al*. 1998; Skinner *et al*. 1991). Badger road casualties are known to be seasonal (Davies *et al*. 1987) with a peak in RTA count during late winter. Climatic conditions in late winter were included in our analysis as a critical period for badger survival, testing for any interaction / association between late winter conditions and RTA rate as a mortality factor. We hypothesise that if mild weather leads to greater badger activity in the winter months, badgers will place themselves at greater risk of exposure to RTAs than if they are securely underground in a seasonal torpor (Davies *et al*. 1987; Fowler and Racey 1988). Our approach highlights the potential for tertiary climate change effects on the population dynamics of a medium-sized mammal.

6.2 Material and Methods

6.2.1 *Study site and badger trapping*

This study was conducted at Wytham Woods, a 424ha mixed semi-natural woodland site, 5 km north west of Oxford, UK (GPS ref: 51:46:26N; 1:19:19W; Mean annual temperature 10.1ºC; mean annual precipitation 644.8mm - Oxford Radcliffe Meteorological station, School of Geography; for details see (Macdonald and Newman 2002; Macdonald *et al*. 2004a). The records used in these analyses cover a 21-year period between 1987 and 2008 for which accurate population size and juvenile cohort survival figures are available for the woodland's population of badgers.

This badger population has been studied continuously since the 1970s (Kruuk 1978b; Kruuk 1978c) and the population has been trapped and marked at least three times per annum since 1987 (For detailed methods see Macdonald and Newman 2002; Macdonald

et al. 2009). All trapping and handling procedures were in accord with the UK Animals (Scientific Procedures) Act, 1992, and approved by institutional ethical review committee. On first capture, each badger was given a unique identifying tattoo in the inguinal region. Morphometric measures of mass, body length (tip of snout to sacrum) and body condition (subcutaneous fat score originally developed for sheep, with 1 being emaciated and 5 being in very good condition; modified from Speedy 1980) were recorded *inter alia* upon each capture.

6.2.2 Climate Data

For each of the 21 years of population data, we consider 2 variables – monthly temperature and rainfall. These data were sourced from the Oxford Radcliffe Meteorological station (School of Geography, University of Oxford). To facilitate the analysis of the potential impacts of different climate variables on demography, we derived standardized variables for monthly rainfall and temperature.

6.2.3 Candidate climate variables for demographic analyses

From the 12 monthly records per year of standardized temperature and rainfall, a set of candidate variables, i.e. climatic variables likely to be associated with demographic parameters, was selected to assess whether they were predictive of demographic trends / responses. These likely associations were informed by knowledge of badger natural history (Macdonald and Newman 2002) and by a preliminary unpublished study investigating a subset of these same data using a reduced data-set (1987 to 2000), and multi-model selection to infer which monthly temperature/rainfall variable best reflected survival or fecundity.

The resulting set of candidate variables reflects critical periods in badger natural history:

(i) spring time: cub emergence thus would be predicted to have an impact on our measure of fecundity;

(ii) late summer - early, autumn, a time when badger body-weight increases in response to generally advantageous foraging circumstances, enabling badgers to have energy

reserve to sustain them during lean winter conditions that would otherwise be detrimental to survival and fecundity in the next year;

(iii) in late winter, when badger RTA rate shows an annual peak, hence the magnitude of this peak might be weather dependent.

We thus focus our analyses on correlations between -

(i) Fecundity and – May rainfall, R_m, May temperature, T_m,and October rainfall from the previous year, R_o^{-1} .

(ii) Survival rate and September temperature , T_s,and October rainfall; R_o .

(iii) Survival rate and February temperature, T_f .

6.2.4 Can demographic parameters be predicted by local weather?

Badger population dynamics can be modelled successfully by characterising a limited set of demographic parameters (Macdonald *et al*. 2009):

i) Juvenile survival (individuals that have not yet reproduced, i.e. less than 2 years old),

ii) Adult survival (individuals of reproductive age, 3 and over), and

iii) Fecundity (number of offspring recorded after first emergence per individual)

We estimated yearly survival and fecundity for the study population using the capture histories for 1225 individuals. In our models demographic parameters were constrained (or not) by our candidate climate variables (associations), then the Akaike Information Criterion (AIC) was applied to evaluate the fit of these models, within the framework of multi-model selection (Burnham and Anderson 2002; Burnham and Anderson 2004). All statistical estimation and analyses of demographic variables were performed using MARK (Lebreton *et al*. 1992; White and Burnham 1999). We note, capture probabilities were left time dependent in these estimates, for each model presented, as we were not concerned with this interaction with climate variables.

6.2.4.1 *Can survival be predicted by the candidate climatic variables?*

Survival was modelled with a binary outcome (survived / died), using the standard *Logit* link function. Both adult and juvenile survival were estimated using the 'Cormack-Jolly-Seber' (CJS) model (Jolly 1965; Lebreton *et al*. 1992). Goodness of fit, for models with year dependency in both demographic parameters, was evaluated using a Boot-strap method (White 2002), facilitating an estimate of the variance inflation factor, $\hat{c}$ (White 2002). This value $\hat{c}$, was subsequently used to correctly evaluate models.

Models with constrained survivals for each combination of the candidate climate variables were constructed and evaluated using the AICc criterion (Grosbois *et al*. 2008). The difference in the AIC_c between any given model and the most supported model (ΔAIC_c) was then used to evaluate relative model fit (Burnham and Anderson 2002; Burnham and Anderson 2004). Models within a ΔAIC_c<2 were considered to be well supported by the data. Finally when an inflation factor, $\hat{c}$, is estimated, AIC_c values can be corrected defining the quasi-AIC: $QAIC_c$ (White 2002).

6.2.4.2 *Can fecundity be predicted by the candidate climatic variables?*

To evaluate recruitment in our closed population (Macdonald and Newman 2002; Macdonald *et al*. 2002), fecundity can be considered to equate with recruitment, as analysed in a '*Pradel'* model (Nichols *et al*. 2000; Pradel 1996; Williams *et al*. 2002). We stress here that our fecundity approximations measure the number of cubs per females but also include a measure of cub survival from birth until emergence (approximately after 3 months). For sake of simplicity we will use the term fecundity henceforth to refer to this apparent fecundity. As recruitment is essentially a count, we applied the *log* link function.

Support/Plausibility for each model was again evaluated using Akaike's weight (Anderson and Burnham 2002; Burnham and Anderson 2002), i.e. where recruitment was / was not constrained by candidate climatic variables of the model was assessed.

In all models investigating fecundity, survival rate and capture probabilities were fixed (i.e. one set of fixed values for survival each year, and one set of fixed values for capture rate per trapping event). The values used were predetermined using a CJS model.

6.2.5 Spring rainfall, fecundity and juvenile parasitic load

Coccidiosis load (prevalence and intensity), of *Eimeria melis*, was measured for 220 cubs in a sub-sample of years from within our total study interval, between 1994 and 1997 (see Chapter 5, section 5.2.2 for details). As *Eimeria melis* typically parasitises young individuals (cubs: see Newman *et al*. 2001a), parasite load was considered an influential variable for cubs.

Newman *et al*. 2001a) propose that the strength of the pathology associated with coccidial infection is in turn influenced by simultaneous weather conditions (with May - weaning as the key month), i.e. the availability of earthworms to infected cubs dictates their capacity to endure (or not) the diarrhoea and malabsoroption of nutrients associated with this disease (Long 1982).

Individual parasite load, with a Poisson distribution (as it is a count) was used as a dependent variable in a generalised linear model, with a *log* link function, with month at which the faecal sample was taken as fixed factor and May rainfall as covariate.

6.2.6 Late summer climatic conditions, survival rates and body-weight

Trapping sessions in June/July and then late-October/November provide the extremes in weight for individuals. Presuming that fatter individuals will have a better chance of survival (in the absence of confounding variables), we propose that this effect would be facilitated by weather which optimised the energetic returns of foraging and the metabolic costs of activity.

For each year of the study, we calculated the variation in weight per individual for 822 badgers between the early summer trapping session and the late autumn trapping. Using a general linear model, we then tested whether September/October's conditions are influential on weight variations. We included month trapped in early summer (June or July) and month trapped in late autumn (late October or November) as fixed factors since these could influence the trend in body weight variation. Sex was also included as fixed factor to correct for dimorphic differences in weight gain/loss.

Accurate records of individual badger body-weight were sparse for the winter period (as most trapping information is collected in early summer, late summer and late autumn),

making it difficult to relate badger body condition with a hypothetical link with February temperature. However, in the following section, we present a potential explanation for a postulated link between survival and February temperature. This explanation is based on national reports of road traffic accidents in South-West Britain, as such detailed records were not available for the Wytham field site, which would also be too localised to support this analysis if considered in isolation (see below).

6.2.7 Analysis of climate-based impacts and influences on badger Road Traffic Accidents (RTAs)

Local records of badger RTAs for the vicinity of our study population at Wytham Woods were insufficient for robust analyses. Because of an interest in their role in bovine tuberculosis transmission, however, a large data set was available for badger RTAs between 1972 and 1999, gathered largely in southwest England (Avon, Cornwall, Devon, Dorset). These data were provided by the Department of Environment Food and Rural Affairs (DEFRA) and the Veterinary Laboratories Agency (VLA), and were used at the regional scale to test for any relationship between RTAs and temperature, to supplement our local study. We tested for relationships between the monthly prevalence of RTAs associated with the corresponding monthly mean temperature (appropriate regional temperature data were obtained from the Met-Office at http://www.metoffice.gov.uk/education/data/; see Parker and Horton 2005 for details).

Since the sampling intensity of this badger carcass recovery programme was unlikely to be constant between years, we used a generalized mixed model (Crawley 2007) to infer the link between RTA counts and monthly temperature (procedure glmmPQL in R). The response variable, "RTA count", was modelled as a function of month as a fixed effect (to account the known seasonal pattern of RTA), monthly temperature as covariate and year as a random effect. This model allowed us to correct the within- year monthly carcass count according to the annual effort put into recovering carcasses. Thus, different slopes for month-temperature interaction would reveal any significant effect of temperature on RTA count for each month specifically. We stress that we are not testing seasonal impact on RTA count (as this has already been established, see (Davies *et al*. 1987), but rather whether the temperature in a particular month influences the RTA count for that month.

6.3 Results

6.3.1 Survival rates and climate variables

From the 1125 badgers' life histories recorded between 1987 and 2008, annual adult and juvenile survivals were determined using a '*Cormack-Jolly-Seber* ' model. Using a bootstrap method (100 replications) goodness of fit for these data was assessed giving a corrected variance inflation factor of $\hat{c} = 1.73$ ($\hat{c} = 1.73$). All outputs from estimation of survival rates were thus adjusted for this value.

Survival rates showed strong evidence for a negative relationship with T_s; and some evidence of weaker links with T_f (negative) and R_o (positive) (Table 6.1). A model with survival rates constrained by T_s, with a negative correlation, gained the greatest support ($w = 0.32$). The model with the second greatest AICc weight ($w = 0.27$), in addition to the previous model parameter, also constrained survivals by R_o, with a positive correlation. An added negative correlation with T_f was also well supported ($w = 0.20$). Finally, constraining survivals by T_s and T_f only also received reasonable support ($w = 0.20$).

6.3.2 Fecundity and climate variables

Fecundity showed strong evidence for a negative correlation with rainfall in May, R_m (Table 6.2). The two models with greatest support were both constrained for R_m and accounted for 99% for the Akaike weight. Strong evidence indicated that fecundity was positively correlated with R_o, with some support also for a negative correlation with T_m .

model	$\Delta QAIC_c$	w_{QAICc}	No. Par.	β_0	β_0^{ad}	β_{Ts}	β_{Ro}	β_{Tf}
$\{\varphi(Ts, g)\}$	0	0.32	75	0.73 (0.12)	0.73 (0.14)	-0.22 (0.06)		
$\{\varphi(Ts, Ro, g)\}$	0.37	0.27	76	0.73 (0.12)	0.74 (0.14)	-0.25 (0.06)	0.09 (0.07)	
$\{\varphi(Ts, Ro, Tf, g)\}$	0.90	0.20	77	0.71 (0.12)	0.76 (0.14)	-0.25 (0.06)	0.10 (0.07)	-0.09 (0.07)
$\{\varphi(Ts, Tf, g)\}$	0.95	0.20	76	0.73 (0.12)	0.75 (0.14)	-0.22 (0.06)		-0.08 (0.07)
$\{\varphi(Tf, g)\}$	11.33	0.001	75	0.72 (0.12)	0.74 (0.14)			-0.11 (0.07)
$\{\varphi(., g)\}$	11.44	0.001	74	0.73 (0.12)	0.72 (0.14)			
$\{\varphi(Ro, Tf, g)\}$	13.26	<0.001	76	0.72 (0.12)	0.74 (0.14)		0.02 (0.07)	-0.11 (0.07)
$\{\varphi(Ro, g)\}$	13.48	<0.001	75	0.73 (0.12)	0.73 (0.14)		0.01 (0.07)	

Table 6.1

Statistical summary of stage-specific survival rate models. Parameters ($\beta's$) standard errors are given in parentheses. The given parameter values link the survivals to a particular set of variables (group, temperature, rainfall) within a logistic regression. Model fit is indicated by: $\Delta QAIC_c$, the difference between $QAIC_c$, AIC values are corrected for small sample and for the variance inflation factor, and by w_{QAICc} , the Akaike weight (Burnham and Anderson 2004).

We note a strong indication for a negative relationship between stage-specific survival rates and September temperature, i.e. the first 3 models included this effect and accounted for over 99% of the AICc weight. A positive relationship between survivals and October rainfall was also well supported. Finally some support for a negative link between February temperature and survivals was found. Models were corrected for the variance inflation factor ($\hat{c} = 1.73$).

model	ΔAIC_c	w_{AICc}	No. Par.	β_0	β_{Rm}	β_{Ro}^{-1}	β_{Tm}
$\{f(Rm, Ro, Tm)\}$	0	0.78	5	-0.33 (0.02)	-0.34 (0.04)	0.17 (0.05)	-0.11 (0.05)
$\{f(Rm, Ro)\}$	2.57	0.21	4	-0.33 (0.02)	-0.33 (0.04)	0.14 (0.05)	
$\{f(Rm)\}$	10.3	0.004	3	-0.33 (0.02)	-0.29 (0.04)		
$\{f(Rm, Tm)\}$	10.7	0.004	4	-0.33 (0.02)	-0.28 (0.04)		-0.06 (0.05)
$\{f(Tm)\}$	60.5	<0.001	3	-0.33 (0.02)			-0.07 (0.05)
$\{f(.)\}$	60.7	<0.001	2	-0.33 (0.02)			
$\{f(Ro, Tm)\}$	63.4	<0.001	4	-0.33 (0.02)		0.01 (0.04)	-0.07 (0.05)
$\{f(Ro)\}$	62.7	<0.001	3	-0.33 (0.02)		-0.003 (0.04)	

Table 6.2

Statistical summary of fecundity models. Parameters are given with their standard error in parentheses and link the climate variables, temperature and rainfall, to the *log*-transformed fecundity. We note strong support for models including May rainfall as constraining factors and some support to constrain fecundity with October rainfall and may temperature. While May climatic conditions show negative correlation with fecundity, October rainfall shows a positively correlation with fecundity.

6.3.3 Spring rainfall, fecundity and juvenile parasitic load

Using a generalised linear model, juvenile parasitic load was positively related to May rainfall (Table 6.3).

The more rainfall was recorded for May, the greater the observed level of parasitic infection.

	Df	Likelihood-ratio χ^2	Wald χ^2	p-value	β covariate
Model	6	240734.3		<0.001	
R_m	1		12510.2	<0.001	0.54
M	5		132077.4	<0.001	

Table 6.3

Spring weather and parasitic infection. Statistical summary of a generalised linear model linking the level of parasite load (count of parasite) with the period at which the sample was taken (M) as a fixed factor, and the rainfall in May, R_m, as covariate. Temperature in May, as well as sex, was excluded from the model as non significant covariate, factor. We observe higher parasitic load correlates with greater level of May rainfall.

6.3.4 Late summer climatic conditions, survival rates and body weight

Using the variation in weight of 882 individuals during the study period, we found badgers generally increase their weight by 1.9 kg between summer - M_1: June / July - and autumn -M_2: late October / November. This weight gain was also influenced by the months in which weight was measured (M_1, M_2 and their interactions), by sex and by the climatic conditions prevalent in the late summer and early autumn trapping periods (Table 6.4). Specifically, T_s was negatively correlated with variation in weight, while R_o was positively correlated with weight variation.

	Df	F	p-value	R-sq	β covariate
Model	6	41.64	<0.001	0.22	
T_s	1	45.38	<0.001		-0.43
R_o	1	196.42	<0.001		0.86
sex	1	20.92	<0.001		
M_1	1	20.06	<0.001		
M_2	1	9.79	0.002		
$M_1 \times M_2$	1	14.39	<0.001		

Table 6.4

Weight gain in autumn. Statistical summary of a general linear model linking the variation weight with the period at which the samples were taken (M_1 and M_2) as a fixed factor, the temperature in September, T_s, and the rainfall in October, R_o, as covariate. We observe greater weight gain correlate with lower temperature in September and higher level of October rainfall.

6.3.5 Road Traffic Accidents

Badger RTA rates show considerable differences both within and between years (see Table 6.5, Figure 6. 1).

Our generalized mixed linear model indicated that RTA count and temperature were positively and strongly correlated only in January and February ($p < 0.001$ level: t-test, Table 6.5). The higher the average temperature is in February, the greater the RTA rate.

In November RTA count and temperature were negatively correlated, however this effect was less significant (t-test: $p<0.05$) and occurred within a month where RTA rate was less prominent (Figure 6. 1) resulting in little relative impact on the population.

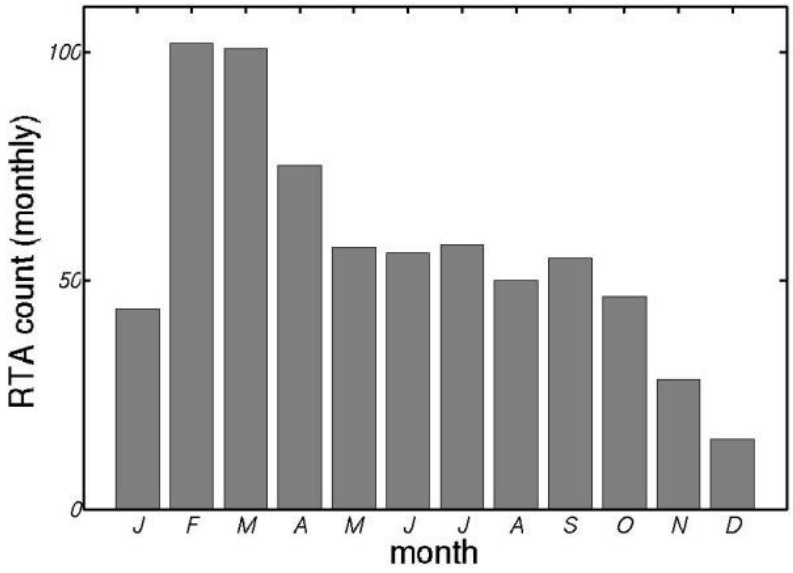

Figure 6.1

Mean RTA count nationwide in England by month. This graph shows a peak in RTA incidence during February and March.

Random effect: year												
			Variance components				Intercept			Residual		
							25.8%			74.2%		
Interaction: month-temperature												
	Jan	Feb	Mar	Apr	May	Jun	Jul	Aug	Sept	Oct	Nov	Dec
Slope - β	0.12	0.12	~0	~0	~0	~0	~0	~0	~0	~0	-0.13	~0
p-value	***	***									**	
t-test testing the null hypothesis $\beta = 0$,** p-value<0.01, *** p-value<0.001												

Table 6.5

Influence of temperature on RTA count. Summary result for the generalized mixed model. The top row indicate that 26% of the variance in the data analysed were due to effect of differences in year (carcass recovery effort), and that 74% of the residual variance remained to be explained. The bottom part summarise the interaction effect, testing the homogeneity of slopes RTA count vs. temperature for different month (with Poisson distributed error). It is clear that only January and February temperature have a very strong impact: high RTA count for those months correlated with higher temperature. November temperature seems to have an impact but as discussed would not greatly influence the population because of low rates of RTA this month.

6.4 Discussion

Climatic conditions are a defining element in the ecological niche characteristics in which organisms have evolved to live (Peterson *et al*. 1999; VanValen 1965), i.e. selection for a range of temperature and humidity to which their physiology is adapted and their behaviour optimised (Peterson *et al*. 2002). By extension, species consuming another organism (at all trophic levels) require climatic conditions suitable to ensure sufficient prey abundance. Interactions between climatic and anthropogenic pressures (e.g. road traffic accidents) could thus exacerbate the declining viability, or success, of a population.

The primary objective of this chapter was to evaluate if and how life history indices in badgers (in this case derived from Capture-Mark-Recapture models) correlate with climate indices. We found complex interactive effects, some of which were more intuitive than others. First, early autumn conditions presented a critical period for all aspects of badger population dynamics; mild (relatively cold) and moist conditions were beneficial for survival (juvenile and adult) and fecundity. This is consistent with the cycle of weight gain observed for badgers in the lead up to typically harsher winter conditions (see Macdonald and Newman 2002). Weather patterns that increase earthworm availability during this time of year are advantageous and here we found a positive benefit on bodyweight both within the population demographic data as well as at the individual level.

Secondly, spring weather was important for the fecundity of this population. That is, dry and cold springs promoted higher reproductive success. As wetting fur has been shown to halve its insulative properties (Webb and King 1984), we postulate that cub survival until first capture in early June benefits from drier conditions (i.e. cubs are vulnerable to hypothermia and exposure in their early weeks above ground), thus accounting for the observed increase in fecundity with drier/warmer spring conditions.

Thirdly, badger cubs are also highly susceptible to a coccidian parasite *Eimeria melis* (Anwar *et al*. 2000), which has a 100% prevalence when cubs are first trapped in late May / early June (Newman *et al*. 2001a), indicating a pervading pathology and morbidity through the period of development in the natal nest chamber. *E. melis* causes malabsorption of nutrients, diarrhoea, steatorrhoea, and subsequent fluid loss and

electrolyte imbalance (Lindsay *et al*. 1997). Therefore, harsh conditions persisting into the spring would additionally expose vulnerable cubs to hypothermic stress, which could tip the balance for their survival, reflected in apparent fecundity (i.e. our measure of how many cubs we trap, post-weaning, per female). We tested and confirmed a link between high rainfall in spring and higher level of parasitic infection in cubs, again reinforcing our population demography results. It is thus possible to suggest a possible mechanistic explanation where the link between cubs' survival and climate could be mediated by a link between on one hand climate and parasitic infection and on the other hand cub's survival and parasitic infection.

A further, somewhat counter-intuitive, result (see (Macdonald and Newman 2002) across this extensive data interval, however, guided us toward a significant climatic impact on badger populations. Our analysis revealed that warm conditions late into winter were disadvantageous for survival of both juveniles and adults. This unexpected improvement in badger survival under harsher weather conditions was a consistent trend in the data for both juveniles and adults. The explanation lies in the tendency of badgers to enter carnivorean lethargy in cold winters, and to be more active in mild winters. Our analyses indicated that there was a strong predictive relationship between temperature (especially in February) and RTA rate within the established seasonality of badger road traffic accident patterns (Clarke *et al*. 1998; Davies *et al*. 1987). Badgers are adapted to survive the winter months underground in their setts, going into extended periods of physiological torpor to conserve energy during cold weather when feeding opportunities are limited (Fowler and Racey 1988). However, during milder conditions they continue to be active above ground, exposing themselves to greater risks than if they were securely inactive (Davies *et al*. 1987; Neal and Cheeseman 1996). Crossing roads can be hazardous for wildlife (Caro *et al*. 2000; Case 1978; Oxley *et al*. 1974). Crossing roads in winter poses additional risks, with long periods of darkness, fog, highway-spray etc reducing the motorists' ability to observe a medium-sized grey animal in the road. Case (1978) highlights several species for which RTA incidences are annually bimodal with the lowest rates occurring in winter when activity is at its lowest. Philcox *et al*. (1999) report that RTAs for otters (*Lutra lutra*) peak in early and late winter in the UK, when crepuscular emergence times coincide with evening and morning rush hours.

National data show that badger RTAs are most prevalent in February, and road mortality is exacerbated in milder years. As the post-partum mating season of the

Eurasian badger also starts in February, it is likely that milder conditions result in longer excursions including more road crossings to find potential mating partners. February is also a time when juvenile dispersal has been reported to peak in some populations, prior to the next cohort's birth (Neal and Cheeseman 1996). Although dispersal is low in our study population (Macdonald *et al*. 2008), we record in this study that in warmer Februarys fewer juveniles survive. Dry soil conditions in the winter, and particularly January were also detrimental to survival, especially for juveniles, which may be driven to forage further afield, exposing them to greater RTA risk, rather than succumbing directly to starvation. Coulson (1997) reports that eastern grey kangaroos (*Macropus giganteus*), and swamp wallabies (*Wallabia bicolor*) are susceptible to climate-related rates of RTAs, with drought exacerbating mortality rates. Saeki and Macdonald (2004) also report significant seasonal variation in RTA rates for the raccoon dog (*Nyctereutes procyonoides viverrinus*) in Japan, but with no reference to any inter-annual effect of temperature on RTA rate within season or month. Inbar and Mayer (1999) report spatio-temporal trends in armadillo (*Dasypus novemcinctus*) RTA rate in central Florida. Like badgers, armadillos tend to be less active in the winter, but this study makes no direct correlation between activity and temperature, simply armadillos expose themselves to less RTA risk with reduced winter activity.

We emphasise here that there are many mechanisms that underlie population regulation, which work simultaneously and interactively. Notably, the advantages warmer winter weather conditions conferred to survival, and thus population size, as observed by Macdonald and Newman (2002; examining a subset of data from this same population, 1987-1998) seem now to be less evident, or more complicated, with the population at a higher, seemingly climate-mediated, carrying capacity (see also Macdonald *et al*. 2009). Mild winters in combination with protracted cold into wet late spring appear to be detrimental for badger populations; the reverse being positive. Mild and wet conditions during late summer early autumn had positive impact on both survival and fecundity. Importantly, equinoctial conditions produced significant population driver effects. That is, while summers will always be relatively warm compared to winters, spring and autumn weather can be more variable. In phenological terms, the gradient of change in weather conditions between the solstices, and the duration of nominally productive vs non-(less-) productive seasons appeared to coincide with the most pronounced life-history parameter effects.

The finding that climatic trends, through proximate changes in weather patterns, might influence a population intrinsically through interaction with vital demographic rates, mediated by food supply, proved to be only part of the story. Seasonal mortality, mediated by activity patterns and consequently road traffic accidents, adds an intriguing dimension to mechanisms regulating badger populations. That RTA rate was also a direct and highly significant product of seasonal temperature only serves to underline the intricate ways in which changing climate might interact with anthropogenic agents to influence population processes of a variety of species.

6.5 Acknowledgements

This study would not have been possible without the efforts of the badger trapping team, past and present. We are especially grateful for comments from Stephen Dobson, Tim Coulson, Sarah Randolph and Mike Bonsall on this manuscript, which directed much of our approach to this study. The contribution of RTA data by Stephen Coleman and Andy Mitchell at DEFRA / VLA was also extremely helpful. The Peoples Trust for Endangered Species generously supported much of this core study, with additional financial support from the Earthwatch Institute. Work was carried out under Natural England Licences, currently 20001537 and Home Office Licence PPL 30/2318.

Chapter 7

Can Unpredictable Weather Predict Population Dynamics?

Long-term Responses to Increasing Climate Instability in a Population of European Badgers (*Meles meles*)

A slightly modified version of this chapter was submitted to *Plos Biology*. Authors of the submitted paper are listed below:

Pierre Nouvellet, Christina D. Buesching, Chris Newman, David W. Macdonald

Abstract

Climate influences population in numerous ways, from determining home range size through primary productivity to tuning demographic parameters through survivorship. Rapid climate change could thus have a dramatic impact on biodiversity by reshaping local species diversities. Many species having evolved in a 'stable' environment, and changing climate is likely to have fitness consequences as a result of selection to adapt to new conditions. We present a new index, the Weather Unpredictability Index (WUI), that reflects inconsistency of prevailing weather patterns relative to historical conditions. This index, based on local climatic conditions, is sensitive to change in averages, timing and variation around average conditions.

For a site near Oxford, a WUI for temperature confirms a trend towards increasing unpredictability. There was no such trend for a rainfall WUI. A long-term monitoring program of badger in the area allowed us to test whether such WUIs were correlated with demographic parameters, e.g. survival and fecundity. We found strong evidence of a negative link between temperature unpredictability and all demographic parameters. Evidence for a similar link with the unpredictability of rainfall was weaker, perhaps reflecting the observed lack of increase in that WUI.

The WUI provides a new approach to facilitate rapid assessment of the likely impact of climate change scenarios on species. From simulated data, badger populations are at minor risk from climate change due to their adaptability as reflected in their wide Eurasian distribution.

7.1 Introduction

Life history strategies are shaped by environmental constraints. Stable conditions, where 'typical' environmental conditions are well defined and thus more predictable, generally favour specialist species while changing environments will benefit more generalist species (Begon *et al*. 2006b). Changes in stable environmental conditions thus have fitness consequences (Reed *et al*. 2009).

Climate is a defining characteristic of an ecosystem (Begon *et al*. 2006b), and thus its variability has been investigated extensively in population ecology (Andrewartha and Birch 1960; Birch 1957; Root *et al*. 2003; Stenseth *et al*. 2002; Thomas *et al*. 2004; Walther *et al*. 2002). In the context of climate change, recent climatic variations may have important implications for the phenology, distribution and the population dynamics of animals and plants in both terrestrial and aquatic ecosystems (Drake 2005; Jonzen *et al*. 2006; McCarty 2001; Parmesan 2006; Parmesan *et al*. 1999; Post and Stenseth 1999; Root *et al*. 2003; Saino *et al*. 2007; Visser and Both 2005; Walther *et al*. 2002). This has raised serious concerns about the potential for climate change to impact on global biodiversity (IPCC 2002; IPCC 2007b; Parmesan 2006; Thomas *et al*. 2004; Visser and Holleman 2001; Visser *et al*. 1998).

Recent climate changes represent a departure from established environmental conditions, that is, the frequency and amplitude of more extreme events is exceeding the time-dependent average range of conditions within which natural, and human, coping mechanisms have developed (Alley *et al*. 2003; IPCC 2008; le Roux and McGeoch 2008). While climate change can benefit some species (e.g. generalist species), evidence of negative impacts of climatic instability on species demography has been accumulating (Adler and Drake 2008; Drake 2005; Hughes 2000; IPCC 2007b). Species extinction – from local extirpation (Thomas *et al*. 2004) to catastrophic global species loss (Parmesan 2006), is the most severe consequence of negative climatic interactions. Demographic interactions with climate, however, may be more subtle, manifesting as a decrease in survival or fecundity parameters (Kausrud *et al*. 2008; Stenseth *et al*. 1999; Stenseth *et al*. 2003), a detrimental phenological adjustment (Visser and Holleman 2001; Visser *et al*. 1998) resulting in asynchronous inter-specific interactions (Parmesan 2006), or reduction in species distribution (Parmesan 2006; Parmesan *et al*. 1999).

Observing historical records of temperature for a particular day (e.g. 1st of January) provides an estimation of the distribution of temperature for that day. If a recent temperature for that date is contrasted with the estimated distribution and represents an outlier, this may perturb an organism in terms of its capacity to accurately anticipate conditions and optimise its behavioural or physiological response.

Thus, the more extreme, or the more often perturbations occur, the less successful the animal's established life-history strategy, and the more strained its capacity for short-term tactical adaptation. Defining the degree of deviation of weather conditions from historical expectations thus establishes a Weather Unpredictability Index (hereafter WUI), with high WUI values reflecting highly unpredictable climatic conditions, i.e. the higher the WUI value, the greater the potential perturbation to population demographics. WUI is sensitive to changing in climatic parameters, as defined previously (i.e. changes in averages, time-dependencies, variation around averages, and the frequency/intensity of extreme events).

In this final research chapter, considering WUIs as predictors of demographic responses, we aim to demonstrate that:

1) WUIs have increasing values during the last 5 decades, as climate is changing.
2) At the demographic level, increasing unpredictability will be associated with a decrease in demographic parameters, such as survival and fecundity, resulting in a negative correlation with increasing WUI values.
3) Finally we aim to establish the possible impacts of climate change on particularly vulnerable species using projections of risk analysis.

We model our investigation on a badger, *Meles meles*, population at Wytham Woods, Oxfordshire, UK. The population dynamics of badgers at this location have been well established from a long-term monitoring programme (Macdonald and Newman 2002; Macdonald *et al*. 2009) and these consistent and continuous data can be contrasted with long-term weather data for the same region (*Oxford Radcliffe Meteorological station, School of Geography* Oxford, UK). The badger is an exemplary species with which to consider potential climate change impacts on population dynamics as *Meles* has an extensive geographical range, stretching across Europe and Asia from the Arctic Circle to the Mediterranean, and exhibits considerable socio-spatial adaptability (reviewed by (Kruuk 1978c; Macdonald and Newman 2002; Woodroffe *et al*. 1995).

Badger populations are regulated principally by the fluctuating availability and dispersion of food resources (e.g. Carr and Macdonald 1986; Dasilva *et al*. 1993; Johnson *et al*. 2002; Kruuk 1978a; Macdonald and Newman 2002). Badgers have no contemporary predators in Britain; thus, aside from disease (e.g. (Newman *et al*. 2001b) there are few natural factors that could result in "top-down" population regulation (*sensu* (Vucetich and Peterson 2004). Previous analyses of population dynamics have already detected links with climatic trends (Johnson *et al*. 2002; Macdonald and Newman 2002).

7.2 Materials and methods

7.2.1 Study site and population

The study site and population was as described in the previous Chapter (see Chapter 6 section 6.2.1).

From 1987 to 2008 inclusive, 1125 badger life histories were included in this study. 70.7% of the badger population was first caught as cubs, highlighting the high capture rate in our study. A low degree of immigration/emigration in this population was recorded allowing the use of closed models (Macdonald *et al*. 2008).

7.2.2 Climate data

Daily temperature and monthly rainfall figures were obtained from the Radcliffe Meteorological station, School of Geography, University of Oxford. Daily temperatures were available from 1881 to 2008, and monthly rainfalls (daily figures were not available) from 1767 to 2008.

7.2.2.1 *Estimation of expected climate based on historical record:*

In order to determine the 'stable' climate conditions under which a population became established (here our focal badger population), historical mean temperature and rainfall

data for as many years as possible are advantageous. However if climate has changed recently, ideally, analyses would be based on historical data prior to any recent climatic change. As climate has changed most dramatically, due to anthropogenic forcing, during the last 50 years (IPCC 2007b; IPCC 2008), we opted to define the historical pattern as that prevailing up to 1950. A study of great tits at this same research site location (Charmantier *et al*. 2008) showed most pronounced changes in temperature during the last 40-50 years, giving us confidence in our defined study interval. Thus analyses of long-term daily temperature and monthly rainfall averages are defined by the periods between the instigation of weather recording (1881 and 1767 respectively) and 1950.

For reasons of biological relevance, we define 'years', hereafter, to run from 1st March, which corresponds approximately with the peak date of parturition in our study population.

Expectations for daily temperature were taken to equal the predicted values of a linear model relating day of the year, as covariate, with daily temperatures observed between 1881 and 1950. The degree of the regression (i.e. quadratic or cubic regression) was assessed using an F-test, and predicted values are taken from the most parsimonious model. Expectations for monthly rainfall were derived similarly, using the 1767-1950 dataset.

7.2.2.2 *Defining and calculating temperature and rainfall unpredictability indices*

Yearly indices for temperature and rainfall were defined to reflect weather unpredictability. These indices are the mean of the squared anomaly in temperature (or rainfall) for any particular year. This anomaly is defined as the deviation from historical expectation, as derived above.

Specifically, temperature unpredictability index for year *j*, ΔT_j, was defined:

$$\Delta T_j = \frac{\sum_{i=1}^{n}\left(t_{i,j} - T_i\right)^2}{n}$$

With $t_{i,j}$ representing the temperature on day *i* of year *j*, and T_i representing the expected temperature from historical record for day *i*. Year *j* has n days.

Similarly, rainfall unpredictability index for year *j*, ΔR_j, was defined as

$$\Delta R_j = \frac{\sum_{i=1}^{n}\left(r_{i,j} - R_i\right)^2}{n}$$

With $r_{i,j}$ representing the rainfall during month *i* of year *j*, and R_i representing the expected rainfall from the historical record for month *i*. Year *j* has n months.

Where typical conditions are established and defined from historical data, increasing values of the WUI will reflect deviant conditions that would be regarded as unpredictable.

It is important to note here that the index presented will not be specific of the change but rather will be sensitive to any kind of change (i.e. increase in the amplitude of seasonal change in weather or increase in fluctuation around the expected values). Furthermore, we need to be careful using them as the frequency of weather records (i.e. either daily or monthly) will have a great effect on their values.

7.2.3 Using WUIs to predict demographic parameters (survival and fecundity)

Badger population dynamics have been modelled successfully using stage-classified matrix models (Macdonald *et al*. 2009) also known as Leslie matrices (Leslie 1945). In the matrices we define the survival of sexually mature and immature individual's (juveniles [cubs to <1 year old] and adults [1 and >1]: P_j *and* P_a), and fecundity (*F*). Here we estimated survival and fecundity sequentially, using the mark-recapture framework (implemented in the MARK program, (White and Burnham 1999, version 6.0).

Our focus is on demography change rather than behavioural adaptation per se, so capture rate was treated as both time- and group-dependent (i.e. for juveniles and adults) for all model scenarios.

Throughout our study we rely on a demographic history file stretching from 1987 to 2008, documenting the capture events of 1125 individual badgers, each of which was caught between 1 and 33 times.

7.2.3.1 *The link between survival rates and WUIs*

Estimates of juvenile and adult survival rates, using the '*Cormack-Jolly-Seber* ' model (Jolly 1965; Lebreton *et al*. 1992), were used to construct a primary model, dependent upon year, $\{\varphi(y, g)\}$. This model was checked for goodness of fit using bootstrap methods (White 2002), allowing approximation of a corrected variance inflation factor ($\hat{c}$). Intervals between trapping sessions (between 2 and 7 months) were not constant throughout the study, thus we defined the time interval between trapping events manually to obtain yearly survival values. In all models presented survival rates were considered to be binomially distributed with a binary response (survived or not/died) and thus modelled using logistic regressions.

Using a multi-model selection procedure (Burnham and Anderson 2002; Burnham and Anderson 2004; Whittingham *et al*. 2006), we compared a number of models with which to describe variation in P_j *and* P_a, constraining some with WUIs. We began with the simplest model: survival held constant, $\{\varphi(.\,, g)\}$, subsequently assessed the implication of adding WUIs as constraints to survival, $\{\varphi(\Delta T, g)\}$ $\{\varphi(\Delta R, g)\}$ $\{\varphi(\Delta T, \Delta R, g)\}$, and finally modelled WUIs constraints operating to independent extents on adult and juveniles, $\{\varphi(\Delta T * g)\}$ $\{\varphi(\Delta T * g, \Delta R)\}$ $\{\varphi(\Delta R * g)\}$ $\{\varphi(\Delta T, \Delta R * g)\}$ $\{\varphi(\Delta T * \Delta R * g)\}$.

7.2.3.2 *The link between fecundity and WUIs*

The estimate of fecundity, *F*, in our closed population, was equivalent to the estimate of recruitment, directing us to use the '*Pradel'* model in this analysis (Pradel 1996). Because the Pradel approach, however, does not allow the specification of age classes, a full model estimating both P_j and P_a, and fecundity *F* was not feasible. This leads us to perform separate analyses for survival and fecundity. Fecundity was estimated as the number of emerging offspring (surviving at least their 3 first month) per individual and per year, displaying a Poisson distribution, directing us to model it using a *log* link function. Again, we stress here that our fecundity approximations measure the number of cubs per females but also include a measure of cub survival from birth until

emergence (approximately after 3 months). For sake of simplicity we will use the term fecundity henceforth to refer to this apparent fecundity

In these 'Pradel' models, recruitment was constrained to a non-zero value only for the first trapping per annum following March (e.g. early June), the time when cubs are born. A set of models, with F as a constant, or dependent upon WUIs, was evaluated: $\{f(.)\}$, $\{f(\Delta T)\}$, $\{f(\Delta R)\}$, $\{f(\Delta T, \Delta R)\}$.

The values for survival and capture probabilities were fixed to predetermined values. Those values were estimated using a CJS model with survival rates dependent on year and capture rate dependent on trapping occasion.

7.2.4 Projection of future population viability

In establishing a relationship between demographic parameters, $\{Pj\ , Pa$ and $F\}$, and WUIs, $\{\Delta T$ and $\Delta R\}$, it becomes possible to project viability scenarios for the population under different future weather regimes.

Two conservative scenarios were considered: (i) future WUIs follow the same trend (in increasing levels of unpredictability) that has been observed during the 5 past decades, (ii) future WUIs stabilise at the most recently level observed (i.e. the *expected* value, from the regression line see Figure 7.1a, of WUIs for 2008 will remain steady onward).

To generate realistic projections of possible future WUIs under both scenarios, one needs to define not only trends (see above case (i) or (ii)) but also the extent of associated variation around these trends (Boyce *et al*. 2006). We assume, for simplicity, that variance in a WUI is unaffected by climate change thus could be directly measured from the data. WUIs values were considered as normally distributed.

A thousand stochastic estimates (reflecting different realisations of the same trend) of weather variability were constructed for the next 500 years following each scenario. Survival rates and fecundity values (linked to WUIs) were determined using results from accompanying analyses, with initial populations ranging from 15 to 1000 individuals. Finally, for both scenarios and each initial population size, we compute an expected extinction probability (here extinction was defined as a population size of less than 10 individuals).

Finally, using simulation, we establish the critical value of ΔT that is predicted to lead to population extinction.

7.3 Results

7.3.1 Climate data

7.3.1.1 *Estimation of expected climate based on historical record*

Within-year, daily temperature (from 1881 to 1950) showed a periodic variation (Figure 7.1.a inset) that could be accounted for by a four-degree polynomial (R^2=0.698 and $p<0.05$). Predicted values for daily temperature are shown in the Figure 7.1.a -inset. These values are used subsequently as the expected historical baseline values, with which we calculate the Temperature Unpredictability Index, ΔT.

Within-year, monthly rainfall (from 1767 to 1950) showed only a slight periodic variation (Figure 7.1.b -inset) that could be accounted for by a two-degree polynomial (R^2=0.068 and $p<0.05$). The low value of R^2 indicates that most of the variance in rainfall remains unexplained after month is taken into account. The predicted values for monthly rainfall are shown in the Figure 1.a -inset. These values are used subsequently as the expected historical baseline values with which we calculate the Rainfall Unpredictability Index, ΔR.

7.3.1.1 *Calculation and trends in WUIs*

From predicted daily temperature values (solid line inset of Figure 7.1.a), Temperature Unpredictability Index, ΔT, was derived for each year (from 1950 to 2008) and plotted in Figure 1.a (main). ΔT showed a significant (R^2=0.08, $p<0.05$) and increasing trend with time (solid line in Figure 7.1.a -main). This is indicative of temperature becoming increasingly unpredictable over the last 5 decades.

From predicted monthly rainfall values (solid line inset of Figure 7.1.b), a Rainfall Unpredictability Index, ΔR , was also derived for each year and plotted in Figure 7.1.b

(main). No significant changes were observed in ΔR in Oxford during the last 50 years, indicating that there was no trend during this period.

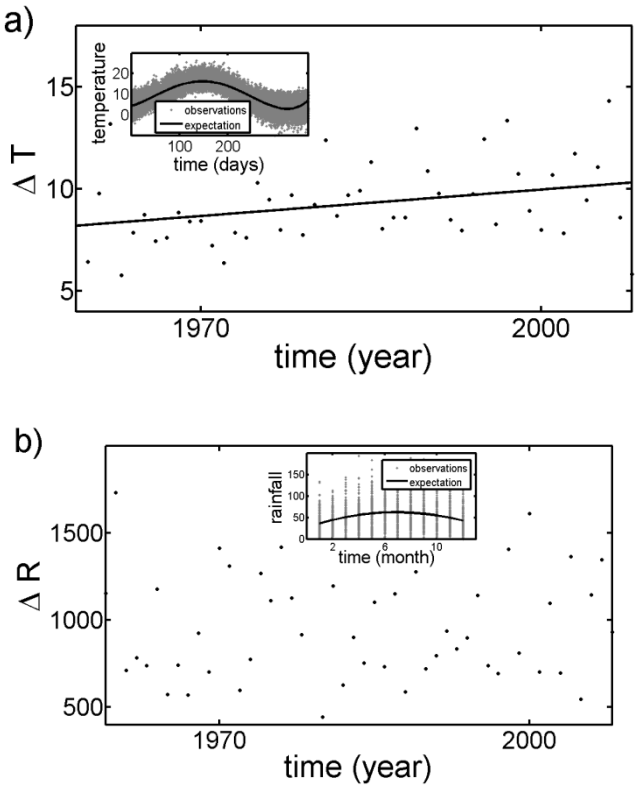

Figure 7.1

Temperature (**a**) and Rainfall (**b**) Unpredictability Index (ΔT and ΔR), in Oxford for the last 5 decades. WUIs were calculated as the mean square anomalies over a year. Anomalies in this context were derived against the historically predicted variation of temperature or rainfall during the year, see inset. Daily historical expectations of temperature were derived from a 4-degree polynomial of daily temperature from 1881 to 1950, leading to the solid curve/line (predicted daily temperature) in Figure **a** -inset. Monthly historical expectations of rainfall were derived from a 2-degree polynomial of rainfall from 1967 to 1950, leading to the solid curve/line (predicted monthly rainfall) in Figure **b** -inset.

ΔT, (points shown in main Figure **a**), increased during the last 50 years (R^2=0.08, $p<0.05$) as illustrated by the solid curve/line in the main figure; no trend was found for ΔR ($p>0.05$), (points in main Figure **b**).

7.3.2 Using WUIs to predict demographic parameters (survival and fecundity)

7.3.2.1 *Survival rates and WUIs*

The 'goodness of fit' of the model, a '*Cormack-Jolly-Seber*' model to derive annual adult and juvenile survival rates (from 1125 badger life histories), was assessed using a bootstrap method (100 replications) and a corrected variance inflation factor was determined ($\hat{c} = 1.73$). All outputs from the estimation of survival rates were thus adjusted for this value.

P_j *and* P_a both showed strong evidence for a negative relationship with ΔT; while ΔR showed a less supported, but positive, correlation with survival rates (Table 7.1). A model with P_j *and* P_a both constrained in the same way by ΔT, gained the greatest support (*w = 0.36*). The model with the second greatest AICc weight (*w = 0.22*, $\Delta QAIC_c = 0.97$), in addition to the previous model parameters, also constrained survival rates by ΔR (in the same way for adults and cubs), followed by a model constrained by ΔT only (*w = 0.13*, $\Delta QAIC_c = 2.05$) but a slightly different trend (regression slope) for P_j and P_a against ΔT.

P_j and P_a were thus mainly influenced by ΔT, with little influence of ΔR, and weak evidence of an interaction term (i.e. P_j and P_a being linked differently to a WUI). Survival of both adults and juveniles thus seems to be correlated negatively with ΔT., i.e. the more unpredictable temperature the lower survival rates.

model	$\Delta QAIC_c$	w_{QAICc}	No. Par.	β_0	β_0^{ad}	$\beta_{\Delta T}$	$\beta_{\Delta R}$	$\beta_{\Delta T}^{int}$ (apply to adult)	$\beta_{\Delta R}^{int}$ (apply to adult)
$\{\varphi(\Delta T, g)\}$	0	0.36	75	1.87 (0.41)	0.75 (0.14)	-0.11 (0.04)			
$\{\varphi(\Delta T, \Delta R, g)\}$	0.97	0.22	76	1.53 (0.52)	0.75 (0.14)	-0.11 (0.04)	0.0003 (0.0003)		
$\{\varphi(\Delta T * g)\}$	2.05	0.13	76	1.90 (0.70)	0.70 (0.83)	-0.11 (0.07)		0.005 (0.08)	
$\{\varphi(\Delta T, \Delta R * g)\}$	2.26	0.12	77	1.26 (0.61)	1.16 (0.49)	-0.10 (0.04)	0.0006 (0.0004)		-0.0004 (0.0005)
$\{\varphi(\Delta T * g, \Delta R)\}$	3.01	0.08	77	1.59 (0.76)	0.66 (0.83)	-0.11 (0.07)	0.003 (0.003)	0.009 (0.08)	
$\{\varphi(\Delta T * \Delta R * g)\}$	4.32	0.04	78	1.27 (0.84)	1.14 (1.01)	-0.11 (0.07)	0.0006 (0.0004)	0.002 (0.08)	-0.0004 (0.0005)
$\{\varphi(\Delta R, g)\}$	5.92	0.02	75	0.34 (0.29)	0.73 (0.14)		0.0004 (0.0003)		
$\{\varphi(., g)\}$	6.12	0.02	74	0.73 (0.12)	0.72 (0.13)				
$\{\varphi(\Delta R * g)\}$	6.87	<0.01	76	0.06 (0.39)	1.22 (0.48)		0.0007 (0.0004)		-0.0005 (0.0005)

Table 7.1

Statistical summary of stage-specific survival rate models. Parameter values link survival rates to a particular set of variables (group, ΔT or ΔR) within a logistic regression. Standard errors are given in parentheses.

We note a strong negative relationship between stage-specific survival rates and ΔT, i.e. the first 6 models included this effect and accounted for 97% of the AICc weight. A relationship between ΔR and survival rates was supported only weakly and the associated parameter, $\beta_{\Delta R}$, had a large standard error. Models were corrected for the estimated variance inflation factor ($\hat{c} = 1.73$).

7.3.2.1 *Fecundity and WUIs*

Fecundity was constrained by either ΔT, ΔR, or both, of which the latter gave the best fit ($w = 0.55$) (Table 7.2). A model constrained by ΔT only was also well supported ($w = 0.37$), i.e. fecundity was negatively correlated with temperature unpredictability, ΔT (strong evidence), and rainfall unpredictability, ΔR (weaker evidence).

model	ΔAIC_c	w_{AICc}	No. Par.	β_0	$\beta_{\Delta T}$	$\beta_{\Delta R}$
$\{f(\Delta T, \Delta R)\}$	0	0.55	4	1.00 (0.33)	-0.10 (0.03)	-0.26E-3 (0.17E-3)
$\{f(\Delta T)\}$	0.37	0.45	3	0.69 (0.26)	-0.10 (0.02)	
$\{f(.)\}$	14.31	<0.01	2	-0.33 (0.02)		
$\{f(\Delta R)\}$	15.27	<0.01	3	-0.17 (0.16)		-0.17E-3 (0.17E-3)

Table 7.2

Statistical summary of fecundity models. Parameter values link variables ΔT and ΔR, to the *log*-transformed fecundity. Standard errors are given in parentheses. We note good support for models including both ΔT and ΔR, as constraining factors, and for ΔTalone (55% and 45% of the AICc weight respectively), indicative of a negative relationship between fecundity and both ΔT and ΔR.

7.3.3 Projection of future population viability

Both juvenile and adult survival rates and fecundity were linked to temperature unpredictability, ΔT. Based upon the observation that the current (last 50 years) trend in ΔT was to increase (Figure 7.1), we constructed a set of predicted yearly ΔT values *over the next* 500 years, on the assumption that :

- (i) trend of ΔT to increase with time will persist, i.e. we determine

$$\Delta T_y = \beta_0 + \beta_1 y + \varepsilon$$

With y, the year of interest, $\beta_0 = -78.21$ and $\beta_1 = 4.42 \times 10^{-2}$ from Figure 7.1a -main, and ε drawn from normally distributed random variables with mean 0 and $\sigma=2.11$ (standard deviation of the residual generated from the relation between ΔT and years).

- (ii) future ΔT remains similar to ΔT in 2008, i.e:

$$\Delta T_y = \beta_0 + 2008\,\beta_1 + \varepsilon$$

With the same notation as above.

In scenario (i), with ΔT projected to continue its trend to increase, our projections result in inevitable long-term population failure; that is, out of 1000 iterations, all finished below the critical threshold of 10 individuals. This result was independent of initial population size values (from 15 to 1000). The average time to crash was approximately 170 years (157 years, *SE* 0.24 when starting with 15 individuals; 183 years, *SE* 0.20, when starting with 1000 individuals).

By contrast, in scenario (ii), where ΔT remained constant from 2008 onwards, no simulations, regardless of the initial population size, showed decreases below the critical threshold value (e.g.: probability of extinction $p<0.001$).

Similarly using simulation we determine that regardless of the initial population, if ΔT takes values greater than 14.1, then more than 95% of the thousand simulated populations would decrease below the critical threshold value. We must stress that this values of ΔT is highly specific upon the frequency of recorded temperature.

7.4 Discussion

The study of climate and population dynamics can be categorised into those using local measures of climate (Charmantier *et al*. 2008; Husby *et al*. 2009; Saino *et al*. 2007; Valeix *et al*. 2008; Visser and Holleman 2001) and those using global indices of climate (e.g. El Niño, the North Atlantic Oscillation) (Hallett *et al*. 2004; Sandvik *et al*. 2008; Stenseth *et al*. 2002; Stenseth *et al*. 2003; Vargas *et al*. 2006; Vargas *et al*. 2007).

An advantage of analysing local weather is to reveal the direct mechanistic link between local conditions and population dynamics (Ben Ari *et al*. 2008; Charmantier *et al*. 2008; IPCC 2002; Sandvik *et al*. 2008). However, characterising relevant candidate variables (temperature, humidity, wind, etc.) and the timing of importance (i.e. winter vs. summer temperature) is difficult, and the problem can be overcome only by a thorough knowledge of the focal species natural history (Sandvik *et al*. 2008; Visser 2008). Moreover, if the aim is to predict future population status, further difficulties arise when trying to establish future trends for local weather (IPCC 2008).

In contrast, global indices are readily available and may correlate with greater veracity with demographic parameters as they reflect various aspects of local weather (Hallett *et al*. 2004). Also, global indices, by bypassing the mechanistic links between climate and demography, offer advantages when conclusions need to be drawn quickly (but, hopefully, not precipitously). In the context of climate change, and particularly for species at risk of extinction, this may be crucial, as the need for mitigation may be urgent (IPCC 2002; Thomas *et al*. 2004). As the nature of the relationships between atmospheric dynamics, ocean circulation and local condition changes (Alley *et al*. 2003; Karl and Trenberth 2003; Meehl *et al*. 2000) however, there is considerable uncertainty as to how past relationships between biological systems and these global indices might reflect responses to ongoing anthropogenic climate change.

In this context, a WUI, as presented here, offers numerous advantages. It is locally defined, guaranteeing the stability of the direct mechanistic link between the organism and climate, and its use does not require such a thorough appreciation for the nuances of the organism's life history. It is also more straightforward to generate future projections for WUIs (IPCC 2008).

One could argue that the approach presented here have undesirable properties. First weather could be unpredictable in many ways, i.e. increase in global average, increase in seasonal variability or increase in daily fluctuations. Our index of weather variability does not distinguish between those effects and thus we are unable to specify which component is effectively influencing population dynamics. Secondly, values of the WUIs are highly sensitive to the frequency of climate record, thus making comparative study difficult. However we believe it is still a useful approach as being very pragmatic and easy to implement.

In this study, we hypothesised that climate change would be reflect in WUIs and that, more importantly, such indices would incur population dynamic responses.

Badger population demographic trends showed strong negative correlations with the increasing WUI for temperature, thus we conclude that changes in the historically established pattern of temperature variations are detrimental to badger survival rates and fecundity. The link between demographic parameters and a rainfall WUI was less supported and of lesser magnitude. While unpredictable rainfall would notionally also be detrimental for fecundity (see Chapter 6), no strong signal is detected as the level of unpredictability observed in rainfall recently remains similar to the historical baseline.

Having established the link between demographic parameters and WUI, our simulations of future population viability projected that unpredictability could threaten the population's tolerance for adaptive response. Such a scenario, under which the unpredictability of weather increases steadily, might be extreme, however in such circumstance our parameter values indicate that this badger population would become extinct within 200 years. Less dramatic scenarios of future trends of weather unpredictability would be less damning for the badger population, reflecting their capacity climatic adaptability.

Species can be classified on a continuum between generalist/opportunist to specialist (Begon *et al*. 2006b) reflecting different sensitivities to environmental change. The potential to adapt to rapid climatic changes through phenotypic plasticity varies intra-specifically (Charmantier *et al*. 2008; Husby *et al*. 2009; Visser *et al*. 1998); therefore when phenotypical plasticity is limited, there could be serious implication for the viability of the species. While generalists may be less susceptible to the immediate

implications of changing climatic pressures (Bernays and Funk 1999), they remain vulnerable to perturbations (McDermott *et al*. 2008).

In conclusion we present here a new method using an index of weather condition unpredictability, and demonstrate a link between this index and the population dynamics of a badger population. It is clear that climatic unpredictability could become a significant population stressor for this population, and populations of many other species in the future, which would test their capacity for optimal risk prospecting and tactical behavioural responses, in turn bringing future demographic viability into question. Thus appropriately informed conservation strategies will become ever-more essential.

7.5 Acknowledgements

This study would not have been possible without the efforts of the badger trapping team, past and present. We thank Tim Coulson for helpful discussion which helped define the core concept of this paper. We are especially grateful for comments from Paul Johnson on this manuscript. The Peoples Trust for Endangered Species generously supported much of this core study, with additional financial support from the Earthwatch Institute. Work was carried out under Natural England Licences, currently 20001537 and Home Office Licence PPL 30/2318.

Chapter 8

General Conclusions and Future Work

The work presented for this thesis is close to the format of research articles, hence each chapter includes its own discussion of the results. The following concluding remarks draw general conclusions, and explore possible avenues for future research.

In the first part of this thesis, we explored the foraging behaviour of Pharaoh's ants. The first chapter described a new model to investigate correlated random walk. Its novelty relies on two characteristics: the movement is described in continuous time as to reflect with greater accuracy its biological features; focus is brought on the mean square displacement as the essential quantity underlying animal movement. This model was shown to remarkably well predict characteristics of real ants' movement (i.e. their angular distribution when discretised). Finally this model may prove very useful as animal trajectories can not only be described accurately but also simulated under the same framework. The second chapter applied this to simulate foraging behaviour. Using an extensive range of simulations, I investigated the optimal walking strategies of animal while searching for food. Various predictions are made which could be testable given the appropriate knowledge of the species of interest. Finally, an important feature when considering foraging behaviour, and somehow related to animal movement, is the rate at which individuals explore their environment. In the final chapter, I constructed an explicit null model describing the rate of exploration of ants and showed again great

accuracy in predictions based on experiments involving ants. Importantly this model relies on the assumption that no interaction between individuals regulates their exiting behaviour. This model thus provides a method to test this assumption for a wide range of species or situation.

A striking feature of the ants system studied during this work is the apparent lack of social organisation, i.e. each individual seems to behave with apparently negligible interactions with individuals surrounding it. The initial project, at the start of this DPhil, was exploring trail usage, i.e. the behaviour of individuals following preferred routes marked by the ants via pheromone deposition. It quickly became apparent that a deeper knowledge of individual movement was required prior to explore movement at the colony level. The approaches presented, and somewhat surprising results, could be used for future studies of socially interacting individuals. By establishing a 'neutral' theory, i.e., where no interactions are apparent, one could observe deviation from the predictions exposed and quantify the impact of interactions on the behaviour of individuals.

In the second part of this thesis, I explored the ecology of badgers. In its first chapter, I demonstrated a link between maculation patterns of badgers and their level of developmental stress. Then I explored the interactions between climate and population dynamics. In chapter 6, estimates of survival and apparent fecundity (including pre-emergence survival) are related to local monthly climatic conditions. The link between climate and population dynamics is shown to be in agreement with the correlation between climate and parasitic infections, body condition and road traffic accident. Such a study required an extended knowledge of various components of the animals' life histories. As those are not always available, I finally presented a method that can be used, with limited knowledge, to explore interactions between climate and population dynamics. This method is applied to our badger population and I demonstrated a negative influence of weather unpredictability on both survival and fecundity. While present level of weather unpredictability is shown not to threaten badger population, this might prove wrong if trend linked with climate change are to continue.

A striking feature of the badger system is its complexity, reflecting the importance of considering individuals as part of a whole system. In this thesis, I furthered knowledge at the intersection between population and individual ecology by exploring the

population dynamics on one hand, individual characteristics on the other, and linking both of them to environmental conditions.

Overall this work, while providing a good example of the importance of statistical modelling to investigate biological systems, deepened my understanding of ants' and badgers' ecology. By working on those two different systems, I could contribute to the understanding and quantification of some very specific behaviours linked to foraging and of how environment, by shaping individuals qualities, influences the biology of the population as a whole. This DPhil, however, opened at least as many questions as it answered and I will now explore the potential future work directly emerging from the presented thesis.

A first project would rely on the combination of previous work on ant foraging by use of trails (see Acosta *et al.* 1993) and work that has started on badger use and modification of their landscape.

8.1 Border or Byway: The Relationship between Badger Paths and Latrine Location and Function, in the Wytham Woods Population

Since the earliest consideration of the role of latrines, a notional functionality was imposed by extrapolation from other social species, that in particular was derived from Kruuk's formative work on hyenas. While badger latrines are used as a means of communication with members of the same and different social groups (Roper *et al*, 1993, Buesching & Macdonald, 2001), there is little substantive evidence for "active defence" (i.e. agonistic behaviours) associated with latrine-marked borders (Stewart *et al.* 2001).

Earlier work (Stewart *et al.* 1997; Stewart *et al.* 2001) proposed that badger latrine-use patterns might best be explained by a Passive Range Exclusion Hypothesis (PREH), where latrines signalled a contour line of resource depletion, rather than an exclusive boundary. Kilshaw *et al*'s (2009) findings lend more support to a pattern of Active Territorial Defence (Stewart *et al.* 1997a; Stewart *et al.* 2001), with apparent evidence that badgers may cooperate systematically to defend their territories. What is clearly in evidence in this population is that anti-kleptogamy per se is apparently not an effective

function of latrine marked borders as evidenced by Dugdale *et al.*'s (2007) discovery that about 50% of cubs are fathered by males from neighbouring social groups, suggesting that groups are neither spatially, nor genetically, discrete.

A third and potentially more parsimonious hypothesis may also explain the perplexing role of latrines in badger society: "information nodes along a path network".

The use of paths by badgers has been under-investigated, and is thus an under-estimated behaviour which has been broadly considered an inevitable corollary of badger activity. We hypothesise that these paths are, functionally, highly significant in badger spatial relationships. They invariably link a series of latrines in a dendritic network and while recognising that latrines serve to communicate olfactory information, this could include navigational cues, and "notes to self" or "notes to others" about the previous nights foraging success and resource depletion. Although previous studies have noted that badger latrines are often found near conspicuous landmarks, field and wood margins and at fence lines (Kruuk, 1978a, Delahay *et al.* 2000; Stewart *et al.* 2002), work investigating the fundamental relationship between path location and use and latrine location and activity has been lacking, owing to implicit and un-tested assumptions.

Our observations note that latrines often correspond with path intersections or forks and latrines will also frequently occur where a well-used path intersects a perpendicular landscape feature, such as dipping under a fence line. Our hypothesis would envisage paths radiating from setts according to established optimal foraging vectors until they intercept similar paths radiating from neighbouring setts. As stated by the PREH, foraging into the neighbouring group's already resource depleted range would not be optimal (with or without active defence); thus convergent paths, marked by a latrine node, will flow toward points of mutual resource abundance. Where "tributaries" intersect this main flow, latrines will occur as "sign-posts" or "information nodes". Further, in areas of poor resource availability, the fluvial dynamics of the path system will militate for a single well-reinforced riverine path. Here resources are more abundant and flow rate will decrease leading to apparent delta-like braiding of paths, which may cease to be detectable over this zone, only to re-converge beyond this point, again marked by a latrine. Also latrines will act to sign-post the confluence of major paths.

As well as faeces marking at latrines (Stewart *et al.* 2002), badgers also use a secretion from sub-caudal glands to mark their environment (object-marking) (Buesching & Macdonald, 2000), and con-specifics (allo-marking) (Buesching & Macdonald 2002, Buesching *et al.* 2003) The use of restricted sites for defecation rather than random defecation while foraging, along with the potential information to be obtained from various secretions, could be investigated in the context of providing nodes of olfactory information along a path network. Scent marking and its associated latrine use is a primary form of communication for species such as the badger and is likely to hold the key to understanding their social dynamics (Hutchings & White, 2000).

Understanding path and latrine use interactions is important for two reasons. Firstly, badgers are one of the few species that live together socially but there is little evidence of co-operative behaviour and the advantages of communal living are not clear (Woodroffe & Macdonald, 2000). Secondly, studies have indicated that badgers represent a large reservoir of bovine TB and that the main route of transmission is probably via cattle contact with pasture contaminated with badger excreta (White *et al.* 1993, Hutchings & Harris, 1997, Hutchings & Harris, 1999); a contamination facilitated by path position and enacted by latrine use.

A second project, somehow more general and to a certain extent encompassing the previous one, would explore animal movement using as foundation work presented in this thesis.

8.2 Animal movement in biased environments

Virtually all environments have spatial heterogeneity. On land, there are barriers, such as streams, which have a strong impact on animal movement (Turchin 1991, Crist *et al.* 1992, Challet *et al.* 2005, Conradt and Roper 2006). In water, there may be persistent temperature and chemical gradients, which affect movement (Mori and Ohishima 1995). These represent physical biases. In addition, environments may have biotic biases or constraints. For instance, some species deposit pheromones, which strongly influence the movement of other conspecifics (Wilson 1962, Goss *et al.* 1989). An interesting continuation of the work presented in this thesis would be to carry out

observations/experiments in concert with detailed mathematical modelling to produce a flexible, predictive and widely applicable theory of animal movement which covers biased environments. A systems-biology approach to the problem, based on the detailed interplay between observations and mathematical modelling and simulation would be an ideal approach. In the modelling cycle, observations made would motivate the construction or modification of a mathematical model. This could then be used to make predictions, via mathematical analysis or simulations, which could be tested on further measurements/observations. In this way the accuracy and components of the model could be successively modified until a valid mathematical description of movement is obtained.

I have set the foundations for this work in the first chapter of this thesis, where I established that, for a single species of ant (the Pharaoh's ant, *Monomorium pharaonis*), a new mathematical model, based on the simplest piece of mathematics capable of describing the continuous random movement of animals, works extraordinarily well. The model is based on an equation with randomness within it – a stochastic differential equation –which contains the random tendencies of animals to move, but with a degree of persistence in direction.

This work establishes that a robust quantity that underlies animal movement is a single distance related quantity: the mean square distance moved by an animal in a given time. Knowledge of this quantity allows prediction of all aspects of animal movement in the model, and remarkably, the mean square displacement (as a function of the time taken to make the displacement) fully characterises all properties of animal movement in unbiased (i.e. pristine) environments. The robustness of the model was shown by the remarkably good fit between modelled and real data on ant movement.

Building on this model, further work would:

1. Fully characterise the movements of a variety of different organisms in homogeneous two-dimensional environments within the framework of our model. Mathematically analyse the differences in behaviour in terms of correlation times and other descriptive parameters.

2. Establish and test an extended version of the model by incorporating biases in the environment, of physical origin, and by performing the modelling cycle of: observation, modifying the model, generation of predictions, observation.

3. Extend the model to accommodate environmental biases of a purely biological origin.

The variety of organisms observed to motivate mathematical modelling could range from the unicellular to mammals, with the aim of obtaining a general theory. I note that the model would potentially be applicable to single-cell movement within an organism (Nossal and Weiss 1974, Zygourakis 1996). Cell motility is involved in a range of critical activities (reproduction, development, bone formation, wound healing etc.) and disease (spread of malignant cells). Thus extensive ramifications could be explored beyond that of purely animal movement.

Literature cited

Abramowitz, M. and I. A. Stegun. 1970. Handbook of Mathematical Functions, Dover Publications, Inc., New York.

Adler, P. B., and J. M. Drake. 2008. Environmental Variation, Stochastic Extinction, and Competitive Coexistence. American Naturalist 172:186-195.

Adler, F. R. and Gordon. D. M., 1992. Information collection and spread by networks of patrolling ants. American Naturalist 40, 373-400

Alley, R. B., J. Marotzke, W. D. Nordhaus, J. T. Overpeck, D. M. Peteet, R. A. Pielke, Jr., R. T. Pierrehumbert *et al*. 2003. Abrupt Climate Change. Science 299:2005-2010.

Ame, J. M., J. Halloy, C. Rivault, C. Detrain, and J. L. Deneubourg. 2006. Collegial decision making based on social amplification leads to optimal group formation. Proceedings of the National Academy of Sciences of the United States of America 103:5835-5840.

Ame, J. M., C. Rivault, and J. L. Deneubourg. 2004. Cockroach aggregation based on strain odour recognition. Animal Behaviour 68:793-801.

Andrewartha, H. G., and L. C. Birch. 1960. Some recent contributions to the study of the distribution and abundance of insects. Annual Review of Entomology 5:219-242.

Anwar, M. A., C. Newman, D. W. Macdonald, M. E. J. Woolhouse, and D. W. Kelly. 2000. Coccidiosis in the European badger (*Meles meles*) from England, an epidemiological study. Parasitology 120:255-260.

Anderson, T. W., and D. A. Darling. 1952. Asymptotic theory of certain goodness of fit criteria based on stochastic processes. Annals of Mathematical Statistics 23:193-212.

Anderson, D. R. and K. P. Burnham. 2002. Avoiding pitfalls when using information-theoretic methods. Journal of Wildlife Management, 66, 912-918.

Aron, S., J. M. Pasteels, and J. L. Deneubourg. 1989. Trail-laying behavior during exploratory recruitment in the argentine ant, *iridomyrmex-humilis* (mayr). Biology of Behaviour 14:207-217.

Aron, S., J. M. Pasteels, J. L. Deneubourg, and J. L. Boeve. 1986. Foraging recruitment in *leptothorax-unifasciatus* - the influence of foraging area familiarity and the age of the nest-site. Insectes Sociaux 33:338-351.

Arzoumanian, Z., J. Holmberg, and B. Norman. 2005. An astronomical pattern-matching algorithm for computer-aided identification of whale sharks *Rhincodon typus*. Journal of Applied Ecology 42:999 - 1011.

Auger-Methe, M., and H. Whitehead. 2007. The use of natural markings in studies of long-finned pilot whales (*Globicephala melas*). Marine Mammal Science 23:77-93.

Austin, D., W. D. Bowen, and J. I. McMillan. 2004. Intraspecific variation in movement patterns: modeling individual behaviour in a large marine predator. Oikos 105:15-30.

Bartumeus, F., M. G. E. Da Luz, G. M. Viswanathan, and J Catalan, 2005. Animal search strategies: A quantitative, random-walk analysis. Ecology 86: 3078-3087.

Bartumeus, F., J.Catalan, G. M Viswanathan, E. P. Raposo, and M. G. E. da Luz, 2008. The influence of turning angles on the success of non-oriented animal searches. J. Theo. Biol. 252: 43-55.

Bates, D., and M. Maechler (2009). lme4: Linear mixed-effects models using S4 classes. R package version 0.999375-32.

Beckers, R., J. L. Deneubourg, and S. Goss. 1992. Trail laying behaviour during food recruitment in the ant *Lasius niger* (L.). Insectes Sociaux 39:59-72.

Begon, M., C. R. Townsend, and J. L. Harper. 2006, Ecology.

Begon, M., C. R. Townsend, and J. L. Harper. 2006, Ecology: From Individuals to Ecosystems, Blackwell Science.

Ben Ari, T., A. Gershunov, K. L. Gage, T. Snall, P. Ettestad, K. L. Kausrud, and N. C. Stenseth. 2008. Human plague in the USA: the importance of regional and local climate. Biology Letters 4:737-740.

Benhamou, S. 1992. Efficiency of area-concentrated searching behavior in a continuous patchy environment. Journal of Theoretical Biology 159:67-81.

Benhamou, S. 2004. How to reliably estimate the tortuosity of an animal's path: straightness, sinuosity, or fractal dimension? J. Theo. Biol. 229: 209-220.

Bernays, E. A., and D. J. Funk. 1999. Specialists make faster decisions than generalists: Experiments with aphids. Proc. of the Roy. Soc. B-Biological Sciences 266:151-156.

Birch, L. C. 1957. The role of weather in determining the distribution and abundance of animals. Cold Spring Harbor Symposia on Quantitative Biology 22:203-218.

Bonabeau, E., G. Theraulaz, J.-L. Deneubourg, S. Aron, and S. Camazine. 1997. Self-organization in social insects. Trends in Ecology & Evolution 12:188-193.

Bonabeau, E., G. Theraulaz, and J. L. Deneubourg. 1998. The synchronization of recruitment-based activities in ants. Biosystems 45:195-211.

Bond, A. B. 1980. Optimal foraging in a uniform habitat - search mechanism of the green lacewing. Animal Behaviour 28:10-19.

Bovet, P. and S. Benhamou. 1988. Spatial analysis of animals' movements using a correlated random walk model. J. Theo. Biol. 131: 419-433.

Bovet, P. and S. Benhamou. 1991. Optimal sinuosity in central place foraging movements. Anim. Behav.. 42: 57-62.

Boyce, M. S., C. V. Haridas, and C. T. Lee. 2006. Demography in an increasingly variable world. Trends in Ecology & Evolution 21:141-148.

Broom, M., P. Nouvellet, J. P. Bacon, and D. Waxman. 2007. Parameter-free testing of the shape of a probability distribution. Biosystems 90:509-515.

Brown, R. 1828. A brief account of microscopical observations made in months of June, July and August, 1827, on the particles contained in the pollen of plants; and the general existence of active molecules in organic and inorganic bodies. Philos. Mag. 4: 161-173

Brown, T. 1964. Oral pigmentation in the aborigines of Kalumburu, North-West Australia. Archives of oral biology 9:555-564.

Buesching, C. D., and D. W. Macdonald. 2000, Scent-marking behaviour of the European badger (Meles meles): Resource defence or individual advertisement? A.

Marchlewska Koj, J. J. Lepri, and D. Muller Schwarze, eds. 9th International Symposium on Chemical Signals in Vertebrates:321-327.

Buesching, C. D., C. Newman, and D. W. Macdonald. 2002. Variations in colour and volume of the subcaudal gland secretion of badgers (Meles metes) in relation to sex, season and individual-specific parameters. Mammalian Biology 67:147-156.

Buesching, C. D., P. Stopka, and D. W. MacDonald. 2003. The social function of allo-marking in the European badger (Meles meles). Behaviour 140:965-980.

Burnham, K. P. and D. R. Anderson. 2002. Model selection and multi-model inference: A practical information-theoretic approach. Springer Verlag, New York.

Burnham, K. P. and D. R. Anderson. 2004. Multimodel inference - understanding aic and bic in model selection. Sociological Methods & Research, 33, 261-304.

Byers, J. A. 2001. Correlated random walk equations of animal dispersal resolved by simulation. Ecology 82: 1680-1690.

Caro, T. M., J. A. Shargel and C. J. Stoner. 2000. Frequency of medium-sized mammal road kills in an agricultural landscape in California. American Midland Naturalist, 144, 362-369.

Carr, G. M. and D. W. Macdonald. 1986. The sociality of solitary foragers - a model based on resource dispersion. Animal Behaviour, 34, 1540-1549.

Case, R. M. 1978. Interstate highway road-killed animals: A data source for biologists. Wildlife Society Bulletin, 6, 8-13.

Cezilly, F., and S. Benhamou. 1996. Optimal foraging strategies: a review. Revue d ecologie-la terre et la vie 51:43-86.

Challet, M., V. Fourcassié, S. Blanco, R. Fournier, G. Theraulaz and C. Jost. 2005. A new test of random walks in heterogeneous environments. Naturwissenschaften 92: 367-370.

Childerhouse, S. J., S. M. Dawson, and E. Slooten. 1996. Stability of fluke marks used in individual photoidentification of male sperm whales at Kaikoura, New Zealand. Marine Mammal Science 12:447-451.

Charmantier, A., R. H. McCleery, L. R. Cole, C. Perrins, L. E. B. Kruuk, and B. C. Sheldon. 2008. Adaptive Phenotypic Plasticity in Response to Climate Change in a Wild Bird Population. Science 320:800-803.

Clarke, G. P., P. C. L. White and S. Harris. 1998. Effects of roads on badger *Meles meles* populations in south-west England. Biological Conservation, 86, 117-124.

Cleary, G. P., L. A. L. Cornerb, J. O'keeffec and N. M. Marples. 2009. The diet of the badger *Meles meles* in the republic of Ireland. mammalian biology, in press.

Codling, E. A. and N. A. Hill. 2005. Sampling rate effects on measurements of correlated and biased random walks. J. Theo. Biol. 233: 573-588.

Codling, E. A., M. J. Plank and S. Benhamou. 2008. Random walk models in biology. Journal of the royal society interface 5:813-834.

Conradt, L., and T. J. Roper. 2006. Nonrandom movement behavior at habitat boundaries in two butterfly species: Implications for dispersal. Ecology 87:125-132.

Coulson, G. 1997. Male bias in roadkills of macropods. Wildlife Research, 24, 21-25.

Crawley, M. J. 2005. Statistics: An Introduction using R, Wiley.

Crawley, M. J. 2007. The R book, Wiley.

Crist, T. O., D. S. Guertin, J. A. Wiens and B. T. Milne. 1992. Animal Movement in Heterogeneous Landscapes: An Experiment with *Eleodes* Beetles in Shortgrass Prairie. Functional Ecology 6: 536-544.

Crist, T. O. and J. A. MacMahon. 1991. Individual foraging components of harvester ants: movement patterns and seed patch fidelity. Insectes Sociaux 38: 379-396.

Da Silva, J., R. Woodroffe and D. W. Macdonald. 1993. Habitat, food availability and group territoriality in the European badger, *Meles meles*. Oecologia, 95, 558-564.

Davies, J. M., T. J. Roper and D. J. Shepherdson. 1987. Seasonal distribution of road kills in the European badger (*Meles meles*). J. Zool., 211, 525-529.

Dejean, A., and S. Benhamou. 1993. Orientation and foraging movements in a patchy environment by the ant serrastruma-lujae (formicidae-myrmicinae). Behavioural Processes 30:233-243.

Delahay, R. J., J. A. Brown, P. J. Mallinson, P. D. Spyvee, D. Handoll, L. M. Rogers, and C. L. Cheeseman. 2000. The use of marked bait in studies of the territorial organization of the European Badger (Meles meles). Mammal Review 30:73-87.

Deneubourg, J. L., S. Aron, S. Goss, and J. M. Pasteels. 1990. The self-organizing exploratory pattern of the argentine ant. Journal of Insect Behavior 3:159-168.

Deneubourg, J. L., S. Aron, S. Goss, J. M. Pasteels, and G. Duerinck. 1986. Random behavior, amplification processes and number of participants - how they contribute to the foraging properties of ants. Physica D 22:176-186.

Depickère, S., D. Fresneau, and J.-L. Deneubourg. 2004. The influence of red light on the aggregation of two castes of the ant, *Lasius niger*. Journal of Insect Physiology 50:629-635.

Depickère, S., D. Fresneau, and J.-L. Deneubourg. 2008. Effect of social and environmental factors on ant aggregation: A general response? Journal of Insect Physiology 54:1349-1355.

Depickere, S., D. Fresneau, and J. L. Deneubourg. 2004a. A basis for spatial and social patterns in ant species: Dynamics and mechanisms of aggregation. Journal of Insect Behavior 17:81-97.

Depickere, S., D. Fresneau, and J. L. Deneubourg. 2004b. Dynamics of aggregation in *Lasius niger* (Formicidae): influence of polyethism. Insectes Sociaux 51:81-90.

Detrain, C., J. Deneubourg, S. Goss, and Y. Quinet. 1991. Dynamics of Collective Exploration in the Ant *Pheidole Pallidula*. Psyche 98:21-31.

Domingo-Roura, X., C. Newman, F. Calafell and D. W. Macdonald. 2001. Blood biochemistry reflects seasonal nutritional and reproductive constraints in the Eurasian badger (M*eles meles*). Physiological and Biochemical Zoology, 74, 450-460.

Dornhaus, A.; Chittka, L., 2004. Information flow and regulation of foraging activity in bumble bees (*Bombus* spp.).Apidologie, 35, 183-192.

Drake, J. M. 2005. Population effects of increased climate variation. Proceedings of the Royal Society B-Biological Sciences 272:1823-1827.

Dufault, S., and H. A. L. Whitehead. 1995. An assessment of changes with time in the marking patterns used for photoidentification of individual sperm whales, *physeter macrocephalus*. Marine Mammal Science 11:335-343.

Dufour, K. W., and P. J. Weatherhead. 1998. Bilateral symmetry and social dominance in captive male red-winged blackbirds. Behavioral Ecology and Sociobiology 42:71-76.

Dugdale, H. L., D. W. Macdonald, L. C. Pope, and T. Burke. 2007. Polygynandry, extra-group paternity and multiple-paternity litters in European badger (*Meles meles*) social groups. Molecular Ecology 16:5294-5306.

Dugdale, H. L., P. Nouvellet, T. Burke, L. C. Pope, and D. W. Macdonald. 2010. Fitness Measures in Selection Analyses: Sensitivity to the Overall Number of Offspring Produced in a Lifetime. Journal of Evolutionary Biology, in press.

Edler, R. J. 2001. Background Considerations to Facial Aesthetics. J. Orthod. 28:159-168.

Edwards. A. M., R. A. Phillips, N. W. Watkins, M. P. Freeman, E. J. Murphy, V Afanasyev, S. V. Buldyrev, M. G. E. da Luz, E. P. Raposo, H. E. Stanley and G. M. Viswanathan. 2007. Revisiting levy flight search patterns of wandering albatrosses, bumblebees and deer. Nature 449: 1044-1049.

Fagan, W. F., and E. E. Holmes. 2006. Interactive Individual Identification Software (I3S) Quantifying the extinction vortex. Ecology Letters 9:51 - 60.

Falconer, D. S., and T. F. C. Mackay. 1996. Introduction to Quantitative Genetics. Harlow, Longman.

Forcada, J., and A. Aguilar. 2000. Use of photographic identification in capture-recapture studies of Mediterranean monk seals. Marine Mammal Science 16:767-793.

Fortin, D. 2003. Searching behavior and use of sampling information by free-ranging bison (*Bos bison*). Behavioral Ecology and Sociobiology 54:194-203.

Fortin, D., H. L. Beyer, M. S. Boyce, D. W. Smith, T. Duchesne, and J. S. Mao. 2005. Wolves influence elk movements: Behavior shapes a trophic cascade in Yellowstone National Park. Ecology 86:1320-1330.

Frankel, J. S. 1991. Inheritance of body marking patterns in the half-banded barb, *barbus-semifasciolatus*. Journal of Heredity 82:250-251.

Fourcassie, V., and J. L. Deneubourg. 1994. The dynamics of collective exploration and trail-formation in Monomorium pharaonis: experiments and model. Physiological Entomology 19:291-300.

Fowler, P. A. and P. A. Racey. 1988. Overwintering strategies of the badger, *Meles-meles*, at 57-degrees-n. Journal of Zoology, 214, 635-651.

Fragoso, C. and P. Lavelle. 1992. Earthworm communities of tropical rain forests. Soil Biology and Biochemistry, 24, 1397-1408.

Franks, N., and T. Richardson. 2006. Teaching in tandem-running ants. Nature 439:153-153.

Fuqua, W. C., Winans S. C., and Greenberg E. P., 1994. Quorum sensing in bacteria: the LuxR/LuxI family of cell density-responsive transcriptional regulators. J. Bacteriol. **176,** 269-275

Gangestad, S. W., and R. Thornhill. 1998. Menstrual cycle variation in women's preferences for the scent of symmetrical men. Proceedings of the Royal Society of London. Series B: Biological Sciences 265:927-933.

Gangestad, S. W., and R. Thornhill. 1999. Individual differences in developmental precision and fluctuating asymmetry: a model and its implications. Journal of Evolutionary Biology 12:402-416.

Garcia, R., F. Moss, A. Nihongi, J. R. Strickler, S. Göller, U. Erdmann, L. Schimansky-Geier, and I. M. Sokolov. 2007. Optimal foraging by zooplankton within patches: The case of Daphnia. Math. Biosciences 207: 165-188.

Garnier, S., J. Gautrais, M. Asadpour, C. Jost, and G. Theraulaz. 2009. Self-Organized Aggregation Triggers Collective Decision Making in a Group of Cockroach-Like Robots. Adaptive Behavior 17:109-133.

Gerard, B. M. 1967 Factors affecting earthworms in pastures. Journal of Animal Ecology, 36, 235-252.

Gilmour, A. R., B. J. Gogel, B. R. Cullis, and R. Thompson. 2006. Asreml User Guide Release 2.0 VSN International Ltd, Hemel Hempstead, UK.

Gope, C., N. Kehtarnavaz, G. Hillman, and B. Wursig. 2005. An affine invariant curve matching method for photo-identification of marine mammals. Pattern Recognition 38:125 - 132.

Gordon, D. M. 1988. Group-Level Exploration Tactics in Fire Ants. Behaviour 104:162-175.

Gordon, D. M., 1995. The development of an ant colony's foraging range. Animal Behaviour 49, 649-659

Goss, S., S. Aron, J. L. Deneubourg, and J. M. Pasteels. 1989. Self-organized shortcuts in the Argentine ant. Naturwissenschaften 76:579-581.

Gowans, S., and H. Whitehead. 2001. Photographic identification of northern bottlenose whales (Hyperoodon ampullatus): Sources of heterogeneity from natural marks. Marine Mammal Science 17:76-93.

Grant, P. R. 1999. Ecology and evolution of Darwin's finches, Princeton.

Grosbois, V., O. Gimenez,, J. M. Gaillard., *et al*. 2008. Assessing the impact of climate variation on survival in vertebrate populations. Biological Reviews, 83, 357-399.

Guenther, M. M., G. W. Ferguson, H. L. Snell, and H. Snell. 1993. The variation and genetic-basis of dorsal color pattern in the desert side-blotched lizard, *uta-stansburiana-stejnegeri*. Journal of herpetology 27:199-205.

Gunn, D. L., J. S. Kennedy and D. F. Pielou. 1937. Classification of taxes and kineses. Nature 140: 1064.

Haigh, J., 2002. Probability Models. Springer, London.

Hallett, T. B., T. Coulson, J. G. Pilkington, T. H. Clutton-Brock, J. M. Pemberton, and B. T. Grenfell. 2004. Why large-scale climate indices seem to predict ecological processes better than local weather. Nature 430:71-75.

Halloy, J., G. Sempo, G. Caprari, C. Rivault, M. Asadpour, F. Tache, I. Said *et al*. 2007. Social integration of robots into groups of cockroaches to control self-organized choices. Science 318:1155-1158.

Hamilton, W. J., and K. E. F. Watt. 1970. Refuging. Annual Review of Ecology and Systematics 1:263-286.

Hamilton, W. D. 1971. Geometry for the selfish herd. J Theor Biol 31:295-311.

Harkness, R. D., and N. G. Maroudas. 1985. Central place foraging by an ant (*Cataglyphis bicolor Fab*.): a model of searching. Animal Behaviour 33:916-928.

Henderson, C. R. 1976. A simple method for computing the inverse of a numerator relationship matrix used in prediction of breeding values. Biometrics 32:69-83.

Hereford, J., T. F. Hansen, D. Houle, and C. Fenster. 2004. Comparing strengths of directional selection: how strong is strong? Evolution 58:2133-2143.

Hill, N. A. and D. P. Hader. 1997. A biased random walk model for the trajectories of swimming micro-organism. J. Theo. Biol. 186: 503-526.

Hofer, H. 1988 Variation in resource presence, utilization and reproductive success within a population of European badgers (*Meles-meles*). Mammal Review, 18, 25-36.

Hogg, R. V., and E. A. Tanis. 2006, Probability and Statistical Inference.

Hölldobler B, Wilson E. O., 1990. The ants. Cambridge, MA, Harvard University Press

Houle, D. 1998. Review: High Enthusiasm and Low R-Squared. Evolution 52:1872-1876.

Hughes, L. 2000. Biological consequences of global warming: is the signal already apparent? Trends in Ecology & Evolution 15:56-61.

Husby, A., L. E. B. Kruuk, and M. E. Visser. 2009. Decline in the frequency and benefits of multiple brooding in great tits as a consequence of a changing environment. Proceedings of the Royal Society B: Biological Sciences 276:1845-1854.

Hutchings, M. R., and S. Harris. 1997. Effects of farm management practices on cattle grazing behaviour and the potential for transmission of bovine tuberculosis from badgers to cattle. Veterinary Journal 153:149-162.

Hutchings, M. R., and S. Harris. 1999. Quantifying the risks of TB infection to cattle posed by badger excreta. Epidemiology and Infection 122:167-173.

Inbar, M. and R. T. Mayer. 1999 Spatio-temporal trends in armadillo diurnal activity and roadkills in central Florida. Wildlife Society Bulletin, 27, 865-872.

IPCC. 2002. Intergovernmental panel on climate change, working group II, Climate Change and Biodiversity.

IPCC. 2007. Intergovernmental panel on climate change, The AR4 Synthesis Report.

IPCC. 2008, Climate Change 2007: The Physical Science Basis: Contribution of Working Group I to the Fourth Assessment Report of the Intergovernmental Panel on Climate Change.

Jackson, D. E., Holcombe, M., and Ratnieks, F. L . W. 2004. Trail geometry gives polarity to ant foraging networks. *Nature* ***432***, 907-909.

Jeanson, R., C. Rivault, J.-L. Deneubourg, S. Blanco, R. Fournier, C. Jost, and G. Theraulaz. 2005. Self-organized aggregation in cockroaches. Animal Behaviour 69:169-180.

Johnson, D. D. P., W. Jetz, and D. W. Macdonald. 2002 Environmental correlates of badger social spacing across Europe. Journal of Biogeography, 29, 411-425.

Jolly, G. M. 1965 Explicit estimates from capture-recapture data with both death and immigration-stochastic model. Biometrika, 52, 225-.

Jonzen, N., A. Linden, T. Ergon, E. Knudsen, J. O. Vik, D. Rubolini, D. Piacentini *et al*. 2006. Rapid advance of spring arrival dates in long-distance migratory birds. Science 312:1959-1961.

Karanth, K. U., and J. D. Nichols. 1998. Estimation of tiger densities in India using photographic captures and recaptures. Ecology 79:2852 - 2862.

Kareiva, P. M. and N. Shigesada. 1983. Analyzing insect movement as a correlated random walk. Oecologia 56: 234-238.

Karl, T. R., and K. E. Trenberth. 2003. Modern global climate change. Science 302:1719-1723.

Karlsson, O., L. Hiby, T. Lundberg, M. Jussi, I. Jussi, and B. Helander. 2005. Photo-identification, site fidelity, and movement of female gray seals (*Halichoerus grypus*) between haul-outs in the Baltic Sea. Ambio 34:628 - 634.

Kausrud, K. L., A. Mysterud, H. Steen, J. O. Vik, E. Ostbye, B. Cazelles, E. Framstad *et al*. 2008. Linking climate change to lemming cycles. Nature 456:93-U93.

Kelly, M. J. 2001. Computer-aided photograph matching in studies using individual identification: An example from Serengeti cheetahs. Journal of Mammalogy 82:440-449.

Kilshaw, K.; Newman, C.; Buesching, C., Bunyan J., and D. Macdonald. 2009. Coordinated latrine use by european badgers, meles meles: potential consequences for territory defense. *Journal of mammalogy* 90:1188-1198.

Krebs, J. R., A. Kacelnik, and P. Taylor. 1978. Test of optimal sampling by foraging great tits. Nature 275:27-31.

Krebs, J. R., J. C. Ryan, and E. L. Charnov. 1974. Hunting by expectation or optimal foraging - study of patch use by chickadees. Animal Behaviour 22:953.

Kruuk, H. 1978a. Foraging and spatial-organization of European badger, *Meles-meles* l. Behavioral ecology and sociobiology 4:75-89.

Kruuk, H. 1978b. Spatial-organization and territorial behavior of European badger *Meles-meles*. Journal of Zoology 184:1-19.

Kruuk, H. 1989. The social badger: Ecology and behaviour of a group-living carnivore (*Meles meles*), Oxford University Press.

Kruuk, L. E. B. 2004. Estimating genetic parameters in natural populations using the 'animal model'. Philosophical Transactions of the Royal Society of London. Series B: Biological Sciences 359:873-890.

Kvam, P. H., Vidakovic, B., 2007. Nonparametric Statistics with Applications to Science and Engineering, (Wiley), Hoboken, New Jersey

Lande, R., and S. J. Arnold. 1983. The measurement of selection on correlated characters. *Evolution* 37:1210-1226.

Lauzon-Guay, J. S., R. E. Scheibling, and M. A. Barbeau. 2008. Formation and propagation of feeding fronts in benthic marine invertebrates: a modeling approach. Ecology 89:3150-3162.

Le Roux, P. C., and M. A. McGeoch. 2008. Changes in climate extremes, variability and signature on sub-Antarctic Marion Island. Climatic Change 86:309-329.

Leamy, L. J., and C. P. Klingenberg. 2005. The genetics and evolution of fluctuating asymmetry. Annual Review of Ecology Evolution and Systematics 36:1-21.

Lebreton, J. D., K. P. Burnham, J. Clobert, and D. R. Anderson. 1992. Modeling survival and testing biological hypotheses using marked animals: A unified approach with case studies. Ecological Monographs, 62, 67-118.

Lens, L., S. Dongen, S. Kark, and E. Matthysen. 2002. Fluctuating asymmetry as an indicator of fitness: can we bridge the gap between studies? Biological Reviews 77:27-38.

Leslie, P.H. 1945. On the use of matrices in certain population mathematics. *Biometrica*, 33: 183-212.

Lindsay, D. S., J. P. Dubey, and B. L. Blagburn. 1997 Biology of *isospora* spp. From humans, nonhuman primates, and domestic animals. Clinical Microbiology Reviews, 10, 19-34.

Ligon, J. D., R. Kimball, and M. Merola-Zwartjes. 1998. Mate choice by female red junglefowl: the issues of multiple ornaments and fluctuating asymmetry. Animal Behaviour 55:41-50.

Lilliefors, H. w. 1969. On Kolmogorov-Smirnov test for exponential distribution with mean unknown. Journal of the American Statistical Association 64:387-389.

Long, P. L. (Ed.) .1982. The biology of the coccidia, london, Edward Arnold: 35-62.

Macarthur, R. H., and E. R. Pianka. 1966. On optimal use of a patchy environment. American Naturalist 100:603.

Macdonald, D. W. 1980. The red fox, *Vulpes vulpes*, as a predator upon earthworms, *lumbricus terrestris*. Z. Tierpsychol., 52, 171-200.

Macdonald, D. W. 1983. Predation on earthworms by terrestrial vertebrates. Earthworm Ecology, 393-414.

Macdonald, D. W. and C. Newman. 2002a Population dynamics of badgers (*Meles meles*) in Oxfordshire, UK: Numbers, density and cohort life histories, and a possible role of climate change in population growth. Journal of Zoology, 256, 121-138.

Macdonald, D. W., C. Newman, P. D. Stewart, X. Domingo-Roura, and P. J. Johnson. 2002b. Density-dependent regulation of body mass and condition in badgers (*Meles meles*) from Wytham woods. Ecology, 83, 2056-2061.

Macdonald, D. W., C. Newman, J. Dean, C. D. Buesching, and P. J. Johnson. 2004. The distribution of Eurasian badger, *Meles meles*, setts in a high-density area: field observations contradict the sett dispersion hypothesis. Oikos 106:295-307.

Macdonald, D. W., C. Newman, C. D. Buesching, and P. J. Johnson. 2008 Male-biased movement in a high-density population of the Eurasian badger (*Meles meles*). Journal of Mammalogy, 89, 1077-1086.

Macdonald, D. W., C. Newman, P. Nouvellet, and C. D. Buesching. 2009. Mechanisms for population regulation and the role of density-dependence in the demographics of the Eurasian badger, *Meles meles*: Matrix models applied to a long-term population study. Journal of Mammalogy, in press.

Malyon, C., and S. Healy. 1994. Fluctuating asymmetry in antlers of fallow deer, *Dama dama*, indicates dominance. Animal Behaviour 48:248-250.

Mateos, C., S. Alarcos, J. Carranza, C. B. Sánchez-Prieto, and J. Valencia. 2008. Fluctuating asymmetry of red deer antlers negatively relates to individual condition and proximity to prime age. Animal Behaviour 75:1629-1640.

McCarty, J. P. 2001. Ecological consequences of recent climate change. Conservation Biology 15:320-331.

McCulloch, C. E., and M. L. Cain. 1989. Analyzing discrete movement data as a correlated random walk. Ecology 70:383-388.

McDermott, R., J. H. Fowler, and O. Smirnov. 2008. On the evolutionary origin of prospect theory preferences. Journal of Politics 70:335-350.

McNamara, J. M. And A. I. Houston. 1992. Risk-sensitive foraging: a review of the theory. Bulletin of Mathematical Biology 54, 355-378.

Meehl, G. A., F. Zwiers, J. Evans, T. Knutson, L. Mearns, and P. Whetton. 2000. Trends in extreme weather and climate events: Issues related to modeling extremes in projections of future climate change. Bulletin of the American Meteorological Society 81:427-436.

Miller, M. B., Bassler, B. L., 2001 Quorum sensing in bacteria. Annu Rev Microbiol **55**, 165-199.

Mirenda, J. T., and H. Topoff. 1980. Nomadic behavior of army ants in a desert-grassland habitat. Behavioral Ecology and Sociobiology 7:129-135.

Moller, A. P., J. J. Cuervo, J. J. Soler, and C. Zamora-Muoz. 1996. Horn asymmetry and fitness in gemsbok, Oryx g. Gazella. Behav. Ecol. 7:247-253.

Mori, I., and Y. Ohshima. 1995. Neural regulation of thermotaxis in caenorhabditis-elegans. Nature 376:344-348.

Morris, M. R. 1998. Female preference for trait symmetry in addition to trait size in swordtail fish. Proceedings of the Royal Society of London. Series B: Biological Sciences 265:907-907.

Morrison, D. W. 1978. On the Optimal Searching Strategy for Refuging Predators. The American Naturalist 112:925.

Naeem, S. and S. Li. 1997. Biodiversity enhances ecosystem reliability. Nature, 390, 507-509.

Neal, E. G. and C. L. Cheeseman. 1996. Badgers.

Newman, C., D. W. Macdonald, and M. A. Anwar. 2001 Coccidiosis in the European badger, *Meles meles* in Wytham woods: Infection and consequences for growth and survival. Parasitology, 123, 133-142.

Nichols, J. D., J. E. Hines, J. D. Lebreton, and R. Pradel. 2000. Estimation of contributions to population growth: A reverse-time capture-recapture approach. Ecology, 81, 3362-3376.

Nossal, R. and G. H. Weiss. 1974. A descriptive theory of cell migration on surfaces. J. Theo. Biol. 47: 103-113.

Nouvellet, P., J. P. Bacon, and D. Waxman. 2009. Fundamental Insights into the Random Movement of Animals from a Single Distance-Related Statistic. The American Naturalist 174:506-514.

Nurnberger, B., N. Barton, C. Maccallum, G. Jason, and M. Appleby. 1995. Natural Selection on Quantitative Traits in the *Bombina* Hybrid Zone. Evolution 49:1224-1238.

Oakes, E. J., and P. Barnard. 1994. Fluctuating asymmetry and mate choice in paradise whydahs, Vidua paradisaea: an experimental manipulation. Animal Behaviour 48:937-943.

Othmer, H. G., S. R. Dunbar, and W. Alt. 1988. Models of dispersal in biological systems. J. Math. Biol. 26: 263-298.

Oxley, D. J., M. B. Fenton, and G. R. Carmody. 1974. Effects of roads on populations of small mammals. Journal of Applied Ecology, 11, 51-59.

Palmer, A. R. 2000. Quasireplication and the Contract of Error: Lessons from Sex Ratios, Heritabilities and Fluctuating Asymmetry. Annual Review of Ecology and Systematics 31:441-480.

Parmesan, C. 2006. Ecological and evolutionary responses to recent climate change. Annual Review of Ecology Evolution and Systematics 37:637-669.

Parmesan, C., N. Ryrholm, C. Stefanescu, J. K. Hill, C. D. Thomas, H. Descimon, B. Huntley *et al*. 1999. Poleward shifts in geographical ranges of butterfly species associated with regional warming. Nature 399:579-583.

Parrish, J. K., and L. Edelstein-Keshet. 1999. Complexity, Pattern, and Evolutionary Trade-Offs in Animal Aggregation. Science 284:99-101.

Patalak, C. S. 1953. Random walk with persistence and external bias. Bull. Math. Biophys. 12: 311-338.

Pearson, K. 1905a. The problem of the random walk. Nature 72:294-294.

Pearson, K. 1905b. The problem of the random walk. Nature 72:342-342.

Perry, G., and E. R. Pianka. 1997. Animal foraging: past, present and future. Trends in Ecology & Evolution 12:360-364.

Peterson, A. T., M. A. Ortega-Huerta, J. Bartley, V. Saì-Nchez-Cordero, N, J. Soberoì, R. H. Buddemeler, and D. R. B. Stockwell, 2002. Future projections for Mexican faunas under global climate change scenarios. Nature, 416, 626-629.

Peterson, A. T., J. Soberon, and V. Sanchez-Cordero. 1999. Conservatism of ecological niches in evolutionary time. Science, 285, 1265-1267.

Philcox, C. K., A. L. Grogan, and D. W. Macdonald, 1999. Patterns of otter *Lutra lutra* road mortality in Britain. Journal of Applied Ecology, 36, 748-762.

Polak, M. 1997. Ectoparasitism in Mothers Causes Higher Positional Fluctuating Asymmetry in Their Sons: Implications for Sexual Selection. The American Naturalist 149:955-974.

Possingham, H. P. 1989. The distribution and abundance of resources encountered by a forager. American Naturalist 133:42-60.

Post, E., and N. C. Stenseth. 1999. Climatic variability, plant phenology, and northern ungulates. Ecology 80:1322-1339.

Pradel, R. 1996. Utilization of capture-mark-recapture for the study of recruitment and population growth rate. Biometrics, 52, 703-709.

Pratt, S. C., Mallon, E. B., Sumpter, D. J. T., and Franks, N. R., 2002. Quorum sensing, recruitment, and collective decision-making during colony emigration by the ant *Leptothorax albipennis*. *Behavioral Ecology and Sociobiology*, ***52***, 117–127

Pyke, G. H. 1978. Are animals efficient harvesters? Animal Behaviour 26:241-250.

Pyke, G. H. 1981. Optimal foraging in hummingbirds - rule of movement between inflorescences. Animal Behaviour 29:889-896.

Pyke, G. H. 1984. Optimal foraging theory - a critical-review. Annual Review of Ecology and Systematics 15:523-575.

Rayleigh. 1905. The problem of the random walk. Nature 72:318-318.

Rebetez, M. and M. Beniston. 199.8 Changes in temperature variability in relation to shifts in mean temperatures in the Swiss alpine region this century. The Impacts of Climate Variability on Forests, 49-58.

Reed, D. H., E. H. Lowe, D. A. Briscoe, R. Frankham, and J. Fry. 2009. Fitness and adaptation in a novel environment: effect of inbreeding, prior environment, and lineage. Evolution 57:1822-1828.

Renshaw, E. 1993. Modelling Biological Populations in space and Time. New York CUP.

Richardson T. O, Robinson E. J. H, Christensen K, Jensen H. J., Franks N. R., *et al*. (2010) Record Dynamics in Ants. PLoS ONE 5(3).

Robinson, E. J. H.; Richardson, T. O.; Sendova-Franks, A.B., Feinerman, O., Franks, N. R., 2009. Radio tagging reveals the roles of corpulence, experience and social information in ant decision making. *Behavioral ecology and sociobiology* 63, 627-636.

Roese, J. H., K. L. Risenhoover, and L. J. Folse. 1991. Habitat heterogeneity and foraging efficiency - an individual-based model. Ecological Modelling 57:133-143.

Roff, D., and D. Reale. 2004. The Quantitative Genetics of Fluctuating Asymmetry: A Comparison of Two Models. Evolution 58:47-58.

Roper, T. J., L. Conradt, J. Butler, S. E. Christian, J. Ostler, and T. K. Schmid. 1993. Territorial marking with feces in badgers (*Meles-meles*) - a comparison of boundary and hinterland latrine use. Behaviour 127:289-307.

Root, T. L., D. Liverman, and C. Newman. 2006 Managing biodiversity in the light of climate change: Current biological effects and future impacts.

Root, T. L., D. P.Macmynowski, M. D. Mastrandrea, and S. H. Schneider. 2005. Human-modified temperatures induce species changes: Joint attribution. Proceedings of the National Academy of Sciences of the United States of America, 102, 7465-7469.

Root, T. L., J. T. Price, K. R. Hall, S. H. Schneider, C. Rosenzweig, and J. A. Pounds. 2003. Fingerprints of global warming on wild animals and plants. Nature, 421, 57-60.

Saeki, M. and D. W. Macdonald. 2004 The effects of traffic on the raccoon dog (*nyctereutes procyonoides viverrinus*) and other mammals in Japan. Biological Conservation, 118, 559-571.

Saino, N., D. Rubolini, N. Jonzen, T. Ergon, A. Montemaggiori, N. C. Stenseth, and F. Spina. 2007. Temperature and rainfall anomalies in Africa predict timing of spring migration in trans-Saharan migratory birds. Climate Research 35:123-134.

Sandvik, H., T. Coulson, and B. E. Saether. 2008. A latitudinal gradient in climate effects on seabird demography: results from interspecific analyses. Global Change Biology 14:703-713.

Scheib, J. E., S. W. Gangestad, and R. Thornhill. 1999. Facial attractiveness, symmetry and cues of good genes. Proceedings of the Royal Society of London. Series B: Biological Sciences 266:1913-1917.

Seeley, T. D.., 1995. The wisdom of the hive: The social physiology of honey bee colonies. Cambridge, MA, Harvard University Press

Seeley, T.D., Visscher, P.K. and Passino, K.M., 2006. Group decision making in honey bee swarms. *American Scientist* 94, 220-229

Sibani P, Dall J 2003 Log-Poisson statistics and full aging in glassy systems. Europhys Lett 64: 8–14.

Skinner, C., P. Skinner, and S. Harris, 1991. The past history and recent decline of badgers *meles-meles* in Essex - an analysis of some of the contributory factors. Mammal Review, 21, 67-80.

Sleeman, P., R. Cussen, T. O'Donoughue, and E. Costello. 2001. Badgers (*Meles meles*) on Fenit Island, and their presence or absence on other islands in Co. Kerry, Ireland. Small carnivore conservation:10-12.

Speed, C., M. Meekan, and C. Bradshaw. 2007. Spot the match - wildlife photo-identification using information theory. Frontiers in Zoology 4:2.

Speedy, A. W., 1980. Sheep Production, Science into Practice. Longman, Harlow/Essex, United Kingdom.

Stenseth, N. C., K. S. Chan, H. Tong, R. Boonstra, S. Boutin, C. J. Krebs, E. Post *et al*. 1999. Common dynamic structure of Canada lynx populations within three climatic regions. Science 285:1071-1073.

Stenseth, N. C., A. Mysterud, G. Ottersen, J. W. Hurrell, K. S. Chan, and M. Lima. 2002. Ecological effects of climate fluctuations. Science 297:1292-1296.

Stenseth, N. C., G. Ottersen, J. W. Hurrell, A. Mysterud, M. Lima, K. S. Chan, N. G. Yoccoz *et al.* 2003. Studying climate effects on ecology through the use of climate indices: the North Atlantic Oscillation, El Nino Southern Oscillation and beyond. Proceedings of the Royal Society of London Series B-Biological Sciences 270:2087-2096.

Stephens, D. W., J. S. Brown, and R. C. Ydenberg. 2007. Foraging: Behavior and Ecology. Chicago, IL, The University of Chicago Press.

Stephens, D. W., and J. R. Krebs. 1987. Foraging theory: Princeton.

Stewart, P. D., C. Anderson, and D. W. Macdonald. 1997. A mechanism for passive range exclusion: Evidence from the European badger (Meles meles). Journal of Theoretical Biology 184:279-289.

Stewart, P. D., D. W. Macdonald, C. Newman, and C. L. Cheeseman. 2001. Boundary faeces and matched advertisement in the European badger (Meles meles): a potential role in range exclusion. Journal of Zoology 255:191-198.

Stewart, P. D., D. W. Macdonald, C. Newman, and F. H. Tattersall. 2002. Behavioural mechanisms of information transmission and reception by badgers, Meles meles, at latrines. Animal Behaviour 63:999-1007.

Stillman, R. A., and W. J. Sutherland. 1990. The optimal search path in a patchy environment. Journal of Theoretical Biology 145:177-182.

Strobeck, C. 1997. Fluctuating asymmetry and developmental stability: heritability of observable variation vs. Heritability of inferred cause. Journal of Evolutionary Biology 10:39-49.

Sudd, J. H. 1960. The foraging method of Pharaoh's ant, *Monomorium pharaonis* (L.). Animal Behaviour 8:67-75.

Thomas, C. D., A. Cameron, R. E. Green, M. Bakkenes, L. J. Beaumont, Y. C. Collingham, B. F. N. Erasmus *et al*. 2004. Extinction risk from climate change. Nature 427:145-148.

Thornhill, R., and S. W. Gangestad. 1999a. Facial attractiveness. Trends in Cognitive Sciences 3:452-460.

Thornhill, R., and S. W. Gangestad. 1999b. The Scent of Symmetry: A Human Sex Pheromone that Signals Fitness? Evolution and Human Behavior 20:175-201.

Tuomenvirta, H. 2000. Trends in Nordic and arctic temperature extremes and ranges. Journal of Climate, 13, 977-990.

Turchin, P. 1991. Translating foraging movements in heterogeneous environments into the spatial distribution of foragers. Ecology 72: 1253-1266.

Valeix, M., H. Fritz, S. Chamaille-Jammes, M. Bourgarel, and F. Murindagomo. 2008. Fluctuations in abundance of large herbivore populations: insights into the influence of dry season rainfall and elephant numbers from long-lterm data. Animal Conservation 11:391-400.

Van Tienhoven, A. M., J. E. Den Hartog, R. A. Reijns, and V. M. Peddemors. 2007. A computer-aided program for pattern-matching of natural marks on the spotted ragged tooth shark *Carcharias taurus*. Journal of Applied Ecology 44:273-280.

Vandongen, S., L. Lens, and G. Molenberghs. 1999. Mixture analysis of asymmetry: modelling directional asymmetry, antisymmetry and heterogeneity in fluctuating asymmetry. Ecology Letters 2:387-396.

Vanvalen, L. 1962. Study of fluctuating asymmetry. Evolution 16:125-142.

Vanvalen, L. 1965. Morphological variation and width of ecological niche. American naturalist, 99, 377-390.

Vargas, F. H., S. Harrison, S. Rea, and D. W. Macdonald. 2006. Biological effects of El Nino on the Galapagos penguin. Biological Conservation 127:107-114.

Vargas, F. H., R. C. Lacy, P. J. Johnson, A. Steinfurth, R. J. M. Crawford, P. D. Boersma, and D. W. Macdonald. 2007. Modelling the effect of El Nino on the

persistence of small populations: The Galapagos penguin as a case study. Biological Conservation 137:138-148.

Verhaeghe, J. 1982. Food recruitment in *Tetramorium impurum* (Hymenoptera: Formicidae). Insectes Sociaux 29:67-85.

Verhaeghe, J., and J. Deneubourg. 1983. Experimental study and modelling of food recruitment in the ant *Tetramorium impurum* (Hym. Form.). Insectes Sociaux 30:347-360.

Visscher, P.K. and Seeley, T.D., 2007. Coordinating a group departure: who produces the piping signals on honeybee swarms? *Behavioral Ecology and Sociobiology*. 61, 1615-1621

Visser, M. E. 2008. Keeping up with a warming world; assessing the rate of adaptation to climate change. Proceedings of the Royal Society B-Biological Sciences 275:649-659.

Visser, M. E., and C. Both. 2005. Shifts in phenology due to global climate change: the need for a yardstick. Proceedings of the Royal Society B-Biological Sciences 272:2561-2569.

Visser, M. E., and L. J. M. Holleman. 2001. Warmer springs disrupt the synchrony of oak and winter moth phenology. Proceedings of the Royal Society of London Series B-Biological Sciences 268:289-294.

Visser, M. E., A. J. van Noordwijk, J. M. Tinbergen, and C. M. Lessells. 1998. Warmer springs lead to mistimed reproduction in great tits (*Parus major*). Proceedings of the Royal Society of London Series B-Biological Sciences 265:1867-1870.

Viswanathan, G. M., V. Afanasyev, S. V. Buldyrev, E. J. Murphy, P. A. Prince, and H. E. Stanley. 1996. Levy flight search patterns of wandering albatrosses. Nature 381: 413-415.

Von Frish, K. 1967. The Dance Language and Orientation of Bees. Cambridge, Belknap Press (Harvard University Press).

Vucetich, J. A. and R. O. Peterson. 2004. The influence of top-down, bottom-up and abiotic factors on the moose (*Alces alces*) population of Isle Royale. Proceedings of the Royal Society of London Series B-Biological Sciences, 271, 183-189.

Walther, G. R., E. Post, P. Convey, A. Menzel, C. Parmesan, T. J. C. Beebee, J. M. Fromentin *et al*. 2002. Ecological responses to recent climate change. Nature 416:389-395.

Webb, D. R. and J. R. King. 1984. Effects of wetting of insulation of bird and mammal coats. Journal of Thermal Biology, 9, 189-191.

White, P. C. L., J. A. Brown, and S. Harris. 1993. Badgers (*Meles-meles*), cattle and bovine tuberculosis (mycobacterium-bovis) - a hypothesis to explain the influence of habitat on the risk of disease transmission in southwest England. Proceedings of the Royal Society of London Series B-Biological Sciences 253:277-284.

White, G. C. 2002. Discussion comments on: the use of auxiliary variables in capture-recapture modelling. An overview. Journal of Applied Statistics 29:103-106.

White, G. C., and K. P. Burnham. 1999. Program MARK: Survival estimation from populations of marked animals. Bird Study 46:S120-S139.

Whitlock, M. C., 2005. Combining probability from independent tests: the weighted Z-method is superior to Fisher's approach. *Journal of evolutionary biology*, 18, 1368-1373

Whitlock, M., and D. Schulter. 2008, The Analysis of Biological Data, Roberts And Company Publishers.

Whitney, W. O., and C. J. Mehlhaff. 1987. High-rise syndrome in cats. Journal of the American Veterinary Medical Association 191:1399-1403

Whittingham, M. J., P. A. Stephens, R. B. Bradbury, and R. P. Freckleton. 2006. Why do we still use stepwise modelling in ecology and behaviour? Journal of Animal Ecology 75:1182-1189.

Williams, B. K., J. D. Nichols, and M. J. Conroy. 2002. Analysis and management of animal populations. Academic Press.

Williamson, C. E. 1981. Foraging behavior of a fresh-water copepod - frequency changes in looping behavior at high and low prey densities. Oecologia 50:332-336.

Wilmers, C. C., S. Sinha, and M. Brede. 2002. Examining the effects of species richness on community stability: An assembly model approach. Oikos, 99, 363-367.

Wilson, E. O. 1962. Chemical communication among workers of the fire ant *Solenopsis saevissima* (Fr. Smith) 1. The Organization of Mass-Foraging. Animal Behaviour 10:134-147.

Wilson, E. O. 1984. The relation between caste ratios and division of labor in the ant genus *Pheidole* (Hymenoptera: Formicidae). Behavioral Ecology and Sociobiology 16:89-98.

Woodroffe, R. and D. W. Macdonald. 1993. Badger sociality - models of spatial grouping. Symp. Zool. Soc. Lond., 65, 145-169.

Woodroffe, R., D. W. Macdonald, and J. Dasilva. 1995. Dispersal and philopatry in the European badger, *Meles-meles*. Journal of Zoology 237:227-239.

Woodroffe, R., and D. W. Macdonald. 2000. Helpers provide no detectable benefits in the European badger (Meles meles). Journal of Zoology 250:113-119.

Woolf, C. M. 1989. Multifactorial inheritance of white facial markings in the Arabian horse. Journal of Heredity 80:173-178.

Wu, H.-i., Li, B.-L., T. A. Springer, and W. H. Neill. 2000. Modelling animal movement as a persistent random walk in two dimensions: expected magnitude of net displacement. Ecological Modelling 132: 115.

Zimmerman, M. 1979. Optimal foraging - case for random movement. Oecologia 43:261-267.

Zollner, P. A., and S. L. Lima. 1999. Search strategies for landscape-level interpatch movements. Ecology 80:1019-1030.

Zuckerkandl, E., L. Pauling, V. Bryson, and H. J. Vogel. 1965. Evolutionary divergence and convergence in proteins, Pages 97-166 Evolving Genes and Proteins. New York, Academic Press.

Zygourakis, K. 1996. Quantification and regulation of cell migration. Tissue Engineering 2: 1-16.

Appendices

Appendix A2.1

Introducing a Mathematical Model for Correlated Random Walks

In this Appendix we give details of the mathematical model introduced in this work.

The model describes properties of the "displacement" at time *t*, namely the position of an animal at time *t*, *relative* to its position at time $t = 0$. Since an animal moves in two dimensions, the displacement involves two coordinates and is written $\mathbf{R}(t) = \big(X(t),\ Y(t)\big)$ and by definition vanishes at time $t = 0$: $\mathbf{R}(0) = (0,0)$. In this formulation, $X(t)$ represents the change in coordinate along the X-axis from the initial position up to time *t*.

We take the displacement, $\mathbf{R}(t)$, to obey the simplest equation governing its continuous changes over time, namely a linear differential equation. A degree of randomness is incorporated into this equation to represent random aspects of the biology of the problem that results in changes of displacement. We take this randomness to be a Gaussian random function of time. For the purposes of this Online Appendix and Online Appendix C, we use a physical analogy that allows us to refer to the random function as a *force*, since forces *drive* movement in physics. We then allow the *force* to be correlated with itself over time. This is a very simple and natural way to incorporate the tendency of animals to move with some persistence of direction. Since the animals move in two dimensions, the *force*, denoted $\boldsymbol{\eta}(t)$, has two components and we write $\boldsymbol{\eta}(t) = \big(\eta_x(t),\ \eta_y(t)\big)$. Since the force is random in character, the displacement $\mathbf{R}(t)$ obeys the *stochastic* differential equation

$$d\mathbf{R}(t)/dt = \boldsymbol{\eta}(t). \tag{A2.1}$$

which can be viewed as a generalisation of a Weiner process.

The mathematical formulation of the problem requires a degree of flexibility that allows an efficient parameterisation of a range of observed behaviours. We accommodate this flexibility by allowing the correlations of the force to be arbitrarily specified.

The statistical properties of the two components of the force, $\eta_x(t)$ and $\eta_y(t)$, are fully characterised by their mean values and by their correlations. The above assumption of foraging means there are no preferred directions of movement. We enforce this by taking $\eta_x(t)$ and $\eta_y(t)$ to be statistically independent and to vanish, when averaged over many animals. This results in X(t) and Y(t) also being statistically independent (for earlier work that employed related ideas, see Tchen 1952; Flory 1969). With $E[...]$ denoting an average or expected value, the correlations of the force, namely $E[\eta_x(t_1)\eta_x(t_2)]$ and $E[\eta_y(t_1)\eta_y(t_2)]$, are taken to be equal and given by the function $\Delta(t_1 - t_2)$, where t_1 and t_2 are arbitrary times. The dependence of correlations on only the time interval, $t_1 - t_2$, means there is no preferred time in the problem.

We term $\Delta(t)$ the *correlation* function and this encapsulates *all* unknown determinants of movement in the model. Conventional Brownian motion adopts a form for $\Delta(t)$ that is an infinitely narrow spike of finite area (in which case $\Delta(t)$ is proportional to a Dirac delta function). This would be the formulation for a Weiner process (see, e.g., Haigh 2002). In the present work we consider more general forms for $\Delta(t)$.

The mean square displacement that is established after time *t* is $E\left[X^2(t) + Y^2(t)\right]$ and we write this this as $\sigma^2(t)$. From the model, the mean square displacement, $\sigma^2(t)$, can be explicitly expressed in terms of the correlation function $\Delta(t)$ (see Appendix 2.2). Exploiting this, we shift emphasis away from $\Delta(t)$ to $\sigma^2(t)$. Thus $\sigma^2(t)$ is the object containing all unknown determinants of movement of the model and flexibility of the model corresponds to the different possible choices that may be made for the dependence of $\sigma^2(t)$ on time *t*.

Literature cited in Appendix A2.1

Flory, P.J. 1969. Statistical Mechanics of Chain Molecules. New York: Wiley.

Tchen, C.M. 1952. Random flight with multiple partial correlations. J. Chem. Phys. 20, 214-217.

Appendix A2.2

Mean Square Displacement and Correlation Function

In this Appendix, we derive the relationship between the correlation function, $\Delta(t)$, and the mean square displacement, $\sigma^2(t)$.

We achieve this by solving the equation that the displacement $\mathbf{R}(t) = (X(t), Y(t))$ obeys, namely Eq. (A1). The solution of Eq. (A1) subject to $\mathbf{R}(0) = (0,0)$ is $\mathbf{R}(t) = \int_0^t \boldsymbol{\eta}(s)ds$, i.e., $X(t) = \int_0^t \eta_x(s)ds$ and $Y(t) = \int_0^t \eta_y(s)ds$. Using these results, the mean square displacement $\sigma^2(t) = E\left[X^2(t) + Y^2(t)\right]$ can be expressed as $E\left[\left(\int_0^t \eta_x(s)ds\right)^2 + \left(\int_0^t \eta_y(s)ds\right)^2\right]$. Both the *x* and *y* components of $\boldsymbol{\eta}$ terms make identical contributions to $\sigma^2(t)$. We thus only consider $E\left[\left(\int_0^t \eta_x(s)ds\right)^2\right]$. Using the definition of the correlation function $E[\eta_x(s_1)\eta_x(s_2)] = \Delta(s_1 - s_2)$, we obtain

$E\left[\left(\int_0^t \eta_x(s)ds\right)^2\right] = \int_0^t \int_0^t \Delta(s_1 - s_2)ds_1 ds_2$. Hence the relation between $\Delta(t)$ and $\sigma^2(t)$ is $\sigma^2(t) = 2\int_0^t \int_0^t \Delta(s_1 - s_2)ds_1 ds_2$. This result can also be written in the simpler form $\sigma^2(t) = 4\int_0^t (t - s)\Delta(s)ds$.

Appendix A2.3

Detailed Analysis of the Model of Correlated Random Walks

In this Appendix we describe the model of a persistent random walk introduced in this work and present details of calculations.

The displacement, $\mathbf{R}(t) = \big(X(t),\ Y(t)\big)$, is the position of an animal at time *t*, relative to its position at time $t = 0$, and obeys Eq. (A1): $d\mathbf{R}(t)/dt = \boldsymbol{\eta}(t)$. The random "force" $\boldsymbol{\eta}(t) = (\eta_x(t), \eta_y(t))$ represents the tendency of displacements to change randomly, but with some persistence of direction. The two components of the random force are taken to be independent and identically distributed Gaussian random processes (functions of time) with vanishing expected values, $E\big[\eta_x(t)\big] = E\big[\eta_y(t)\big] = 0$. Statistical independence yields $E[\eta_x(t_1)\eta_y(t_2)] = 0$ and this is necessary for a rotationally symmetric description, where no direction in the environment is distinguished. The correlations of the random force, $E[\eta_x(t_1)\eta_x(t_2)]$ and $E[\eta_y(t_1)\eta_y(t_2)]$, are equal and given by the function $\Delta\big(t_1 - t_2\big)$, which is termed the *correlation function*. This is symmetric: $\Delta\big(-t\big) = \Delta\big(t\big)$, and is taken to have a finite area: $\int_{-\infty}^{\infty} \Delta\big(t\big)\,dt < \infty$.

To gain some intuition about the nature of the correlations of the random force, we state without proof the property that the probability density of $\eta_x(t_2)$, conditional that the force at some other time t_1 has the value $\eta_x(t_1) = e_1$, is a normal distribution with mean $\Delta(t_2\text{-}t_1)\times e_1/\Delta(0)$ and variance $(\Delta^2(0)\text{-}\Delta^2(t_2\text{-}t_1))/\Delta(0)$. These results confirm the way that that $\Delta(t)$ characterises correlations. In particular, such a conditional probability density deviates considerable from the unconditional distribution when $\Delta(t_2\text{-}t_1)$ is close to $\Delta(0)$ and approaches the unconditional distribution when $\Delta(t_2\text{-}t_1) << \Delta(0)$.

The solution of Eq. (A1) for $\mathbf{R}(t)$, subject to $\mathbf{R}(0)=(0,0)$, is $\mathbf{R}(t)=\int_0^t \boldsymbol{\eta}(s)ds$. Explicitly, this means $X(t)=\int_0^t \eta_x(s)ds$ and $Y(t)=\int_0^t \eta_y(s)ds$. These are integrals (equivalent to sums) of independent normal random processes. It follows that at fixed *t*, both $X(t)$ and $Y(t)$ are independent and identically distributed normal random variables. Furthermore, given the statistical properties of $\boldsymbol{\eta}$, it follows that $X(t)$ and $Y(t)$ have mean 0 and equal variances: $E[X^2(t)]=E[Y^2(t)]$, which we write as $\sigma^2(t)/2$. In Appendix 2.2 it is shown that $\sigma^2(t)=4\int_0^t (t-s)\Delta(s)ds$ and this last result means the information contained in $\Delta(t)$ is also contained in the mean square displacement $E\left[X^2(t)+Y^2(t)\right]=\sigma^2(t)$.

Even incomplete information about $\Delta(t)$, such as the value of its area, has implications for the behaviour of a $\sigma^2(t)$. For example, if $\Delta(t)$ has a non-zero area $\left(\int_{-\infty}^{\infty}\Delta(s)ds\neq 0\right)$, then there is diffusive behaviour at sufficiently long times, and the mean square displacement ultimately becomes proportional to time t. By contrast, if $\Delta(t)$ has a vanishing area $\left(\int_{-\infty}^{\infty}\Delta(s)ds=0\right)$ then the mean square displacement, $\sigma^2(t)$, exhibits some form of subdiffusive behaviour at long times.

We note that normality of $X(t)$ and $Y(t)$ has a direct implication; in terms of the quantity $\|\mathbf{R}(t)\|=\sqrt{X^2(t)+Y^2(t)}$ (the magnitude of the displacement at time *t*), there is a unique time independent value for the ratio $E\left[\|\mathbf{R}(t)\|\right]\Big/\sqrt{E\left[\|\mathbf{R}(t)\|^2\right]}$ (Bovet & Benhamou 1988). We calculate the ratio using the normal probability density of $X(t)$ and $Y(t)$, which we write as $\phi(x,y)=\dfrac{\exp(-(x^2+y^2)/(2\sigma^2(t)))}{2\pi\sigma^2(t)}$. We can express $E\left[\|\mathbf{R}(t)\|\right]$ and $E\left[\|\mathbf{R}(t)\|^2\right]$ as integrals which can be evaluated by direct calculation,

using Cartesian coordinates. We have

$E\left[\|\mathbf{R}(t)\|\right] = \int_{-\infty}^{\infty}\int_{-\infty}^{\infty}\sqrt{x^2+y^2}\,\phi(x,y)dxdy = \sqrt{\pi/2}\,\sigma(t)$ and

$E\left[\|\mathbf{R}(t)\|^2\right] = \int_{-\infty}^{\infty}\int_{-\infty}^{\infty}\left(x^2+y^2\right)\phi(x,y)dxdy = 2\sigma^2(t)$. Thus $E\left[\|\mathbf{R}(t)\|\right]\Big/\sqrt{E\left[\|\mathbf{R}(t)\|^2\right]}$ has the value $\sqrt{\pi/4} \approx 0.8862$ (Bovet & Benhamou 1988).

An illustrative example of the mean square displacement, $\sigma^2(t)$, follows from the correlation function $\Delta(t) = D\exp\left(-|t|/T\right)/(2T)$ where T is a constant representing a single timescale in the problem and *D* is a constant associated with the magnitude of fluctuations of the random force. This correlation function leads to $\sigma^2(t) = 2D\left[t - T + T\exp(-t/T)\right]$. When the time *t* is large compared with the timescale *T*, we have $\sigma^2(t) \approx 2Dt$ which is typical of standard diffusion. We consider two special cases of the correlation function $\Delta(t) = D\exp\left(-|t|/T\right)/(2T)$.

(i) The first special case is when $\Delta(t)$ has all variation contained in the shortest possible range, as arises when the timescale, *T*, approaches 0. In this limit, $\Delta(t)$ becomes a zero width, infinite height spike of area *D* that is concentrated at $t = 0$. It follows that $\Delta(t)$ is proportional to a Dirac delta function $\delta(t)$, i.e., $\Delta(t) = D \times \delta(t)$. In this case, the resulting variance is proportional to time *t* for all times: $\sigma^2(t) = 2Dt \propto t$, and the displacement takes the form $\mathbf{R}(t) = \sqrt{D}\left(W_x(t),\ W_y(t)\right)$ where $W_x(t)$ and $W_y(t)$ are independent Wiener processes (see, e.g., Haigh 2002). This is two-dimensional *Brownian motion*, which has no persistence of direction.

(ii) The second special case is when $\Delta(t)$ changes extremely slowly, such that over the *time-interval of interest*, it may be treated as a constant, independent of time *t*. This occurs when the timescale, *T*, has a very large value compared with *t*. An expansion of $\sigma^2(t) = 2D\left[t - T + T\exp(-t/T)\right]$ in powers of the small quantity $1/T$ yields, to leading

order, a variance that is proportional to the square of time: $\sigma^2(t) = Dt^2/T \propto t^2$. This behaviour is characteristic of *ballistic motion* and the displacement takes the form $\mathbf{R}(t) = \sigma(t) \times \left(Z_x,\ Z_y\right)/\sqrt{2}$ where Z_x and Z_y are independent normal random variables with mean 0 and variance 1. When ballistic motion occurs, the movement of any animal is in a straight line at constant speed, but different animals have different realisations of Z_x and Z_y and hence in general, move at different constant speeds in different directions.

In the case of general correlations, i.e., general forms of $\Delta(t)$, an animal path exhibits a level of persistence of direction, and corresponds to a continuous version of a correlated (or persistent) random walk. When we sample animal paths at time intervals of τ, and consider the angle made between two straight line segments joining the displacement, $\mathbf{R}(t)$, at three adjacent times (e.g., τ, 2τ and 3τ), the distribution of angles can be expressed in terms of a single parameter, $\zeta(\tau)$, which is determined solely by the mean square displacement, $\sigma^2(t)$, evaluated at the times τ and 2τ. This is explicitly shown below and the results are given in Eqs. (2) and (3) of the main text.

Derivation of a property of discretely sampled paths

The normality and correlations of $\boldsymbol{\eta}(t)$ determine the distribution of angles associated with discretely sampled paths. Sampling at time intervals of τ, a piecewise linear approximation of a path $\mathbf{R}(t)$ is obtained by joining the positions on the path at the times $t = 0, \tau, 2\tau, 3\tau, \ldots$, with straight lines (see Figure 7.1). The angles characterising such a path are between adjacent straight-line segments. With $j = 0,1,2,\ldots$, adjacent straight line segments are defined by the two vectors $\mathbf{A} = \mathbf{R}((j+1)\tau) - \mathbf{R}(j\tau) = \int_{j\tau}^{(j+1)\tau} \boldsymbol{\eta}(s)ds$ and

$\mathbf{B} = \mathbf{R}((j+2)\tau) - \mathbf{R}((j+1)\tau) = \int_{(j+1)\tau}^{(j+2)\tau} \boldsymbol{\eta}(s)ds$ and these differ in direction by the angle α. The joint probability density (i.e., distribution) of $\mathbf{A}$ and $\mathbf{B}$ factorises into the

product $\psi(a_x,b_x)\times\psi(a_y,b_y)$ where $\psi(a_x,b_x)$ is the joint distribution of the x components of **A** and **B** and is identical to the corresponding distribution of y components. The factorisation occurs because of statistical independence of the x and y components of $\boldsymbol{\eta}$. We adopt the convention that angles, α, lie in the range $-\pi$ to π. The distribution of angles is then given by

$\phi(\alpha)=\int\delta\left(\alpha-\operatorname{atan}2(a_xb_y-a_yb_x,a_xb_x+a_yb_y)\right)\psi(a_x,b_x)\psi(a_y,b_y)da_xda_ydb_xdb_y$ where: all integrals range from $-\infty$ to ∞; the quantity $\delta(x)$ denotes a Dirac delta function; $\operatorname{atan}2(y,x)$ is the *four sector* arctangent function. This returns a unique angle in the range $-\pi$ to π and has the property $\operatorname{atan}2(k\sin\theta,k\cos\theta)=\operatorname{atan}2(\sin\theta,\cos\theta)$ for all positive k. Using polar coordinates, we can write $a_x=\rho\cos\beta$, $a_y=\rho\sin\beta$, $b_x=\lambda\cos\gamma$ and $b_y=\lambda\sin\gamma$, where ρ and λ range from 0 to ∞ and the angles β and γ can cover any interval of width 2π. For multiple integrals with different limits of integration, we write the integration measures (such as $d\rho$) immediately to the right of the integral sign, so no ambiguity exists about the range of each integral. We then find the distribution of angles is

$\phi(\alpha)=\int_0^\infty d\rho\int_0^\infty d\lambda\int_0^{2\pi}d\beta\;\rho\lambda\psi(\rho\cos\beta,\lambda\cos(\alpha+\beta))\psi(\rho\sin\beta,\lambda\sin(\alpha+\beta))$. The distribution $\psi(a,b)$ appearing in this expression is, because of normality of $\boldsymbol{\eta}$, bivariate normal, with vanishing means, $E[A_x]=E[B_x]=0$, equal variances, denoted $P=E[A_x^2]=E[B_x^2]$, and a covariance $Q=E[A_xB_x]$. With $S=P^2-Q^2$, it may be verified that $\psi(a,b)$ has the form

$\psi(a,b)=\left(2\pi\sqrt{S}\right)^{-1}\exp\left(-\left[\left(a^2+b^2\right)P-2abQ\right]/(2S)\right)$. This then yields

$\phi(\alpha)=(2\pi S)^{-1}\int_0^\infty d\rho\int_0^\infty d\lambda\;\rho\lambda\exp\left(-\left[\left(\rho^2+\lambda^2\right)P-2\rho\lambda Q\cos\alpha\right]/(2S)\right)$. Changing variable from λ to $y=\lambda/\rho$ yields *first* a ρ integral, and *then* a *y* integral, which may both be evaluated in closed form. The result is Eq. (3) of the main text, with $\zeta=Q/P$.

Finally, we establish the relation between $\zeta\equiv Q/P$ and the mean square displacement,

$\sigma^2(t)$. We have $P = E\left[\left(X((j+1)\tau) - X(j\tau)\right)^2\right]$. This can also be written in the form $\int_{j\tau}^{(j+1)\tau}\int_{j\tau}^{(j+1)\tau}\Delta\left(t_1 - t_2\right)dt_1 dt_2$ and by shifting integration variables, $t_1 \to t_1 - j\tau$ and $t_2 \to t_2 - j\tau$, it follows that P is independent of j. Similarly, we can show that $Q = E\left[\left\{X((j+2)\tau) - X((j+1)\tau)\right\}\left\{X((j+1)\tau) - X(j\tau)\right\}\right]$ is also independent of j. Setting $j = 0$ and $j = 1$ in the expression for P yields (i) $P = \sigma^2(\tau)/2$, (ii) $P = \sigma^2(2\tau)/2 + \sigma^2(\tau)/2 - 2E\left[X(2\tau)X(\tau)\right]$ and setting $j = 0$ in the expression for Q yields (iii) $Q = E\left[X(2\tau)X(\tau)\right] - \sigma^2(\tau)/2$. Combining (i), (ii) and (iii) allows us to obtain $\zeta = Q/P = \sigma^2(2\tau)/\left[2\sigma^2(\tau)\right] - 1$, which is Eq. (2) of the main text.

Literature cited Appendix A2.3

Haigh, J. 2002. Probability Models, Springer-Verlag, London.

Appendix A2.4

Experimental Set-up

In this Appendix, we provide a description of the experimental setup.

Ants, *Monomorium pharaonis*, were kept in a 15x30cm plastic container, containing a 7x7cm wooden nest box, a constant water supply and a food source (ox's liver with honey). Queens, larvae and pupae naturally established themselves in the nest box while workers exhibited activity both inside and outside the nest box (e.g., looking after young or foraging for food). Temperature and photoperiod were held constant at 26ºC and 12 hours light/dark.

Prior to an experiment, the ants were deprived of food for 2 days but the water supply was not removed. At time t = 0 min, ants were given access, via a bridge, to a new clean platform (the arena) of size 280x400 cm (i.e., approximately A3). Ants were free to travel between the arena and the nest. The application of a layer of *fluon* (fluon PTFE, *Blades Biological*) on the upper part of the walls of the container, prevented ants from climbing above this layer; thus the overall system was closed to ant escape. The experiment lasted 70 minutes. For practical reasons (file size) and because the shape of $\sigma^2(t)$ changed slowly during the course of the experiment, the 70 minutes experiment was sequenced in 35 films, each of 2 minutes in length. For each of those 2 minutes sequences, we extracted a single 30 seconds set of ant paths that were localised in the central 80% of the arena.

Appendix A2.5

Accuracy of Path Reconstruction

In this Appendix, we present evidence of the Accuracy of the path identification procedure.

In the main text, a procedure was briefly described for determining the positions of each ant in each frame, and hence constructing piecewise linear ant paths from the positions of many ants at discrete times. This procedure was performed using the software package Matlab. First, each frame was filtered to remove the background. Three positions of each ant were then determined using the '*bwlabel*' and '*regionprops*' functions which are able recognise and characterise clusters (i.e., ants in each frame). Finally, given the position of a particular ant in one frame, the position of the ant closest to it, in the next frame, was taken as the actual position of the ant in that frame. The accuracy of the procedure was tested via simulation. Ant paths were simulated as persistent random-walks, with a correlation function, $\Delta(t)$ which yielded a mean square displacement, $\sigma^2(t)$ of qualitatively correct form. The $\Delta(t)$ adopted was a reflected exponential, $\Delta(t) = \exp(-|t|/T)/(2T)$, where T is a characteristic timescale of the problem, and was estimated from the data to have the value 2 seconds. The simulated ants were started simultaneously, at random locations, in an *in silico* arena, and allowed to run for a period of 30 seconds. In the simulations, all information on the different ant paths was generated by the computer, and hence known with complete accuracy. Positions on paths were then sampled every 0.125 seconds and the procedure, described above and in the main text, was used to identify the paths and positions of individual ants. Accuracy was measured as the proportion of ant positions correctly assigned. The method adopted was found to correctly identify the paths of ants, for realistic densities, with an accuracy of 98%, in the sense that 98% of the positions that were assigned to a single ant on a path were correctly identified.

Appendix A3.1

Properties of Path Length

In this Appendix we establish the relationship between the mean distance travelled in time *t*, and *t* itself**.**

Given Equation (1), the length of the path travelled up to time *t* is given by: $M(t) = \sqrt{D}\int_0^t \|\eta(s)\| ds = \sqrt{D}\int_0^t \sqrt{\eta_x^2(s) + \eta_y^2(s)} ds$ .Thus the mean path length travelled is:

$$E[M(t)] = \sqrt{D}\int_0^t E\left[\sqrt{\eta_x^2(s) + \eta_y^2(s)}\right] ds \ . \tag{A3.1}$$

We know that at a fixed *s*, the quantity $\eta(s)$ is normally distributed with mean 0 and variance $\Delta(0)/\tau$, thus: $E\left[\sqrt{\eta_x^2(s) + \eta_y^2(s)}\right] = \iint_{-\infty}^{+\infty} \sqrt{x^2 + y^2}\, \frac{1}{2\pi\Delta(0)/\tau} exp\left(-\frac{x^2+y^2}{2\Delta(0)/\tau}\right) dxdy$. Hence we obtain:

$$E[M(t)] = \sqrt{\frac{\pi\Delta(0)D}{2\tau}}\ t \ . \tag{A3.2}$$

Appendix A3.2

Simulating Correlated Random Walks

In this Appendix, we give details of the simulation carried out in this work. For simplicity, we consider only properties of a single component of displacement, X(t). The other component of displacement, Y(t), has identical statistical properties to X(t) and is independent of X(t).

Because we focus on X(t) alone, we drop subscripts on η etc.

With the correlation function having the form of Equation (3.1), we can write:

$$\eta(t) = \frac{1}{\tau}\int_{-\infty}^{t} e^{-(t-s)/\tau}\xi(s)\,ds \qquad \text{(A3.3)}$$

where $\xi(s)$ is a delta correlated random function of time and is fully characterised by

$$E[\xi(t)] = 0 \text{ and } E[\xi(t_1)\xi(t_2)] = \begin{cases} 1 & if \quad t_1 = t_2 \\ 0 & if \quad t_1 \neq t_2 \end{cases}. \qquad \text{(A3.4)}$$

We can thus write $X(t) = \frac{\sqrt{D}}{\tau}\int_0^t \int_{-\infty}^{s} e^{-(s-u)/\tau}\xi(u)\,du\,ds$; which can be simplified to

$$X(t) = \sqrt{D}\left(1 - e^{-t/\tau}\right)\int_{-\infty}^{0} e^{u/\tau}\xi(u)du + \sqrt{D}\int_0^t \left(1 - e^{-(t-u)/\tau}\right)\xi(u)du\,. \qquad \text{(A3.5)}$$

By setting $t_j = j \times \delta$ (with δ a time discretisation), and $X_j = x\left(t_j\right)$, we have $X_0 = 0$ and for $j \geq 1$:

$$X(t) = \sqrt{D}\left(1 - e^{-t/\tau}\right)\int_{-\infty}^{0} e^{u/\tau}\xi(u)du + \sqrt{D}\sum_{k=1}^{j}\int_{t_{k-1}}^{t_k}\left(1 - e^{-(t_k-u)/\tau}\right)\xi(u)du \qquad \text{(A3.6)}$$

Without making any approximation, we note that for a particular value k, $\sqrt{D}\int_{t_{k-1}}^{t_k}\left(1 - e{-}tk{-}u\tau\xi udu\right.$ is a normally distributed random variable with mean 0 and variance:

$$D\int_{t_{k-1}}^{t_k}\left(1-e^{-(t_k-u)/\tau}\right)^2 du =$$

$$D\left[\delta-2\tau e^{-(t_j-t_k)/\tau}\left(1-e^{-\delta/\tau}\right)+\frac{\tau}{2}e^{-2(t_j-t_k)/\tau}\left(1-e^{-2\delta/\tau}\right)\right]. \quad \text{(A3.7)}$$

Thus, if we write $M_{j0}=\sqrt{\frac{D\tau}{2}}\left(1-e^{-t/\tau}\right)$: ,

$M_{jk}=\sqrt{D\left[\delta-2\tau e^{-(t_j-t_k)/\tau}(1-e^{-\delta/\tau})+\frac{\tau}{2}e^{-2(t_j-t_k)/\tau}(1-e^{-2\delta/\tau})\right]}$, and Z_k independent and identically distributed random variables are drawn from a normal distribution with mean 0 and standard deviation M_{jk}, then the position of an individual at time j can be fully determined using:

$$X_j=\begin{cases}0, & j=0\\ M_{j0}Z_0+\sum_{k=1}^{j}M_{jk}Z_k & j\geq 1\end{cases} \quad \text{(A3.8)}$$

Appendix A 3.3

Details on the Simulation Process

Individual trajectories contained 2,000 positions (one per unit time) and were simulated such that their mean speed would equal 20 unit of space per unit time (regardless of the values of *D* or *T* used).

In our simulation each prey items were considered immobile and non-renewable during a foraging bout. A foraging bout was deemed finished when each 1000 individuals with the same walking pattern had foraged (apart of case 4, see Table 3.1, where a foraging bout finishes when *G* individuals have foraged).

A prey item matrix was constructed and each element corresponded to equidistant point on the plane. In cases 1, and 3 to 5 (of Table 3.1), each element takes the value ρ ($\rho = 10^{-4}$ represents the food density) at the beginning of a foraging bout. When a simulated individual 'walks' at a distance *s* from a prey item, it retrieves the food, and the element takes the value 0 indicating no food is available at this location. At the end of the foraging bout, it is possible to simply count the food gathered by each individual. After a foraging bout is simulated, and thus a walking strategy tested, the prey item matrix is reinitiated to test a new walking strategy.

In case 2 of Table 3.1, some elements (determined randomly from a uniform distribution) takes the value 1 while other keep the value 0 such that the food density remains constant over the prey item matrix (ρ). Finally in case 6 of Table 3.1, the values in each element of the matrix take a value according to a normal distribution (in 2 dimension) whose mean is centred around the starting point of the trajectory and with standard deviation σ ranging from 10 to 1000.

Appendix A 4.1

Summary for all Runs

This Appendix contains two tables which summarise the results for the different runs of experiments carried out. The general conclusions we draw in the main text (for experimental run 1) hold for all experiments.

In Table 4.2 we present the results of experiment where replacement is permitted. In this situation we can, for each run, determine the product of the parameters *n* and *r*, but not each parameter separately. We verify the exponential nature of the distribution of time-intervals using the Anderson Darling test (test statistic AD). We also note that a visual estimate of the total number of ants in a nesting area is denoted Ne and is accurate within ±50 ants.

	nr	Ne	Exp. Dist.
run 2	0.08	~500	P ~ 0.1 (AD ~ 1.0)
run 3	0.06	~300	P ~ 0.08 (AD ~ 1.1)
run 4	0.19	~100	P ~ 0.4 (AD ~ 0.5)

Table 4.2

In Table 4.3 we summarise the result of the second set of experiment where replacement was not allowed. In this situation, estimates of both *n* and *r* are given. The distribution of time-intervals appears not to follow an exponential distribution (Anderson-Darling test, test statistic: AD), but cannot be distinguished from a distribution that would be exponential in shape with a shifting parameter (using a Kolmogorov-Smirnov test, test statistic: KS, on transformed time-intervals according to Broom *et al.* 2007).

	N	r	Exp. Dist.	Shift Exp. Dist.
run 2	529 (526-533)	6.8 (6.7-6.9)	$p<0.001$ (AD~29.0)	p~0.2 (KS~0.05)
run 3	527 (523-532)	3.9 (3.8-4.0)	$p<0.001$ (AD~4.2)	p~0.9 (KS~0.02)
run 4	214 (211-218)	5.2 (5.1-5.4)	$p<0.05$ (AD~1.4)	p~0.4 (KS~0.06)

Table 4.3

Appendix A4.2

Statistical Properties of Falling Ants

In this Appendix we determine the statistical properties of the number of ants that have left the nesting area, as predicted by the models of the main text. We use a discrete-time description to derive results, where time t can take only the discrete values $t = j \times \tau$ where $j = 0,1,2,...$ and τ is the value of a discrete-time-step. While the results presented for a finite time-step may have some utility in their own right, we do not employ the finite step results here. Thus, at the end of the calculations, we take the time-step to zero, so time becomes continuous. We note that the models presented have close connections with `pure death' models of population biology (Renshaw, 1993).

The probability of any particular ant to leave/unit time is r hence the probability of any ant to leave in a time-step is taken as $r\tau$ (and only consider $r\tau < 1$). The number of ants leaving during any time-step is the outcome of random sampling, where every ant in the nesting area has an equal probability of being chosen to leave. Hence the number of ants leaving is drawn from an appropriate binomial distribution.

Replacement model

When replacement is allowed, the number of ants present in the nesting area is constant and equal to the initial number, n. The number of ants that have left by time t, namely $N(t)$, is determined by the stochastic difference equation

$$N(t+\tau) = N(t) + B(n, r\tau) \tag{A4.1}$$

with

$$N(0) = 0. \tag{A4.2}$$

In Eq. (A4.1) the quantity $B(n, r\tau)$ represents a random variable that is independently drawn, each time-step, from a binomial distribution with parameters n and $r\tau$. Since a sum of independent and identically distributed binomial random variables is also a

binomial random variable, the number of ants that have left after time *t* also has a binomial distribution. Consequently, we can write $N(t) = B(n, r\tau)$**Error! Bookmark not defined.**. Allowing τ to tend to zero (so time becomes continuous) results in $N(t)$ having a Poisson distribution

$$N(t) \sim Poisson(nrt) \tag{A4.3}$$

This has a mean, $E[N(t)]$, and a variance, $\mathrm{Var}\big(N(t)\big)$, of nrt.

To derive the distribution of time-intervals, we note that given a dropping event occurs at time $j\tau$, the next event will occur at time $(j+k)\tau$ with a probability that results from $k-1$ "failures" followed by a "success." A failure occurs with probability $(1-r\tau)^n$ and a success occurs with probability $1-(1-r\tau)^n$. Hence the distribution of time-intervals between successive events follows a geometric distribution:

$$\psi(k;\tau) = [1-(1-r\tau)^n](1-r\tau)^{n(k-1)}. \tag{A4.4}$$

As τ tends toward zero, we can neglect the probability of more than one ant leaving at any step and an event can be interpreted as a single ant leaving. For a time-interval of Δt the number of time-steps is $k = \Delta t/\tau$. The *probability density* of time-intervals arises from the small τ limit of $\psi(\Delta t/\tau\,;\tau)/\tau$ and from Eq. (A4.4) we obtain the exponential distribution

$$\varphi(\Delta t) = nre^{-nr\Delta t}. \tag{A4.5}$$

The last result we shall determine for the replacement model concerns the distribution of exponentially distributed random numbers. If *U* is a random variable with a uniform distribution on [0,1] then $Y = -\ln(U)/\lambda$ has an exponential distribution with mean $1/\lambda$. Conversely, if Y has an exponential distribution with mean $1/\lambda$, then $e^{-\lambda Y}$ is uniformly distributed on [0,1]. It follows from Eq. (A4.5) that if Δt_j is a random variable with an exponential distribution with mean $1/(nr)$ then $U_j = e^{-nr\,\Delta t_j}$ is uniformly distributed on [0,1].

<u>Without replacement model</u>

When replacement is not allowed, and $N(t)$ ants have left from the nesting area, the number of ants present in the nesting area is $n - N(t)$. This is the number from which a

random sample is selected to leave in the next time-step. It follows that the analogue of Eq. (A4.1) is

$$N(t+\tau) = N(t) + B(n - N(t), r\tau). \tag{A4.6}$$

The solution is subject to Eq. (A4.2). To determine the distribution of $N(t)$ it is convenient to define $M(t) = n - N(t)$, and Eq. (A4.6) becomes equivalent to

$$M(t+\tau) = B(M(t), 1 - r\tau) \tag{A4.7}$$

with

$$M(0) = n. \tag{A4.8}$$

We write the probability distribution of $M(t)$ as $\psi_t(m)$ and Eq. (A4.7) leads to

$$\psi_{t+\tau}(m) = \sum_{k=0}^{n} f_{1-r\tau}(m,k)\psi_t(k) \tag{A4.9}$$

where $f_s(a,b) = \binom{b}{a} s^a(1-s)^{b-a}$ and $\binom{b}{a}$ denotes a binomial coefficient. It may be verified that $\sum_{b=0}^{n} f_s(a,b) f_{s'}(b,c) = f_{ss'}(a,c)$ and this property, combined with Eqs. (17) and (18) leads to $\psi_t(m) = f_{(1-r\tau)^{t/\tau}}(m,n)$ and hence to $M(t)$ having a binomial distribution with parameters n and $(1-r\tau)^{t/\tau}$. As a consequence $N(t)$, has a binomial distribution with parameters n and $1-(1-r\tau)^{t/\tau}$. As we allow τ to tend to zero (and time becomes continuous) we obtain a binomial distribution for $N(t)$ with parameters n and $1-e^{-rt}$:

$$N(t) \sim \text{Binomial}(n, 1 - e^{-rt}). \tag{A4.10}$$

This is characterised by a mean value of

$$E[N(t)] = n(1 - e^{-rt}) \tag{A4.11}$$

and a variance of $\text{Var}\big(N(t)\big) = ne^{-rt}(1 - e^{-rt})$.

To determine the distribution of time-intervals between individual ants leaving at time *t*, we note that when *j* ants have left, the mean time to the next ant leaving follows from Eq. (A4.5) with *n* replaced by *n* – *j* and is given by $1/[(n-j)r]$. At time *t* we approximate the mean time-interval between ants leaving by $1/[(n - E[N(t)])r]$.

Combining this result with Eq. (A4.11) leads to a mean time-interval between ants leaving that depends on time *t* according to

$$E[\Delta t(t)] \approx e^{rt}/(nr). \tag{A4.12}$$

Similar considerations to the "with replacement" case, where we first assume *j* ants have left, and then replace j by $E[N(t)]$, leads to an exponential distribution of time-intervals that depends on the time *t* and is given by

$$\varphi(\Delta t, t) = nre^{-rt}e^{-nre^{-rt}\Delta t}. \tag{A4.13}$$

Furthermore, in the limit of small τ, we have that after *j* events (*j* ants having dropped), the time to the next event is an exponential random variable with mean $1/[(n-j)r]$. Writing this random time as Δt_j we have, following the arguments in the "with replacement" case, that the random variable $V_j = e^{-(n-j)r\,\Delta t_j}$ is uniformly distributed on [0,1].

Appendix 4.3

Record Dynamics Approach

In this Appendix, we compare the random process, which is used in this work to describe the departure of ants from a nest, with the random process adopted by Richardson *et al* (2010) for their experiments. We note that all experiments and analysis of the present work, with the exception of this Appendix, were completed prior to learning of the work by Richardson *et al*. (2010).

To proceed, let t_k denote the time the *k*'th ant left the nest. Richardson *et al* (2010) assumed that differences of the natural logarithms of the times ants left a nest, namely $\ln(t_{k+1}) - \ln(t_k)$, had an exponential distribution. This leads to so called 'record dynamics' and, for some physical systems, is known to imply long range correlations (see e.g., Sibani and Dall, 2003). The logic of Richardson *et al* (2010) is that if $\ln(t_{k+1}) - \ln(t_k)$ has an exponential distribution then this is evidence of interactions (of some kind) between the ants in their experiments. We note that these workers are therefore reasoning by analogy, and are not deriving the dynamics of the ants from a concrete mathematical model of ant behaviour.

By contrast, the results of the present paper are based on the detailed analysis of a specific mathematical model of ant behaviour. This model does not include any interactions between the ants and it predicts that the time intervals between ants leaving the nest without replacement, namely $t_{k+1} - t_k$, are exponentially distributed. A non-trivial outcome of this model is that the mean time interval $E[t_{k+1} - t_k]$ depends on the value of *k* (i.e., on the number of ants that have left the nest).

Description of a log-Poisson process adopted by Richardson *et al*.

The model of Richardson *et al* (2010) is based on the assumption that $\ln(t_{k+1}) - \ln(t_k)$ has an exponential distribution, which is termed a log Poisson process. We shall derive some approximate properties of this process.

To begin, we note that a log Poisson process can be expressed as

$$\ln(t_{k+1}) - \ln(t_k) = -c\ln(U_k) \tag{A4.14}$$

where c is a constant (the expected value of $\ln(t_{k+1}) - \ln(t_k)$), and the U_k are, for different *k*, independent random variables which are uniformly distributed over [0,1]. We make the assumption that the distribution of $\log(t_k)$ changes slowly with *k* so that the parameter *c* in Eq. (23) is small:

$$c \ll 1. \tag{A4.15}$$

To fully define the log Poisson process, we need to specify the time of the initial event and we take t_0 to have the value of unity, so all times are measured from time 1 (we cannot take it as zero due to the properties of logarithms).

From Eq. (23) it follows that $\log(t_1) = -c\ln(U_0)$, $\ln(t_2) = -c\ln(\mathrm{U}_1) - c\ln(U_0)$ and generally $\ln(t_k) = -c\sum_{\mathrm{j}=0}^{\mathrm{k}-1}\ln(U_j)$, or equivalently

$$t_k = U_{\mathrm{k}-1}^{-\mathrm{c}} U_{\mathrm{k}-2}^{-\mathrm{c}} \ldots U_0^{-\mathrm{c}}. \tag{A4.16}$$

Thus

$$\Delta t_k \equiv t_{k+1} - t_k = (U_{\mathrm{k}}^{-\mathrm{c}} - 1) U_{\mathrm{k}-1}^{-\mathrm{c}} U_{\mathrm{k}-2}^{-\mathrm{c}} U_{\mathrm{k}-2}^{-\mathrm{c}} \ldots U_0^{-\mathrm{c}}$$

$$= (U_{\mathrm{k}}^{-\mathrm{c}} - 1) t_k. \tag{A4.17}$$

To obtain an indication of the content of this process, we make two approximations to Eq. (26): (i) we approximate $(U_{\mathrm{k}}^{-\mathrm{c}} - 1)$ by $-c\log(U_k)$ which applies for $c \ll 1$; (ii) we replace t_k by its expected value, $E[t_k] = (1-c)^{-k} \approx \exp(ck)$. Thus

$$\Delta t_k \approx -ce^{kc}\log U_k. \tag{A4.18}$$

Lastly, we wish to infer the distribution of time intervals not after *k* events, but rather, after time *t*. It may be shown that for the log Poisson process, the mean number of events up to time *t* is $\log(t)/c$. Thus to convert Eq. (5) to the time domain we replace *k* by $\log(t)/c$ and obtain $\Delta t(t) \approx -ct\log U$ which means the time intervals, at time *t*, have an exponential distribution with mean *ct*:

$$E[\Delta t(t)] \approx ct \qquad \text{Model of Richardson } et\ al. \tag{A4.19}$$

Equation (A4.19) has been checked by simulations and works reasonably for $c < 0.5$.

Equation (A4.19) is to be contrasted with the prediction of the model of the present work, which is given in Eq. (A4.12) of Appendix A4.2, namely $E[\Delta t(t)] \approx e^{rt}/(nr)$.

We can thus say that the log Poisson model adopted by Richardson *et al* (2010) and the non-interaction model, used in the present work, both predict that mean time intervals increase with the time that has elapsed since the start of an experiment, but that the manner of increase is different.

Experimental evidence

We have subjected data from our 'without replacement' experiments to statistical tests, to see if they can be described by a log Poisson process. We reject a log Poisson process for our data, based on two simple analyses. Firstly, the distribution of logged time intervals $(\ln(t_{k+1}) - \ln(t_k))$ differs significantly from an exponential distribution (Anderson Darling test, $N = 495$, $p < 0.001$). Secondly, and perhaps more strikingly, we plotted the cumulative number of events (ant departures) against time, and used a non-linear fitting procedure to determine the `best choice' for the parameter $c$ in the prediction of a log Poisson process, namely: $E[t_k] = (1-c)^{-k} \approx \exp(ck)$. Figure 4.10 illustrates how ants exit the nest in our `without replacement' experiments, along with the 'best fit' from a log Poisson process. The significant absence of a good fit contrasts very strongly with Figure 4.5 in the main body of this paper, which plots data and a curve from our mathematical model.

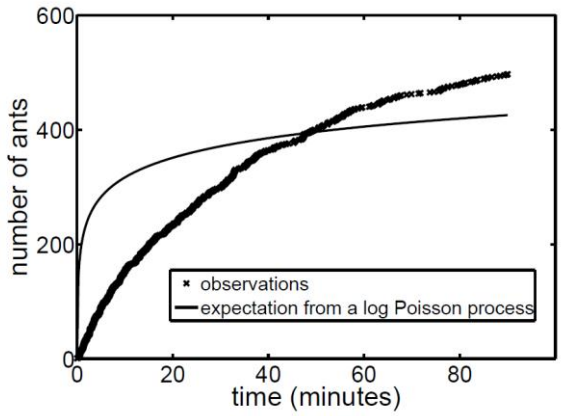

Figure 4.10

Observed number of ants that leave their nest, as a function of time, and its expectation under a log Poisson process (solid curve).

We note that Richardson *et al*. (2010) pointed out that, under a log Poisson process, the survivorship function (calculated as 1 – cumulative distribution) of the logged time intervals and the cumulative number of exits should be linear in log scale. Thus they plotted those functions in their Figures 3 and 4 as evidence to support their model. While we conclude that, for our experiments, a log Poisson process is not a good description of the data (see above), we have plotted survivorship for our data (Figure 4.11a) in the same format as Figure 3 of Richardson *et al* (2010) (i.e., survivorship plotted as a function of $\ln(t_{k+1}/t_k)$). We have also plotted the cumulative number against log time for our data (Figure 4.11b) in the same format of Figure 4 in Richardson *et al* (2010). A visual inspection of these gives little reason to reject a log Poisson process, even though the analysis presented above does, indeed, clearly reject this process. Our view is that adopting a log scale might not be the most appropriate way to plot the data, since it does tend to smooth differences.

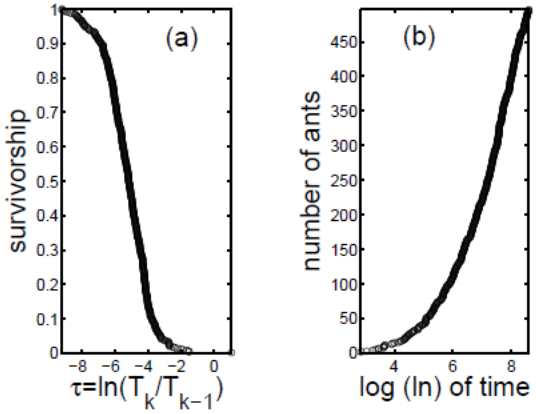

Figure 4.11

(a) A plot of survivorship as a function of the difference of log times. (b) A plot of the cumulative number of ants that had left their nest against the logarithm of time.

Let us, finally, consider the most important evidence adduced by Richardson *et al* (2010) in favour of a log Poisson process. This is the test that the difference of the logarithm time intervals has an exponential distribution (the basic assumption underlying their analysis). In particular the result of the Anderson Darling test presented in Table S1 of their work. In their 'removal situation' (equivalent to 'without replacement' in the present work), out of the total of 13 experiments, we observe that 5 (38%) show evidence to reject the log Poisson process at the 5% confidence level. In their non-removal situation, out of the 7 experiments, 3 (42%) show evidence to reject the log Poisson process. On the assumption that the experiments presented by Richardson *et al*. (2010) are independent on one another, it is possible to perform a small meta-analysis of their results. We used a weighted *Z* method (Whitlock, 2005) to obtain an overall *p* value that is associated with the null hypothesis of Richardson et. al (2010) that the distribution of exit times is a log Poisson process. This overall *p* value takes into account the *p* values from each independent experiment. The *Z* values (back-calculated from the *p* values) were weighted by number of exits from the nest. We found that both in the removal situation of Richardson *et al*. (2010) and in their non-

removal situation, there was significant evidence to reject the null hypothesis of a log Poisson process (in both cases, $p < 0.001$).

Overall, we conclude that in our experiments, there is very strong statistical evidence to reject a log Poisson process. Additionally, on the basis of a limited meta-analysis, we find some statistical evidence to reject the log Poisson process in the experiments of Richardson *et al* (2010).